Radio Resource Management for Automotive Device-to-Device Communication in Future Cellular Networks

vorgelegt von
M. Sc.
Mladen Botsov

von der Fakultät IV - Elektrotechnik und Informatik
der Technischen Universität Berlin
zur Erlangung des akademischen Grades

Doktor der Ingenieurwissenschaften
-Dr.-Ing.-

genehmigte Dissertation

Promotionsausschuss:

Vorsitzender:	Prof. Dr.-Ing. Rafael Schäfer
Gutachter:	Prof. Dr.-Ing. Slawomir Stańczak
Gutachter:	Prof. Erik G. Ström
Gutachter:	Prof. Dr.-Ing. Wolfgang Kellerer

Tag der wissenschaftlichen Aussprache: 16.01.2020

Berlin, 2020

Kurzfassung

Die sogenannte Device-to-Device-Kommunikation (D2D-Kommunikation) wird neulich als effiziente Lösung für das Entladen von Zellen und zur Erhöhung der Kapazität von zukünftigen Mobilfunknetzen angesehen. Dies wird durch die Wiederverwendung von zellulären Radioressourcen für eine örtlich begrenzte Direktübertragung zwischen betroffenen Endgeräten. Die durch das D2D-Paradigma gebotenen Vorteile können die Implementierung zusätzlicher neuer Dienste in einem solchen Hybridsystem ermöglichen. Insbesondere die lokalisierte Natur der direkten Übertragungen und ihre höhere spektrale Effizienz korrelieren gut mit den Eigenschaften von Automotiveanwendungen, die auf der Grundlage von kooperativen intelligenten Transportsystemen (bekannt als C-ITS) erstellt werden. Diese Arbeit untersucht die Implementierung solcher Dienste basierend auf D2D-Kommunikation. Sie befasst sich insbesondere mit dem Problem des Radio Resource Managements (RRM) mit dem Hauptziel, die strengen QoS-Anforderungen (Quality of Service) von sicherheitsrelevanten Automotiveanwendungen zu erfüllen.

Zu diesem Zweck wird eine Analyse der asymptotischen Transportkapazität des beabsichtigten zweischichtigen Netzwerks durchgeführt, um das Potenzial der Unterstützung von C-ITS-Anwendungen in dem D2D-Subnetz zu bewerten. Motiviert durch das ermutigende Systemverhalten und das Fehlen entsprechender Beiträge in der Literatur, wird ein auf Kanalverteilungsinformationen (Channel Distribution Information, CDI) basierendes RRM-Schema definiert, um die QoS-Anforderungen aller sendenden Benutzer sowohl im primären Mobilfunknetz als auch in dem D2D-Subnetz zu erfüllen. Dieses Schema nutzt das Wissen über die (Verteilung der) Kanalkoeffizienten für alle potenziellen (Interferenz-) Verbindungen im System, um eine geeignete Ressourcenzuteilung zu bestimmen. Insbesondere können mehrere Benutzer dieselben Funkressourcen für die zellulare bzw. direkte Kommunikation wiederverwenden, so dass gleichzeitige Übertragungen keine schädlichen gegenseitigen Interferenzen verursachen. Das Sammeln von CDI ist jedoch mit einem enormen Overhead verbunden und in Szenarien mit höherer Netzwerklast nicht realisierbar. Daher wird ein zweites RRM-Schema basierend auf Standortinformationen mit dem Ziel eines minimalen zusätzlichen Aufwands entwickelt. Dieses Schema nutzt das Wissen über die Positionen der Benutzer und leitet basierend auf ihrer räumlichen Trennung eine geeignete Ressourcenzuteilung ab.

Die Leistung der beiden Schemata wird durch umfangreiche Simulationen auf Systemebene bewertet. Es wird eine Analyse der Vor- und Nachteile von CDI- bzw. standortbasiertem RRM durchgeführt. Während beide Schemata in der Lage sind, einige realistische QoS-Anforderungen zu erfüllen, kann das CDI-basierte System eine größere Anzahl von Benutzern unterstützen. Dies geht jedoch mit einem viel höheren Messaufwand einher. Darüber hinaus wird die Notwendigkeit einer Berücksichtigung der QoS-Anforderungen im RRM für C-ITS-Anwendungen gezeigt, da der häufig verwendete opportunistische Ansatz für die D2D-Kommunikation zu einer unbefriedigenden Leistung führt.

Abstract

Device-to-device (D2D) communication as an underlay to future cellular networks has been recently considered as an efficient cell offloading and capacity increasing solution. As such, it is envisioned to help serve the ever increasing cellular traffic. The gains offered by the D2D paradigm may enable the implementation of additional novel services in such a hybrid system. In particular, the localized nature of direct transmissions and their higher spectral efficiency correlate well with the properties of automotive applications built on the basis of Cooperative Intelligent Transport Systems (C-ITS). This work investigates the adoption of such services in the D2D underlay. In particular, it deals with the problem of Radio Resource Management (RRM) with the main objective of satisfying their stringent Quality of Service (QoS) requirements.

To this end, an analysis of the asymptotic transport capacity of the envisioned two-tier network is carried out in order to assess the potential of supporting C-ITS applications in the D2D underlay. Motivated by the encouraging system behavior and the lack of corresponding contributions in the literature, a RRM scheme based on Channel Distribution Information (CDI) is defined to satisfy the QoS requirements of all transmitting users, both in the primary cellular network and in the D2D underlay. This scheme leverages knowledge over the (distribution of the) channel coefficients for all of the potential (interference) links in the system, in order to determine appropriate resource allocation. In particular, it allows for multiple users to reuse the same radio resources for cellular and direct communication, respectively, such that concurrent transmissions do not cause harmful mutual interference. The acquisition of CDI, however, is associated with enormous overhead and is not feasible in scenarios with higher network load. Hence, a second RRM scheme based on location information is developed with the goal of minimal added overhead. This scheme leverages knowledge over the positions of users and derives an appropriate resource allocation based on their separation in space.

The performance of the two schemes is evaluated by means of extensive system level simulations. An analysis of the advantages and disadvantages of CDI- and location-based RRM, respectively, is carried out. While both schemes are capable of satisfying some feasible QoS requirements, the CDI-based one can support a higher number of users. This comes at the cost of much higher measurement overhead, however. Moreover, the necessity of considering QoS requirements in RRM for C-ITS applications is demonstrated, as the commonly used opportunistic approach to D2D communication leads to unsatisfactory performance.

I would like to acknowledge everyone who has assisted me throughout my doctoral studies over the years. I would first like to express my deepest gratitude towards Prof. Dr.-Ing. Slawomir Stańczak for agreeing to serve as my adviser, and for his patience and feedback as I completed my dissertation. Additionally, I would like to thank Prof. Erik G. Ström and Prof. Dr.-Ing. Wolfgang Kellerer for agreeing to serve on my dissertation committee. I truly appreciate all of their time and insightful comments!

A very special thanks is due to my second adviser, Dr. Peter Fertl, with whom I have had the pleasure of working together since 2011. Without Peter's guidance I would not have chosen the path of doctoral studies! With his support I was able to secure a scholarship at the BMW Group within its doctoral program ProMotion. For this opportunity, and all of the educational experiences I had as a participant, I am very grateful. I also wish to thank all other friends and colleagues, which I met at the company, for creating a supportive environment in which my work could flourish. My special thanks goes to my department heads through the years - Karl-Ernst Steinberger and Martin Arend, for their support, as well as to David Gozalves-Serrano and my fellow doctoral students Christian Lottermann, Ren Zhe, and Levent Ekiz for many fruitful discussions. A note of thanks is also due to all contributes to the project METIS, in which the topic of my studies was formed, for numerous inspiring conversations. I would especially like to thank Wanlu Sun for our close collaboration and exchange of ideas.

Last but not least, I would like to thank my loving family for their never-ending encouragement and backing, and for making me the person I am today.

I could not have completed my studies without the support of all these wonderful people!

Mladen Botsov

Contents

Chapter 1

Introduction

1.1 Background

After their introduction in the 1980's, commercial cellular networks have rapidly developed into an integral part of everyday life. Such systems utilize fixed transceivers deployed over the served area, known as base stations, to enable wireless connectivity for mobile devices by means of radio transmissions. In those early days, the supported applications were limited to voice calls. Nevertheless, the added convenience and flexibility over fixed telephone lines encouraged the adoption of cellphones. As the subscriber base grew, so did the effort spent by the telecommunications industry on evolving the cellular technology and expanding the business opportunities it offered. Further success soon followed with the introduction of short text messages (up to 160 characters) as additional means of communication in the 1990's. Slipping into the new Millennium, cellular networks made a revolutionary step forward by adopting packet switching which enabled services such as mobile web browsing, e-mail, and video streaming, and triggered a change in consumer behavior. This change, in conjunction with further technological advancements in the 2010's, has led to a booming demand for mobile multimedia contents. In its most recent report, Cisco predicts that mobile data traffic will grow at a compound annual growth rate of 53% until 2020 [Cis16]. Faced with such ever increasing capacity requirements, current cellular networks will struggle to provide adequate service. Hence, novel system concepts are being studied to cope with the mobile data traffic beyond 2020, when the so called Fifth Generation of Mobile Communication (5G) is expected to be introduced.

1.1.1 Device-to-Device Communication

One of the most promising concepts for the 5G era is commonly referred to as *Device-to-Device (D2D) communication* [JYD+09]. Under this paradigm, the exchange of data between mobile devices, or User Equipment (UE), in close proximity is carried out directly between the UEs while the network infrastructure has merely a control function [DRW+09]. In contrast, the same exchange in a conventional cellular network, where the links are established via the Radio Access Network (RAN) and the core network, requires the data to be relayed between multiple entities. This process is illustrated in Figure 1.1. In a first step, said data is sent by the source to a base station, also known as evolved NodeB (eNB) in current cellular networks, by means of an uplink (UL) transmission. The information is then relayed through gateways in the core network - potentially back to the same eNB or one of its immediate neighbors.

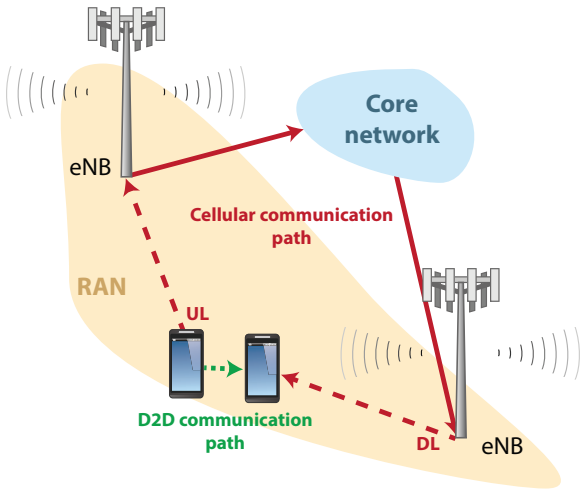

Figure 1.1: Cellular and D2D communication paths between two UEs in close proximity.

Finally, the data is delivered to its intended destination in a downlink (DL) transmission. In comparison, D2D communication enables the so-called *hop gain* [FDM+12], referring to the fact that a single transmission uses radio resources more efficiently than the required pair of UL and DL transmissions in cellular communication. In addition, a direct link also allows for lower End-to-End (E2E) latency by avoiding the processing and queuing delays at eNBs and gateways. Furthermore, it is likely that the distance between the communicating partners is much smaller than the distance between any of the UEs and its serving eNB. Hence, exploiting the more favorable channel conditions, D2D communication enables either higher data rates at the same power consumption or lower power consumption at the same data rate as compared to the UL and DL transmissions that are required in a conventional cellular network. This is referred to as *proximity gain* [FDM+12].

Direct transmissions between proximate UEs under the D2D paradigm can be carried out in an additional frequency band (an approach known as *out-band* D2D communication [AWM14]) or in the spectrum considered for cellular communication (also known as *in-band* D2D communication [AWM14]). In the latter case, cellular transmissions can be separated from direct transmissions by assigning disjoint subbands to the two communication modes. This approach is known as *overlay* D2D communication [AWM14]. Under favorable conditions, however, the localized nature of direct links allows for the reuse of radio resources which are used for cellular transmissions at the same time. In this manner, D2D communication enables the so-called *reuse gain* [FDM+12], hinting at the increased overall spectral efficiency of the system. This is referred to as *underlay* D2D communication [AWM14] and is, for the above reason, the most worthwhile form of network-controlled direct communication. Figure 1.2 shows a graphical representation of the different spectrum utilization options for D2D communication.

With its above mentioned gains, D2D communication establishes an efficient RAN offloading alternative (for local traffic) and is, therefore, expected to be an integral part of 5G networks [MFP+14]. As such, it will not only contribute towards serving the ever increasing mobile data traffic originating from established applications (e.g., mobile video streaming), but can also serve as an enabler for a wide variety of novel proximity-based services.

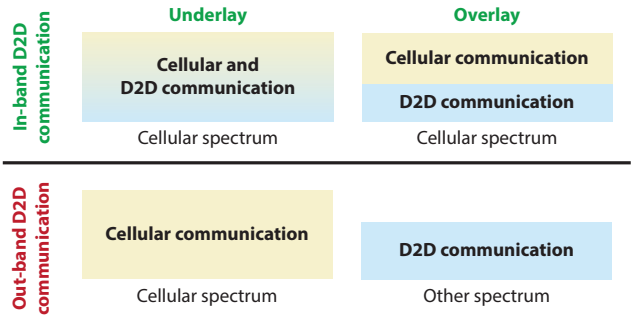

Figure 1.2: Graphical representation of the spectrum utilization in in-band and out-band D2D communication.

1.1.2 Automotive Applications

Among others, the recently explored novel services include automotive applications [FTP+13, CYS15]. The improvement of road traffic safety and efficiency presents the greatest challenge in the transportation of people and goods. Cooperative Intelligent Transport Systems (C-ITS) [ETS13] are envisioned to contribute towards this goal. Cooperative driving applications, such as platooning [JLW+16] or highly automated driving [KTT+02], can reduce travel time, fuel consumption, and CO_2 emissions. Safety services based on the exchange of critical information between vehicles and infrastructure can aid drivers by enhancing their perception horizon beyond the physical limitations of a human being. This aid may include alerting the driver of potential road hazards (e.g., end of a traffic jam on the highway or road damage) as well as actively supporting him in avoiding potential accidents (e.g., by means of automated braking). Moreover, the cooperation between vehicles and vulnerable road users, such as pedestrians or cyclists, may improve traffic safety even further. For example, using mobile communications devices (i.e., smartphones or smartwatches) to announce the approach of a pedestrian from behind a corner with obstructed vision could help prevent potential accidents.

The exchange of messages between vehicles and consumer electronics (CE) devices, however, requires a common communications platform. Such vehicle-to-vehicle, vehicle-to-infrastructure and vehicle-to-device (collectively, V2X) communication could be carried out in cellular networks, as modern vehicles and CE devices already have built-in cellular modules. However, even the most recent Long Term Evolution (LTE) deployments have been shown to be incapable of satisfying the stringent Quality of Service (QoS) requirements of C-ITS applications [LBFM12]. In particular, these requirements may include near 100% availability of the communication links, up to 99.999% reliable transmissions, and E2E latency as low as 5 ms for packets of up to 1600 bytes in the 5G era [FTP+13]. The strongly localized nature of V2X-based services (i.e., the exchanged messages are only relevant for road users in a relatively small area), in conjunction with the previously mentioned gains of underlay D2D communication, can enable support for C-ITS applications in future 5G cellular networks. The ambition of this work is to contribute towards this vision.

1.2 Motivation

Quite some effort has been spent recently on studying and shaping the D2D paradigm in the context of future 5G cellular networks. Support for C-ITS applications with their stringent

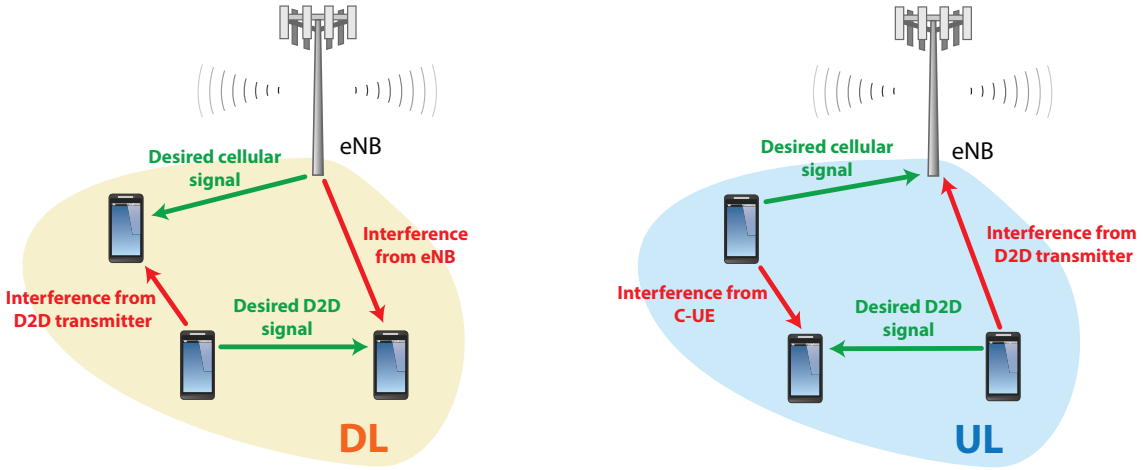

(a) DL resource reuse

(b) UL resource reuse

Figure 1.3: Cross-interference caused in a cellular network with a D2D underlay considering the reuse of DL and UL radio resources.

QoS requirements and the high mobility of vehicles, however, pose a significant challenge. Radio Resource Management (RRM), which plays a key role in the performance of wireless systems, is particularly affected. Although enabling high transmission reliability and timely transmission opportunities, given the stochastic nature of wireless channels, is a complicated task on its own, the complexity of RRM in the context of underlay D2D communication is even higher due to the *cross-interference* between cellular and D2D transmissions. Depending on which radio resources are to be reused for direct communication, two different models need to be considered. A D2D transmitter utilizing DL resources causes interference at the respective receiving cellular UE (C-UE[1]), while the D2D receiver is disturbed by the signal transmitted by the respective eNB (see Figure 1.3a). In the reciprocal case, the D2D transmitter disturbs the UL signal at the eNB, while the D2D receiver suffers from interference due to the respective transmitting C-UE (see Figure 1.3b). This cross-interference can jeopardize the network performance and, hence, needs to be managed carefully.

The RRM problem has been investigated extensively in this regard. For example, [JKR+09] proposes a resource allocation scheme that relies on measuring the interference levels caused by the active C-UEs (in the UL) and eNBs (in the DL) at each potential D2D receiver. This data, along with information about the quality of the cellular links, is gathered at the eNBs to accumulate complete Channel State Information (CSI). The resource allocation for all of the users in the system is then determined (under consideration of the CSI) as the solution of an optimization problem (OP) that maximizes the throughput of the D2D underlay while maintaining a target level of throughput in the primary cellular network.

A simpler scheme with a similar objective has been proposed in [ZHS10]. In this work, radio resources are first allocated to each C-UE in conventional fashion according to the network operator's preferences. In a second step, complete CSI is leveraged to determine the respective potential D2D transmitter expected to cause the least interference to each cellular link. In the case that UL resources are to be reused, this is the one with the weakest channel to the

[1]Hereinafter, UEs that communicate with a eNB (i.e., in cellular manner) will be referred to as C-UEs.

eNB. Conversely, when reusing DL resources, it is the potential D2D transmitter that has the weakest channel to the potentially affected C-UE that needs to be considered. Reuse of the resources allocated for cellular communication in the D2D underlay is only allowed if the additional interference at eNB, C-UE and D2D receiver, respectively, remains below a certain threshold. Otherwise, D2D communication in the resources allocated to a specific cellular link is prohibited.

Another approach to maximize the total system throughput is proposed in [XSH+12], where DL radio resources are allocated to users according to an iterative combinatorial auction. In the auction, all the resources are considered to compete as bidders, while the data packages of D2D transmitters are auctioned off as goods in each round. This is achieved by a non-monotonic descending price auction algorithm which converges in a finite number of iterations.

The main aim of the above mentioned schemes and many other alternative approaches available in the literature (see, e.g., [PLW+09, DYRJ10, MLPH11] and the the survey in [AWM14]) is to maximize the total network throughput while preserving the performance of cellular communication. As a consequence, the D2D underlay is utilized in opportunistic fashion and lacks QoS support. Therefore, such schemes are not suited for automotive applications. At the start of this work, only a limited number of contributions which consider QoS requirements was available. For example, a network-level OP for jointly optimizing mode selection (i.e., selecting between direct links that reuse DL or UL resources, or cellular communication), resource allocation and power assignment has been introduced in [BFA11]. Again building upon complete CSI knowledge, this approach minimizes the total transmit power while satisfying the QoS requirements of individual users. Due to its extreme complexity, however, it is not feasible in practical implementations.

Motivated by this state of the art, the goal of this work is to deliver feasible solutions to the problem of RRM for underlay D2D communication in future 5G networks, with focus on satisfying the strict QoS requirements of C-ITS applications. Details on the contributions to this end can be found in the following section. For the sake of completeness, it should be further mentioned that the research community's interest in QoS-constrained underlay D2D communication has been growing in the meantime. Some of the contributions that emerged in parallel to this work even target automotive applications as well [CYS15, POC+15]. Resource allocation with focus on V2X communication has been explored in [SSB+14, XWW+14, SSB+16, SYSB16], while a scheme for general purpose QoS-aware D2D communication is proposed in [FLY+16], among others.

1.3 Contributions and Outline

The wireless communications network of interest in this work is introduced in details in Chapter 2. Hereby, a system model for a cellular network with vehicular D2D underlay is established, considering the properties of V2X communication and wireless channels. Moreover, the QoS requirements of C-ITS applications are transformed to Key Performance Indicators (KPIs) to be used in the subsequently presented RRM schemes and their performance evaluation. In particular, these parameters include Signal-to-Interference-and-Noise-Ratio (SINR), the probability that a fixed SINR target is not met, E2E transmission delay, and packet transmission probability.

Based on this system model, the asymptotic per-user transport capacity of the considered wireless network is analyzed in Chapter 3. This is done under the consideration of two resource

reuse strategies - one building upon complete knowledge over the channel conditions (i.e., CSI-based), and one building upon the spatial separation of users (i.e., location-based). The results of this study are published in [BSF15b] and indicate that a D2D underlay may be able to support the load of V2X communication. However, intelligent RRM is essential in order to satisfy the stringent QoS requirements of C-ITS applications in an efficient manner.

One such RRM scheme is the subject of Chapter 4. Hereby, starting from the assumption of complete CSI knowledge, the problem of resource allocation is formulated as the minimization of the spectral radius (i.e., the supremum of the absolute eigenvalues) of a square matrix which jointly describes the SINR requirements of each user and the cross-interference due to the reuse of radio resources in D2D underlay manner. Due to the very high complexity of this combinatorial problem, a practical heuristic algorithm is also derived. The results of this work are published in [BSF15a]. Moreover, as complete CSI knowledge is not available in realistic scenarios due to the stochastic nature of wireless channels, the scheme is further developed to accommodate for channel uncertainty. In other words, the scheme is evolved to consider Channel Distribution Information (CDI), i.e., knowledge over the distribution of the channel gains in the system, but not their instantaneous realizations. In such a case, the above mentioned spectral radius becomes a random variable and is difficult to work with. Hence, the initial CSI-based scheme is evolved to consider a deterministic upper bound thereof. Based on this approach, a CDI-based Resource Allocation Algorithm (CDI-bRAA) is developed which bounds the probability with which the SINR targets of the allocated users are not met. The results of this work are published in [BSF16c].

As the acquisition of CSI or CDI may be too costly or even infeasible in the considered cellular network with vehicular D2D underlay, Chapter 5 studies an alternative, location-based, RRM approach for it. This Location Dependent Resource Allocation Scheme (LDRAS) relies on prior knowledge over the radio propagation conditions in the considered deployment. Based on this, each cell is divided into disjoint zones according to criteria that enable the reuse of radio resources for cellular and D2D communication between zones with sufficient spatial separation. A graph coloring approach ensures that the experienced interference by all users is kept at acceptable levels. The initial concept of LDRAS and criteria for its application to an isolated cell with homogeneous non-fading channels are part of the author's master's thesis [Bot13] and are also published in [BKKF14]. In this work, LDARAS is evolved further to consider multi-cell deployments as well as heterogeneous radio propagation environments and the stochastic nature of wireless channels. Hereby, the criteria for the zone topology design are extended to consider inter-cell (cross-) interference and channel uncertainty. The results of this work are published in [BKKF15] and [BSF15a]. Moreover, the definition of the zone topology is formalized by means of hierarchical clustering (as opposed to the initial design by hand) and the performance of LDRAS in heterogeneous propagation environments is improved by means of optimized selection of its control parameters (as opposed to the initial selection by intuition). The results of this work were published in [BSF16b].

Chapter 6 focuses on the performance evaluation of the introduced RRM schemes with respect to the above mentioned KPIs. This evaluation is done based on extensive system level simulations considering a typical urban network deployment. Hereby, a selected state-of-the-art algorithm is used as a reference in order to demonstrate the need for QoS-aware RRM in the considered cellular network with vehicular D2D underlay. In addition, the signaling and management overhead (SMOH) associated with CDI-bRAA and LDRAS is assessed in order to enable a fair comparison between the two. The results of this performance study are published in part in [BSF16a] and in all of the above mentioned publications, and indicate

that CDI-bRAA holds an advantage over LDRAS in scenarios with a high load in the D2D underlay and low load in the cellular network. On the contrary, LDRAS is preferred under high cellular load and medium load in the D2D underlay.

Finally, Chapter 7 summarizes the conclusions of this work and briefly discusses possible future research topics in the context of vehicular D2D communication.

The effort invested in the above listed contributions has also enabled fruitful collaborations on related topics, the results of which are not part of this work. A comparative performance study of ad-hoc and network-controlled RRM for C-ITS applications considering LDRAS (as the network-controlled scheme) is the topic of [CMB+18]. The results thereof show that LDRAS is able to increase the number of users experiencing high QoS as compared to the currently preferred approach in vehicular ad-hoc networks, i.e., IEEE 802.11-2012 [IEE12]. An improvement over this standard that allows vehicles to communicate with a deterministic medium access delay in ad-hoc manner based on out-band D2D communication is proposed in [GEGSBS16]. Another contribution towards the improvement of the performance of vehicular ad-hoc communication is presented in [CMM+18]. Here, a clustering approach is considered to enable more efficient message distribution in a wide area. Furthermore, [HED+16] proposes a novel unified radio frame structure and Medium Access Control (MAC) protocol to enable the communication between users operating under the ad-hoc or network-controlled paradigm, respectively. Finally, the system level simulator developed for the purposes of this work and a preliminary version of CDI-bRAA are used for the comparative evaluation of an akin RRM scheme for vehicular D2D communication in [SBS+16].

Chapter 2

System Model and Notation

2.1 Communications Scenario

As motivated in the previous chapter, the wireless system of interest in this work consists of a future cellular network with a D2D underlay, which is meant to serve as an enabler for C-ITS applications. Figure 2.1 illustrates this setup. For the sake of simpler arguments and notation, hereinafter we consider said D2D underlay to be used exclusively for V2X communication, although a wide variety of additional applications can be adopted seamlessly. In this regard, we use D2D communication and V2X communication as synonyms throughout this work. Moreover, we refer to UEs which communicate in direct manner as vehicular UEs (V-UEs), although this can apply to CE devices as well as vehicles. We use the term *primary network* as synonym for the cellular part of the considered two-tier network. The accent "primary" refers to the fact that the cellular service should not be significantly degraded due to the D2D underlay.

Let $M \in \mathbb{N}_0$ denote the total number of transmissions (also, users or transmitters) that are to be served by this system at a given time instance, either in the DL or the UL. Without loss of generality, we consider the first $K \in \mathbb{N}_0, K \leq M$ transmissions to be between a C-UE and its serving eNB (i.e., cellular transmissions). Hereby, let $C \in \mathbb{N}_0$ denote the number of eNBs or, alternatively, the number of cells deployed over the area of interest. As the messages in the context of C-ITS applications are considered to be relevant for all traffic participants within a certain range $d \in \mathbb{R}_+$ around the source, we label the remaining $L = M - K$ transmissions as broadcast transmissions from a V-UE to its relevant neighboring V-UEs (i.e., the ones within a range of d). Each such broadcast transmission can also be considered as an ensemble of unicast D2D links (all of which using the same transmission configuration in terms of modulation and coding, and transmit power), where the overall performance is determined by the worst-case receiver. Hence, the objective of RRM in the considered wireless system is to guarantee a certain performance level on these worst-case D2D links, as well as on the cellular links. This can be achieved by appropriate allocation of the available radio resources to the M users and appropriate transmit power assignment. In this regard, we consider the radio resources to be organized in Resource Blocks (RBs). Following the Orthogonal Frequency-Division Multiple Access (OFDMA) structure established in LTE [3GP10], each RB consists of a group of 12 subcarriers in the frequency domain and 14 symbols in the time domain, or 168 Resource Elements (REs) in total. Figure 2.2 illustrates this structure. A RB is considered to be the minimal amount of radio resources which can be allocated to a given user in each Transmission

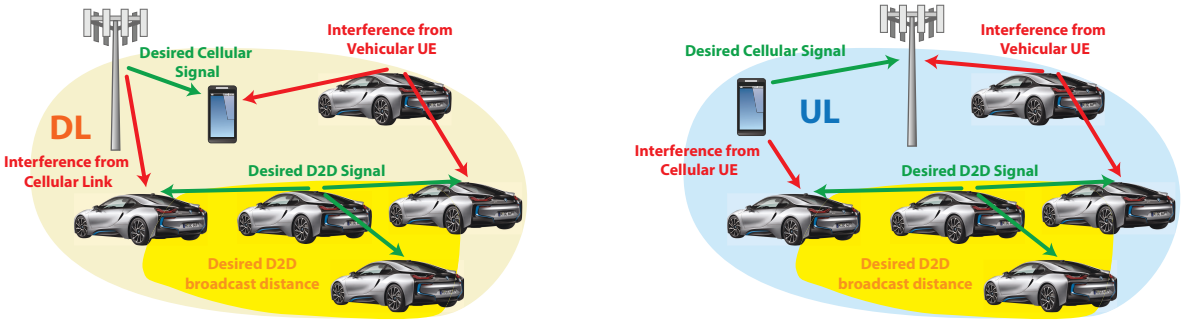

(a) DL resource reuse

(b) UL resource reuse

Figure 2.1: Cellular network with vehicular D2D underlay.

Time Interval (TTI). Each RB is allocated to at most one user served by a given eNB in a given TTI in order to avoid inter-user interference. For the purpose of network management in LTE, the collection of every 10 TTIs is grouped into a frame in order to enable functions such as synchronization between the RAN and UEs, cell (re-)selection, etc. We disregard these system functions (and, correspondingly, the grouping of radio resources in frames) in the context of this work as they are outside its scope. We assume perfect synchronicity among all communicating network nodes and perfect cell selection (i.e., every UE is always served by the eNB with the strongest signal). Moreover, we consider the RAN to operate in Frequency Division Duplex (FDD), where DL and UL transmissions take place in parallel (in the time domain) but in different parts of the spectrum. In the context of this work, the role of RRM is to determine how many and which RBs may be used by each user in the system. In contrast to the OFDMA principle, however, V-UEs are allowed to simultaneously transmit their localized broadcast messages in RBs used for cellular communication.

Each transmission (over all of the allocated RBs in a given TTI) is considered to be subject to sum power constraints, where $P_k \in \mathbb{R}_+$ denotes the total transmit power available to user k. Let $S \in \mathbb{N}_0$ denote the total number of available RBs in the considered wireless system, either in the DL or the UL. Hence, the power constraints can be expressed as

$$\sum_{s=1}^{S} p_k^{(s)} \leq P_k, \tag{2.1}$$

where $p_k^{(s)} \in \mathbb{R}_{\geq 0}$ stands for the transmit power of user k in RB $s \in \mathcal{S} := \{1, \ldots, S\}$.

2.2 Interference Channel Model

Under the D2D paradigm, multiple users (within the coverage area of a given eNB) may be allowed to reuse the same RB. This, in conjunction with the broadcast nature of the direct transmissions, leads to a complex interference environment. Figure 2.3 illustrates the channel model used to describe the interference environment in the context of this work. Any given RB $s \in \mathcal{S}$ is associated with a flat fading channel on all links and $h_{kl}^{(s)} \in \mathbb{C}, k, l \in \mathcal{M} := \{1, \ldots, M\}$, denotes the complex-valued channel coefficient for the link from transmitter k to the (worst-case) receiver associated with user l. Hereby, we consider a Single-Input Single-Output (SISO)

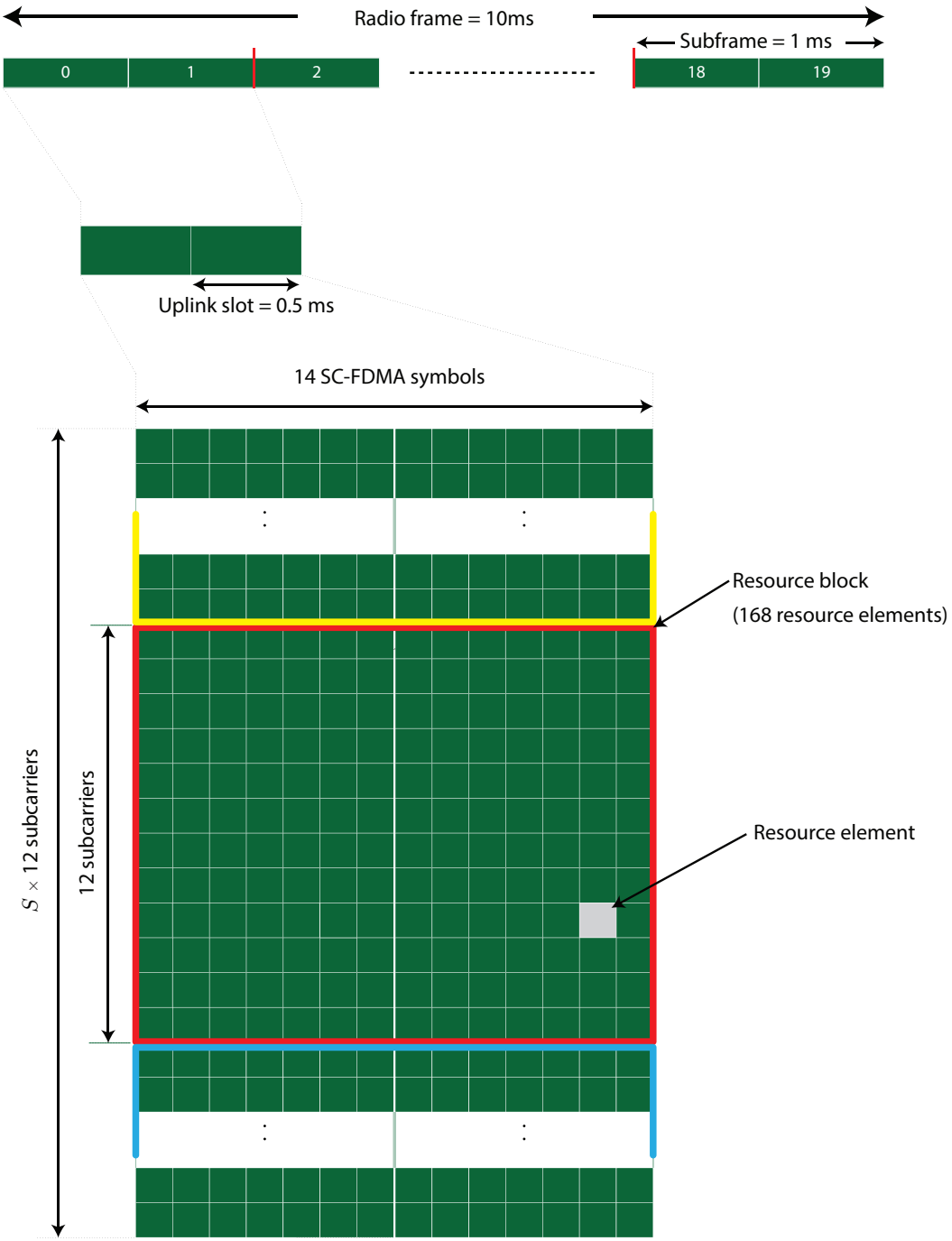

Figure 2.2: LTE frame structure type I and UL resource grid (cf. [3GP10].

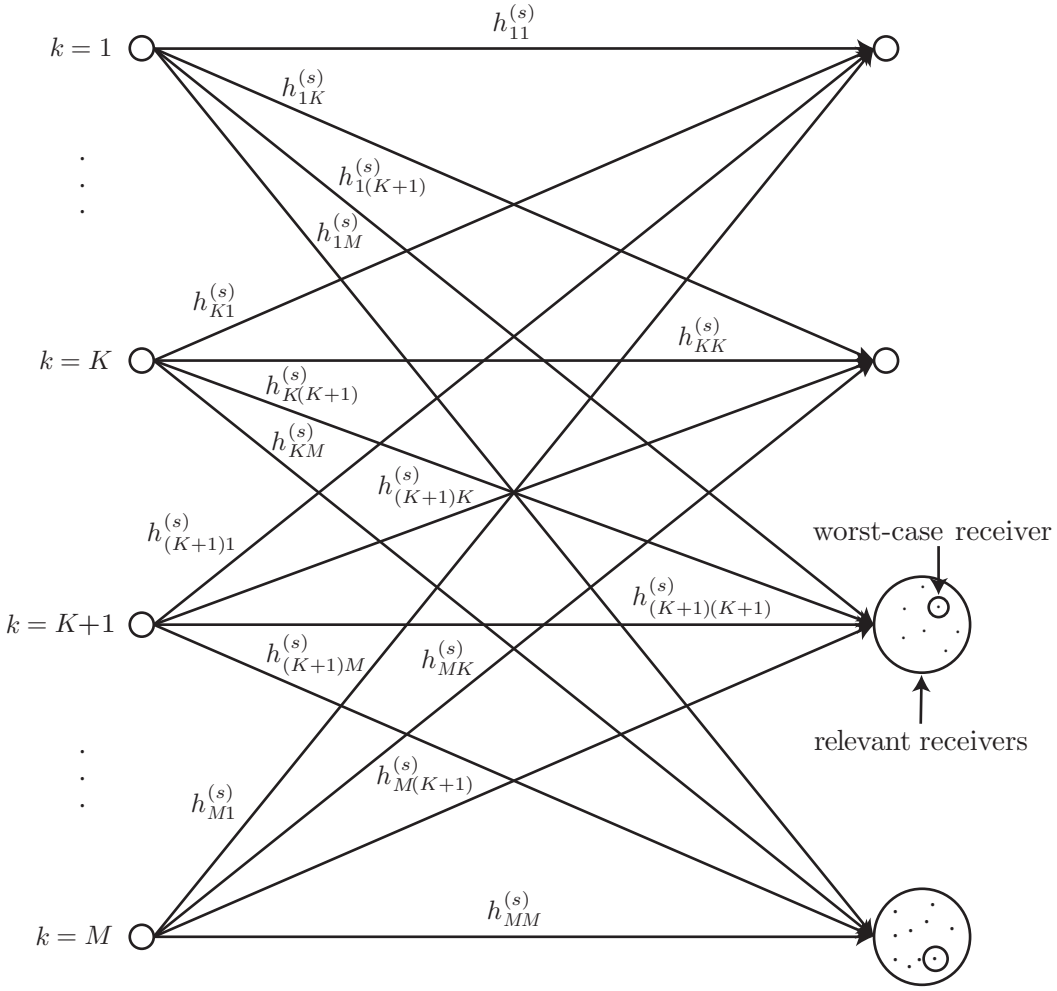

Figure 2.3: Interference channel model.

system, i.e., each transmission in the two-tier wireless network is transmitted and received by a single antenna, respectively. By this definition, $h^{(s)}_{kk}$ characterizes the channel (associated with RB s) from user k to its intended (worst-case) receiver, while $h^{(s)}_{kl}, k \neq l$, characterizes the respective (interference) channel from user k to the intended (worst-case) receiver of user l. The channel gains $|h^{(s)}_{kl}|^2 = d_{kl} z^{(s)}_{kl}$ are considered to be composed of a constant distance/location-dependent component $d_{kl} \in \mathbb{R}_{\geq 0}$ and a random fading component $z^{(s)}_{kl} \in \mathbb{R}_{\geq 0}$ following some distribution.

Note that the (worst-case) receiver of cellular transmissions (i.e., $\forall k \leq K$) is clearly defined as the single intended receiver, i.e., the serving eNB in the case of a UL transmission (cf. Figure 2.1b), or the respective C-UE in the case of a DL transmission (cf. Figure 2.1a). Hence, the channels $h^{(s)}_{lk}$, $\forall s \in \mathcal{S}, l \in \mathcal{M}, k \leq K$, are fixed. In the case of V2X communication, however, a broadcast transmission may be received by multiple V-UEs. In this regard, let $\mathfrak{R}(k)$ denote the set of relevant receivers associated with transmitter k. For $k > K$, the worst-case receiver of the bunch is likely to be determined by the experienced interference and depends on the simultaneously transmitting interferers. Hence, the channels $h^{(s)}_{lk}$, $\forall s \in \mathcal{S}, l \in \mathcal{M}, k > K$,

are defined in fuzzy fashion in the considered channel model. Figure 2.4 illustrates this aspect for the case of UL resource reuse. Consider the source V-UE $\mathfrak{s}$ to broadcast a message to the destinations $\mathfrak{d}_1$, $\mathfrak{d}_2$, and $\mathfrak{d}_3$ in its proximity, using RB s. Moreover, consider this source to be denoted as the transmitter $k > K$ under the established convention with $\mathfrak{R}(k) = \{\mathfrak{d}_1, \mathfrak{d}_2, \mathfrak{d}_3\}$. First, assume that there are no interferers in the environment. Hence, the SINR at each destination is determined by the respective channel gains and noise powers. Assuming that the lowest SINR is experienced at $\mathfrak{d}_2$, the relevant worst-case D2D link associated with transmitter k is formed by the pair $\mathfrak{s}$-$\mathfrak{d}_2$ and $h_{kk}^{(s)}$ refers to this respective channel.

Now assume that only the C-UE $\mathfrak{c}$ is simultaneously active in the same resources as $\mathfrak{s}$. For the sake of this example, assume that it would cause the strongest interference to the closest destination $\mathfrak{d}_1$ and that this interference is so strong that $\mathfrak{d}_1$ experiences the lowest SINR out of the three destinations. Hence, the relevant worst-case D2D link associated with transmitter k is formed by the pair $\mathfrak{s}$-$\mathfrak{d}_1$ and $h_{kk}^{(s)}$ refers to this respective channel. Moreover, the interference channels $h_{lk}^{(s)}$, $\forall l \in \mathcal{M} \setminus k$, are also defined with respect to the destination $\mathfrak{d}_1$.

Alternatively, assume that instead of $\mathfrak{c}$, a second V-UE $\mathfrak{v}$ is simultaneously active in the same resources as $\mathfrak{s}$. In this case, the closest destination suffering from the strongest interference is $\mathfrak{d}_2$. Hence, the relevant worst-case D2D link associated with transmitter k is formed by the pair $\mathfrak{s}$-$\mathfrak{d}_2$ and $h_{kk}^{(s)}$ refers to this respective channel. Similarly, the interference channels $h_{lk}^{(s)}$, $\forall l \in \mathcal{M} \setminus k$, are also defined with respect to the destination $\mathfrak{d}_2$.

Finally, assume that both $\mathfrak{c}$ and $\mathfrak{v}$ are simultaneously causing interference. The worst-case receiver is now determined by the sum-interference and might differ from the ones suffering the most from individual contributions. In this example, assume that $\mathfrak{d}_3$ is the destination experiencing the strongest sum-interference and lowest SINR. Hence, the relevant worst-case D2D link associated with transmitter k is formed by the pair $\mathfrak{s}$-$\mathfrak{d}_3$ and $h_{kk}^{(s)}$ refers to this respective channel. Correspondingly, the interference channels $h_{lk}^{(s)}$, $\forall l \in \mathcal{M} \setminus k$, are also defined with respect to the destination $\mathfrak{d}_3$. With this example it is clear that the composition of the relevant channels $h_{lk}^{(s)}$, $\forall l \in \mathcal{M}, k > K$, depends on the resource allocation and the respective transmit power assignment. Hence, a formal definition for the selection of the worst-case receiving V-UEs will be presented as a part of the respective RRM scheme discussions in Chapter 4 and Chapter 5.

A similar situation arises in the case of DL resource reuse, with the exception that the C-UE $\mathfrak{c}$ is substituted by an eNB. In order to avoid repetitions, hereinafter we present concepts affected by the reuse of radio resources in the D2D underlay on the example of UL resource reuse. Additional clarifications are provided for the case of DL resource if required.

2.3 Key Performance Indicators

As mentioned in Section 1.1.2, C-ITS applications have especially stringent QoS requirements with regards to the availability of radio resources, reliability of transmissions, and the transmission delay. First, we translate the said requirements to appropriate KPIs, in order to use them in the definition of RRM schemes and their performance evaluation.

A reasonable assumption widely used in practice is that the reliability requirement of transmission k is fulfilled if it is received with a SINR of at least a predefined threshold $\gamma_k \in \mathbb{R}_+$ [SWB09]. The following well established model is used in the context of this work in order to

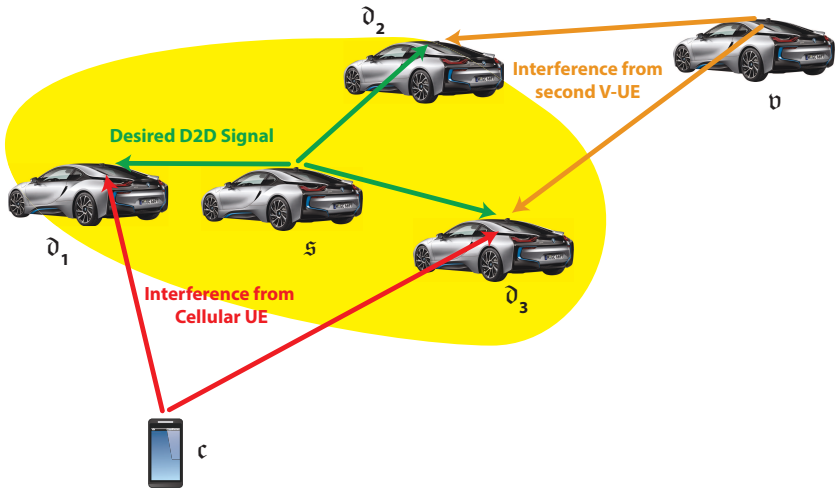

Figure 2.4: Interference caused to receiving V-UEs as a result of the reuse of UL radio resources by a C-UE and an additional transmitting V-UE.

determine said SINR value at the receivers associated with the respective transmission:

$$\mathrm{SINR}_{kr}^{(s)} = \frac{|h_{kk}^{(s)}|^2 p_k^{(s)}}{\sum\limits_{l \in \mathcal{M} \setminus k} |h_{lk}^{(s)}|^2 p_l^{(s)} + \eta_{kr}^{(s)}}, \; \forall k, l \in \mathcal{M}, s \in \mathcal{S}_k, r \in \mathfrak{R}(k). \tag{2.2}$$

Hereby, we consider the SINR to be a function of the users' transmit powers $p_k^{(s)}$ and the RB allocation, where $p_k^{(s)} = 0$ if user k is not allocated to transmit in RB s. Moreover, $\mathcal{S}_k \subseteq \mathcal{S}$ denotes the set of RBs allocated to user k and $\eta_{kr}^{(s)}$ denotes the noise power at the respective receiver $r \in \mathfrak{R}(k)$ in the considered bandwidth.

We refer to the resulting condition $\mathrm{SINR}_{kr}^{(s)} \geq \gamma_k, \forall k \in \mathcal{M}, s \in \mathcal{S}_k, r \in \mathfrak{R}(k)$, as the *SINR requirement* of user k. Considering the stochastic nature of wireless channels, it is not possible to guarantee that said SINR requirement is fulfilled under all channel realizations, although it might be fulfilled under most. Hence, we adopt a more practical interpretation of the reliability requirements in this work, where we consider them to be satisfied if

$$\Pr\left(\mathrm{SINR}_{kr}^{(s)} < \gamma_k\right) \leq \upsilon_k^{\mathrm{out}}, \; \forall k \in \mathcal{M}, s \in \mathcal{S}_k, r \in \mathfrak{R}(k). \tag{2.3}$$

Here, $\upsilon_k^{\mathrm{out}}$, denotes an acceptable outage probability (i.e., probability that the SINR requirement is violated) for transmission k. The criterion in (2.3) builds the foundation of the RRM schemes developed in this work.

The transmission of larger packets often requires more than one RB to be completed. Moreover, larger transmission bandwidths can be leveraged to facilitate a coding gain. Hence, another important KPI is the *effective SINR* over the entire used bandwidth. We use the exponential effective SINR mapping [AATK13] for the performance evaluation of the RRM schemes developed in this work , where

$$\mathrm{SINR}_{kr}^{\mathrm{eff}} = -\beta_{\mathrm{MCS}} \ln\left(\frac{1}{S_k} \sum_{s \in \mathcal{S}_k} \exp\left(-\frac{\mathrm{SINR}_{kr}^{(s)}}{\beta_{\mathrm{MCS}}}\right)\right), \; \forall k \in \mathcal{M}, r \in \mathfrak{R}(k). \tag{2.4}$$

Here $S_k = |\mathcal{S}_k|$ denotes the respective set's cardinality or, in other words, the number of allocated RBs for transmission k. The parameter β_{MCS} is a calibration margin and depends on the chosen Modulation and Coding Scheme (MCS). It is chosen such that the block error probability for the individual RBs matches the block error probability for the effective SINR in an Additive White Gaussian Noise (AWGN) channel [AATK13]. In this regard, we use the distribution of $\text{SINR}_{kr}^{\text{eff}}$ to characterize the transmission reliability.

Furthermore, the E2E latency plays an important role in the context of C-ITS applications. Although additional delay sources (e.g., processing delay at the application layer) may affect their performance, we only consider the E2E transmission delay δ_k^{E2E}. Hereby, it consists of the time needed for the actual packet transmission δ_k^{Tx} and the delay associated with the SMOH needed to obtain resources for said transmission δ_k^{SMOH}, i.e., $\delta_k^{\text{E2E}} = \delta_k^{\text{SMOH}} + \delta_k^{\text{Tx}}$, $\forall k \in \mathcal{M}$. In other words, we define the E2E transmission delay as the time between the generation of a packet and its complete transmission. We use the distribution of this metric to characterize the performance of the proposed RRM schemes.

In this regard, we consider packets whose transmission cannot start within a predefined delay budget (e.g., due to unavailability of RBs) to be no longer relevant and drop them. We use the ratio of the total dropped and generated packets to characterize the performance of the proposed RRM schemes with respect to the availability of radio resources for V2X transmissions.

2.4 Notational Convention

We use the following notation throughout this work: The special set of natural numbers including zero is denoted as $\mathbb{N}_0 = \mathbb{N} \cup \{0\}, \mathbb{N} = \{1, 2, \dots\}$, while the set of real positive numbers is denoted as $\mathbb{R}_+ = (0, +\infty)$, and the set of positive real numbers and zero is denoted as $\mathbb{R}_{\geq 0} = [0, +\infty)$. Further sets are denoted by capital calligraphic letters, e.g., $\mathcal{M}$, with $|\mathcal{M}|$ denoting the respective set's cardinality. Capital mathematical fraktur letters, such as $\mathfrak{R}$, denote auxiliary sets, while small mathematical fraktur letters, such as $\mathfrak{v}$, denote auxiliary scalars used to describe the particularities of a concept. Small and capital letters, such as k and K, represent scalars while small boldface letters, e.g., $\mathbf{p}$, designate column vectors, and capital boldface letters, e.g., $\mathbf{\Gamma}$, denote matrices. Vector inequalities are considered element-wise. The superscript $(\cdot)^{\text{T}}$ stands for the matrix transposition, while the superscript $(\cdot)^{-1}$ denotes the matrix inversion operation. The Hadamard product of two arbitrary matrices $\mathbf{X}$ and $\mathbf{Y}$ of the same size is denoted as $\mathbf{X} \circ \mathbf{Y}$ and $\text{Tr}(\mathbf{Z})$ denotes the trace of a given square matrix $\mathbf{Z}$. Moreover, $\mathbf{1}$ stands for the all-ones column vector of appropriate size, depending on the context in which it appears. Similarly, $\mathbf{I}$ denotes the identity matrix of appropriate size, depending on the context in which it appears. Moreover, the probability of a random event E holding true is denoted as $\Pr(E)$. For the reader's convenience, a list of the symbols used throughout this work is provided in Appendix A.

Chapter 3

Transport Capacity

The current chapter discusses the capacity of the two-tier wireless network of interest in this work (cf. Section 2.1). In particular, we analyze the asymptotic scaling of the mean per-user transport capacity (MPUTC), both for the primary network and the vehicular D2D underlay network. This metric characterizes the amount of data that can be transferred in a certain time interval over a given distance in the network and has the physical dimension *bit per meter and second*. The analysis is carried out both from the perspective of a RRM approach building upon CSI knowledge, and an approach building upon knowledge about the location of terminals. We primarily study the influence of cross-interference between the users in the primary network and the D2D underlay and its implications on the system design. The results of this study are published in [BSF15b] and indicate that careful system design is essential in order to enable additional D2D-based applications (e.g., automotive ones) in the next-generation cellular networks. Notably, the trend of network infrastructure densification and the prioritization of cellular communication over direct links might hinder D2D communication. These results serve as motivation for the contributions presented in the following chapters.

3.1 Preliminaries and Related Work

The capacity of wireless networks has had the attention of the scientific community for quite some time. Among many other significant contributions, Gupta and Kumar investigate the capacity of static ad-hoc networks and show that (even in an optimal case) the per-user throughput diminishes to zero with an increasing number of considered users [GK00]. Zemlianov and de Veciana demonstrate that the support through network infrastructure can help reduce the rate at which the per-user throughput diminishes [ZdV05], while Grossglauser and Tse show that, under the assumption of loose packet delay constraints, the per-user throughput in such networks can be increased dramatically by exploiting node mobility [GT01]. The comprehensive surveys in [WAJ10, LS14] summarize further state-of-the-art results for various wireless network deployments. Such results are often referred to as *Capacity Scaling Laws* and the methods used for obtaining them can be described as *Capacity Scaling Framework (CSF)*.

The two-tier cellular network of interest in this work represents a unique constellation. The CSF can nevertheless be adapted in order to assess its asymptotic MPUTC.

Assumption 3.1 (The network domain is a unit area disk)**.** *Under the CSF, the network domain is modeled as a unit area disk (i.e., a disk with a radius of* $\frac{1}{\sqrt{\pi}}$*), where the* C *eNBs*

are optimally placed such that the mean area a eNB has to provide coverage for is minimized.

Assumption 3.2 (Static network)**.** *Any benefits from exploiting mobility (cf. [GT01]) are disregarded in the context of this work, as the envisioned safety-related services in the D2D underlay are associated with very stringent packet delay requirements and the C-UEs only communicate with their respective serving eNB. Hence, we consider the network to be static at each transmission instance.*

Assumption 3.3 (Uniform user distribution)**.** *For the sake of simplicity, assume that the C-UEs and V-UEs are uniformly distributed within the coverage area of an eNB. Approximating the coverage area of each eNB as a disk of radius $r(C)$ (depending on the number of deployed eNBs), the user coordinates follow the distribution $\left(r(C)\sqrt{U_1}\cos 2\pi U_2, r(C)\sqrt{U_1}\sin 2\pi U_2\right)$, where U_1 and U_2 are independent uniformly distributed random variables on the interval* $[0,1]$*[FLE87, p. 84].*

In addition, the study of the MPUTC considers a more general description of the available radio resources: as a bandwidth of $W \in \mathbb{R}_+$ (in the frequency domain) and a transmission interval of $T \in \mathbb{R}_+$ (in the time domain). This is done for the sake of simpler notation and is well justified, as it has been shown in [GK00] that introducing additional channel structure (e.g., organizing the radio resources into RBs) does not change the asymptotic behavior of wireless systems. We consider two fundamentally different RRM approaches for D2D-enabled cellular networks in the analysis: On the one hand, we investigate the case of resource allocation based on exact knowledge about the channel conditions in the network under, what is hereinafter referred to as, the *CSI-based model*[1]. On the other hand, we consider resource allocation based on sufficient spatial separation between UEs that reuse the same resources in the so called *location-based model*[2]. The following sections are devoted to the asymptotic case and derive upper bounds for the MPUTC in the primary network $\lambda \in \mathbb{R}_+$ and in the D2D underlay $\lambda' \in \mathbb{R}_+$ under the two models. A performance comparison and analysis of the advantages and disadvantages of these two RRM paradigms with regards to a realistic deployment scenario is shown based on the example of practical schemes developed in this work (cf. Chapter 4 and Chapter 5) in Chapter 6.

3.2 CSI-based RRM

Some simplifications to the system model are necessary in order to apply the CSF to the scenario of interest. First, let $p_k \in \mathbb{R}_{\geq 0}$ denote the transmit power of user k under the simplified channel structure (i.e., without the organization in RBs) and let all of the M active users utilize all of the available radio resources. Moreover, let $\mathbf{x}_k$ denote the location of transmitter k and $\mathbf{x}_{\tilde{r}(k)}$ denote the location of its worst-case receiver $\tilde{r}(k) \in \mathfrak{R}(k)$, in some coordinate system with a defined distance metric. The two dimensional space and the Euclidean distance defined on it as $|\mathbf{x}_k - \mathbf{x}_l| = \sqrt{(x_{k,1}-x_{l,1})^2 + (x_{k,2}-x_{l,2})^2}$ [DD16, p. 94] are considered for the purposes of this study. In the context of the CSF, we can simplify the SINR model by setting $|h_{kl}|^2 = |\mathbf{x}_k - \mathbf{x}_{\tilde{r}(l)}|^{-\alpha}$, where $\alpha \in [2, +\infty)$ denotes an environment-dependent

[1] Note that similar models are referred to as *physical models* in the literature. This substitution is necessary to better illustrate the connection between the derived results and the RRM schemes presented in Chapter 4.

[2] Note that similar models are referred to as *protocol models* in the literature. This substitution is necessary to better illustrate the connection between the derived results and the RRM scheme presented in Chapter 5.

path loss exponent. Furthermore, let $\gamma_{\mathrm{C}} \in \mathbb{R}_+$ and $\gamma_{\mathrm{D2D}} \in \mathbb{R}_+$ denote a certain targeted SINR for cellular and D2D communication, respectively, and let $\eta_{kr} = \eta$, $\forall k \in \mathcal{M}, r \in \mathfrak{R}(k)$.

Assumption 3.4 (CSI-based model)**.** *We consider transmissions to be received successfully both in the primary network and in the D2D underlay when the following conditions hold (cf. Section 2.3):*

$$\frac{\frac{p_k}{|\mathbf{x}_k - \mathbf{x}_{\tilde{r}(k)}|^\alpha}}{\eta + \sum\limits_{\substack{l=1,\\ l\neq k}}^{K} \frac{p_l}{|\mathbf{x}_l - \mathbf{x}_{\tilde{r}(k)}|^\alpha} + \sum\limits_{l'=K+1}^{M} \frac{p_{l'}}{|\mathbf{x}_{l'} - \mathbf{x}_{\tilde{r}(k)}|^\alpha}} \geq \gamma_C,\ \forall k \in \mathcal{M}, k \leq K, \tag{3.1}$$

$$\frac{\frac{p_k}{|\mathbf{x}_k - \mathbf{x}_{\tilde{r}(k)}|^\alpha}}{\eta + \sum\limits_{\substack{l'=K+1,\\ l'\neq k}}^{M} \frac{p_{l'}}{|\mathbf{x}_{l'} - \mathbf{x}_{\tilde{r}(k)}|^\alpha} + \sum\limits_{l=1}^{K} \frac{p_l}{|\mathbf{x}_l - \mathbf{x}_{\tilde{r}(k)}|^\alpha}} \geq \gamma_{D2D},\ \forall k \in \mathcal{M}, k > K. \tag{3.2}$$

Assumption 3.5 (Interference-limited network)**.** *Interference between links is the major performance-limiting factor in wireless networks [Uts16]. Hence, we assume that*

$$\eta << \sum_{\substack{l=1,\\ l\neq k}}^{K} \frac{p_l}{|\mathbf{x}_l - \mathbf{x}_{\tilde{r}(k)}|^\alpha} + \sum_{l'=K+1}^{M} \frac{p_{l'}}{|\mathbf{x}_{l'} - \mathbf{x}_{\tilde{r}(k)}|^\alpha}\ \forall k \in \mathcal{M}, k \leq K,$$

$$\eta << \sum_{\substack{l'=K+1,\\ l'\neq k}}^{M} \frac{p_{l'}}{|\mathbf{x}_{l'} - \mathbf{x}_{\tilde{r}(k)}|^\alpha} + \sum_{l=1}^{K} \frac{p_l}{|\mathbf{x}_l - \mathbf{x}_{\tilde{r}(k)}|^\alpha},\ \forall k \in \mathcal{M}, k > K.$$

Theorem 3.1. *Satisfying the above conditions, the MPUTC for the considered two-tier network under the CSI-based model is bounded*

- *in the primary network as:*

$$\lambda \leq \begin{cases} \frac{3}{\delta} \sqrt[\alpha]{\frac{\gamma_C+1}{\gamma_C}} \sqrt[\alpha]{\frac{1}{1+\frac{LP_{V\text{-}UE}}{CP_{C\text{-}UE}}}} W \frac{C^{\frac{3\alpha-2}{2\alpha}}}{K}, & if K >> C, \\ \frac{3}{\delta} \sqrt[\alpha]{\frac{\gamma_C+1}{\gamma_C}} \sqrt[\alpha]{\frac{1}{1+\frac{LP_{V\text{-}UE}}{KP_{C\text{-}UE}}}} W \frac{C\sqrt{C}}{K \sqrt[\alpha]{K}}, & otherwise, \end{cases} \tag{3.3}$$

- *and in the D2D underlay as:*

$$\lambda' \leq \begin{cases} \frac{2}{\sqrt{\pi}\bar{d}} \sqrt[\alpha]{\frac{\gamma_{D2D}+1}{\gamma_{D2D}}} \sqrt[\alpha]{\frac{1}{1+\frac{CP_{C\text{-}UE}}{LP_{V\text{-}UE}}}} W \frac{1}{\sqrt[\alpha]{L}}, & if K >> C, \\ \frac{2}{\sqrt{\pi}\bar{d}} \sqrt[\alpha]{\frac{\gamma_{D2D}+1}{\gamma_{D2D}}} \sqrt[\alpha]{\frac{1}{1+\frac{KP_{C\text{-}UE}}{LP_{V\text{-}UE}}}} W \frac{1}{\sqrt[\alpha]{L}}, & otherwise, \end{cases} \tag{3.4}$$

where $P_{C\text{-}UE}$ denotes the maximum transmit power of C-UEs and $P_{V\text{-}UE}$ denotes the maximum transmit power of V-UEs, and δ and $\bar{d}$ are some positive constants.

Proof. Consider first the case of cellular communication, i.e., $k \in \mathcal{M}, k \leq K$. According to Assumption 3.5, the noise power can be neglected. Hence, by adding the numerator to the denominator on the left-hand side (LHS) in (3.1), the condition can be reformulated as:

$$\frac{\frac{p_k}{|\mathbf{x}_k - \mathbf{x}_{\tilde{r}(k)}|^\alpha}}{\sum\limits_{l=1}^{K} \frac{p_l}{|\mathbf{x}_l - \mathbf{x}_{\tilde{r}(k)}|^\alpha} + \sum\limits_{l'=K+1}^{M} \frac{p_{l'}}{|\mathbf{x}_{l'} - \mathbf{x}_{\tilde{r}(k)}|^\alpha}} \geq \frac{\gamma_\mathrm{C}}{\gamma_\mathrm{C}+1}, \tag{3.5}$$

or equivalently:

$$|\mathbf{x}_k - \mathbf{x}_{\tilde{r}(k)}|^\alpha \leq \frac{\gamma_\mathrm{C}+1}{\gamma_\mathrm{C}} \frac{p_k}{\sum\limits_{l=1}^{K} \frac{p_l}{|\mathbf{x}_l - \mathbf{x}_{\tilde{r}(k)}|^\alpha} + \sum\limits_{l'=K+1}^{M} \frac{p_{l'}}{|\mathbf{x}_{l'} - \mathbf{x}_{\tilde{r}(k)}|^\alpha}}. \tag{3.6}$$

According to Assumption 3.1, the distance between any two network nodes is at most the diameter of the domain (i.e., $|\mathbf{x}_l - \mathbf{x}_{\tilde{r}(k)}| \leq 2/\sqrt{\pi}$, $\forall k, l \in \mathcal{M}$). Considering this property, the following holds:

$$|\mathbf{x}_k - \mathbf{x}_{\tilde{r}(k)}|^\alpha \leq \left(\frac{2}{\sqrt{\pi}}\right)^\alpha \frac{\gamma_\mathrm{C}+1}{\gamma_\mathrm{C}} \frac{p_k}{\sum\limits_{l=1}^{K} p_l + \sum\limits_{l'=K+1}^{M} p_{l'}}. \tag{3.7}$$

Building the sum over all transmissions by C-UEs leads to:

$$\sum_{k=1}^{K} |\mathbf{x}_k - \mathbf{x}_{\tilde{r}(k)}|^\alpha \leq \left(\frac{2}{\sqrt{\pi}}\right)^\alpha \frac{\gamma_\mathrm{C}+1}{\gamma_\mathrm{C}} \frac{\sum\limits_{k=1}^{K} p_k}{\sum\limits_{l=1}^{K} p_l + \sum\limits_{l'=K+1}^{M} p_{l'}}. \tag{3.8}$$

Under the worst case interference scenario (i.e., a scenario where all C-UEs and and all V-UEs transmit at their respective maximal transmit power), $\sum\limits_{k=1}^{K} p_k = n_\mathrm{sim} P_\text{C-UE}$ and $\sum\limits_{l'=K+1}^{M} p_{l'} = n'_\mathrm{sim} P_\text{V-UE}$. Here, $n_\mathrm{sim} \in \mathbb{N}_0$ and $n'_\mathrm{sim} \in \mathbb{N}_0$ denote the respective number of C-UEs and V-UEs that are allowed to transmit in parallel. According to the considered system model, each eNB is able to receive at most one transmission reliably at a given time. Hence, some C-UEs might not be supported and $n_\mathrm{sim} < K$ might need to be selected. In this regard, let $\mathcal{K}_\mathrm{active} = \{k : k \leq K, p_k > 0\} \subset \mathcal{M}$ denote the set of supported C-UEs, where $|\mathcal{K}_\mathrm{active}| = n_\mathrm{sim}$. On the other hand, such restrictions do not apply to transmitting V-UEs and $n'_\mathrm{sim} = L$ can be set (under the assumption of full duplex operation). Furthermore, let $d_{k,\tilde{r}(k)} = |\mathbf{x}_k - \mathbf{x}_{\tilde{r}(k)}|$ for brevity. With this, the following holds:

$$\sum_{k \in \mathcal{K}_\mathrm{active}} d_{k,\tilde{r}(k)}^\alpha \leq \left(\frac{2}{\sqrt{\pi}}\right)^\alpha \frac{\gamma_\mathrm{C}+1}{\gamma_\mathrm{C}} \frac{n_\mathrm{sim} P_\text{C-UE}}{n_\mathrm{sim} P_\text{C-UE} + L P_\text{V-UE}}. \tag{3.9}$$

By Jensen's inequality [RW00], it holds that $\frac{\sum\limits_{k \in \mathcal{K}_\mathrm{active}} d_{k,\tilde{r}(k)}^\alpha}{\sum\limits_{k \in \mathcal{K}_\mathrm{active}} 1} \geq \left(\frac{\sum\limits_{k \in \mathcal{K}_\mathrm{active}} d_{k,\tilde{r}(k)}}{\sum\limits_{k \in \mathcal{K}_\mathrm{active}} 1}\right)^\alpha$. Further considering $\sum\limits_{k \in \mathcal{K}_\mathrm{active}} 1 = n_\mathrm{sim}$, it holds that:

$$\sum_{k \in \mathcal{K}_\mathrm{active}} d_{k,\tilde{r}(k)} \leq \frac{2}{\sqrt{\pi}} \sqrt[\alpha]{\frac{\gamma_\mathrm{C}+1}{\gamma_\mathrm{C}} \frac{n_\mathrm{sim} P_\text{C-UE}}{n_\mathrm{sim} P_\text{C-UE} + L P_\text{V-UE}} n_\mathrm{sim}^{\alpha-1}}. \tag{3.10}$$

Building the transport capacity yields

$$\lambda KT \sum_{k\in\mathcal{K}_{\text{active}}} d_{k,\tilde{r}(k)} \leq \frac{2}{\sqrt{\pi}} \sqrt[\alpha]{\frac{\gamma_{\text{C}}+1}{\gamma_{\text{C}}} \frac{n_{\text{sim}} P_{\text{C-UE}}}{n_{\text{sim}} P_{\text{C-UE}} + L P_{\text{V-UE}}} n_{\text{sim}}^{\alpha-1}} CWT, \tag{3.11}$$

where λKT denotes the total throughput of all users, and CWT is the system capacity, i.e., $\lambda KT \leq CWT$. Let $\bar{d}_{k,\tilde{r}(k)}$ denote the mean distance between a C-UE and its serving (i.e., closest) eNB. Hence, by the law of large numbers [Fel71], it follows that $\sum_{k\in\mathcal{K}_{\text{active}}} d_{k,\tilde{r}(k)} \approx n_{\text{sim}} \bar{d}_{k,\tilde{r}(k)}$ (for large enough n_{sim}) and

$$\lambda KT n_{\text{sim}} \bar{d}_{k,\tilde{r}(k)} \leq \frac{2}{\sqrt{\pi}} \sqrt[\alpha]{\frac{\gamma_{\text{C}}+1}{\gamma_{\text{C}}} \frac{n_{\text{sim}} P_{\text{C-UE}}}{n_{\text{sim}} P_{\text{C-UE}} + L P_{\text{V-UE}}} n_{\text{sim}}^{\alpha-1}} CWT. \tag{3.12}$$

According to Assumption 3.3, it follows that

$$\bar{d}_{k,\tilde{r}(k)} = \int_0^1 \int_0^1 \sqrt{\left(r\left(C\right)\sqrt{U_1}\cos U_2\right)^2 + \left(r\left(C\right)\sqrt{U_1}\sin U_2\right)^2}\,\mathrm{d}U_2\,\mathrm{d}U_1 \tag{3.13}$$

$$= r\left(C\right)\int_0^1 \sqrt{U_1}\,\mathrm{d}U_1 = \frac{2r(C)}{3}. \tag{3.14}$$

Furthermore, as $C \to \infty$ the overlap of the coverage areas of the different eNBs declines in the considered domain. Hence, $\pi r^2(C) \to \frac{1}{C}$ and $r(C) = \frac{\delta}{\sqrt{\pi C}}$ for some constant $\delta > 0$. Hence, it follows that

$$\bar{d}_{k,\tilde{r}(k)} = \frac{2\delta}{3\sqrt{\pi C}}. \tag{3.15}$$

Furthermore, as each eNB can only receive one UL transmission reliably, n_{sim} is either limited by the number of eNBs or the number of C-UEs, i.e.,

$$n_{\text{sim}} = \begin{cases} C, & \text{if } K >> C \\ K, & \text{otherwise} \end{cases}. \tag{3.16}$$

Plugging (3.16) and (3.15) into (3.12), and reformulating, yields the final result in (3.3).

The results for the MPUTC in the D2D underlay can be derived following the same method. To this end, consider $k \in \mathcal{M}, k > K$. Again, according to Assumption 3.5, the noise power in (3.2) can be ignored and adding the numerator to the denominator on the LHS yields

$$\frac{\frac{p_k}{|\mathbf{x}_k - \mathbf{x}_{\tilde{r}(k)}|^\alpha}}{\sum_{l'=K+1}^{M} \frac{p_{l'}}{|\mathbf{x}_{l'} - \mathbf{x}_{\tilde{r}(k)}|^\alpha} + \sum_{l=1}^{K} \frac{p_l}{|\mathbf{x}_l - \mathbf{x}_{\tilde{r}(k)}|^\alpha}} \geq \frac{\gamma_{\text{D2D}}}{\gamma_{\text{D2D}}+1} \tag{3.17}$$

or equivalently:

$$|\mathbf{x}_k - \mathbf{x}_{\tilde{r}(k)}|^\alpha \leq \frac{\gamma_{\text{D2D}}+1}{\gamma_{\text{D2D}}} \frac{p_k}{\sum_{l'=K+1}^{M} \frac{p_{l'}}{|\mathbf{x}_{l'} - \mathbf{x}_{\tilde{r}(k)}|^\alpha} + \sum_{l=1}^{K} \frac{p_l}{|\mathbf{x}_l - \mathbf{x}_{\tilde{r}(k)}|^\alpha}}. \tag{3.18}$$

Considering again that $|\mathbf{x}_l - \mathbf{x}_{\tilde{r}(k)}| \leq 2/\sqrt{\pi}$, $\forall k, l \in \mathcal{M}$, the following holds:

$$|\mathbf{x}_k - \mathbf{x}_{\tilde{r}(k)}|^\alpha \leq \left(\frac{2}{\sqrt{\pi}}\right)^\alpha \frac{\gamma_{\text{D2D}}+1}{\gamma_{\text{D2D}}} \frac{p_k}{\sum\limits_{l'=K+1}^{M} p_{l'} + \sum\limits_{l=1}^{K} p_l}. \tag{3.19}$$

Building the sum over all transmissions by V-UEs yields

$$\sum_{k=K+1}^{M} |\mathbf{x}_k - \mathbf{x}_{\tilde{r}(k)}|^\alpha \leq \left(\frac{2}{\sqrt{\pi}}\right)^\alpha \frac{\gamma_{\text{D2D}}+1}{\gamma_{\text{D2D}}} \frac{\sum\limits_{k=K+1}^{M} p_k}{\sum\limits_{l'=K+1}^{M} p_{l'} + \sum\limits_{l=1}^{K} p_l}. \tag{3.20}$$

Again, considering the worst-case interference scenario, $\sum\limits_{k=K+1}^{M} p_k = n'_{\text{sim}} P_{\text{V-UE}}$ and $\sum\limits_{l=1}^{K} p_l = n_{\text{sim}} P_{\text{C-UE}}$. With $n'_{\text{sim}} = L$, the following holds

$$\sum_{k=K+1}^{M} d_{k,\tilde{r}(k)}^\alpha \leq \left(\frac{2}{\sqrt{\pi}}\right)^\alpha \frac{\gamma_{\text{D2D}}+1}{\gamma_{\text{D2D}}} \frac{LP_{\text{V-UE}}}{LP_{\text{V-UE}} + n_{\text{sim}} P_{\text{C-UE}}}. \tag{3.21}$$

By Jensen's inequality [RW00], it holds that $\frac{\sum\limits_{k=K+1}^{M} d_{k,\tilde{r}(k)}^\alpha}{\sum\limits_{k=K+1}^{M} 1} \geq \left(\frac{\sum\limits_{k=K+1}^{M} d_{k,\tilde{r}(k)}}{\sum\limits_{k=K+1}^{M} 1}\right)^\alpha$, $\sum\limits_{k=K+1}^{M} 1 = L$ and

$$\sum_{k=K+1}^{M} d_{k,\tilde{r}(k)} \leq \frac{2}{\sqrt{\pi}} \sqrt[\alpha]{\frac{\gamma_{\text{D2D}}+1}{\gamma_{\text{D2D}}} \frac{LP_{\text{V-UE}}}{LP_{\text{V-UE}} + n_{\text{sim}} P_{\text{C-UE}}} L^{\alpha-1}}. \tag{3.22}$$

Building the transport capacity yields

$$\lambda' LT \sum_{k=K+1}^{M} d_{k,\tilde{r}(k)} \leq \frac{2}{\sqrt{\pi}} \sqrt[\alpha]{\frac{\gamma_{\text{D2D}}+1}{\gamma_{\text{D2D}}} \frac{LP_{\text{V-UE}}}{LP_{\text{V-UE}} + n_{\text{sim}} P_{\text{C-UE}}} L^{\alpha-1} LWT}, \tag{3.23}$$

where $\lambda' LT$ denotes the total throughput of all transmitting V-UEs, and LWT is the system capacity of the vehicular underlay network, i.e., $\lambda' LT \leq LWT$. Let $\bar{d}_{k,\tilde{r}(k)}$ denote the mean distance between a vehicular transmitter and its worst-case receiver. For large enough vehicle density this mean distance is equivalent to the intended broadcast distance $\bar{d}$ determined by the deployed application (and normalized to the unit area disk domain). With this, it holds that $\sum\limits_{k=K+1}^{M} d_{k,\tilde{r}(k)} = L\bar{d}$ and

$$\lambda' LT L\bar{d} \leq \frac{2}{\sqrt{\pi}} \sqrt[\alpha]{\frac{\gamma_{\text{D2D}}+1}{\gamma_{\text{D2D}}} \frac{LP_{\text{V-UE}}}{LP_{\text{V-UE}} + n_{\text{sim}} P_{\text{C-UE}}} L^{\alpha-1} LWT}. \tag{3.24}$$

Considering the two operation modes in the primary network (cf. (3.16)) and reformulating yields the final result in (3.4). This concludes the proof. □

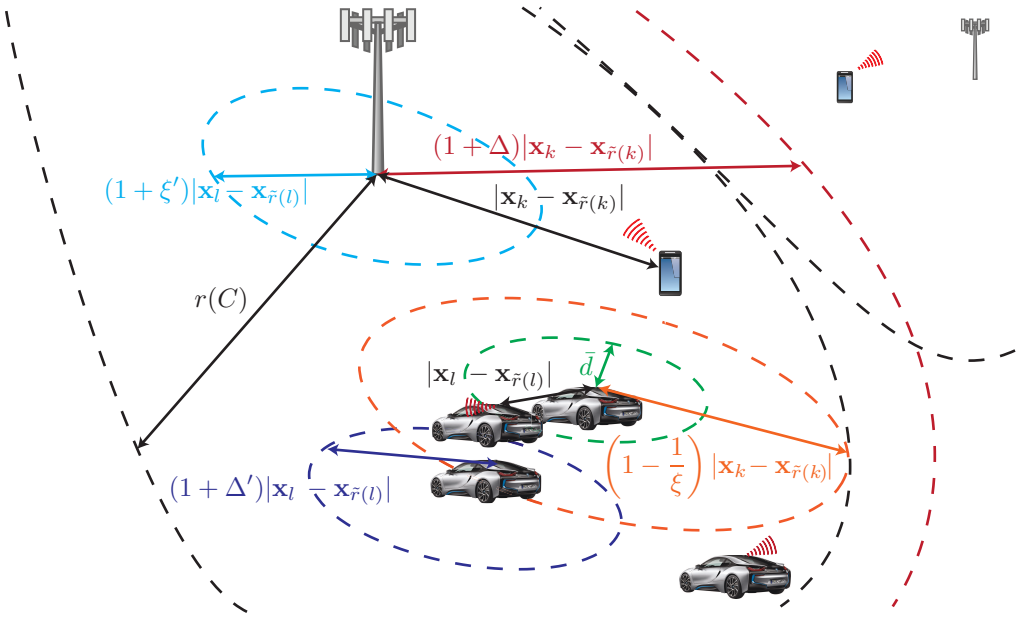

Figure 3.1: Depiction of the considered two-tier network and the required separation between network nodes for successful communication under the location-based model.

3.3 Location-based RRM

This second approach assumes that a transmission is successfully received when certain criteria on the separation between the considered network nodes are met (see Figure 3.1 for a graphical representation).

Assumption 3.6. *First, we require that each receiver is within the designed range from the respective transmitter, i.e.,*

$$|\mathbf{x}_k - \mathbf{x}_{\tilde{r}(k)}| \leq r(C), \forall k \in \mathcal{M}, k \leq K, \tag{3.25}$$
$$|\mathbf{x}_k - \mathbf{x}_{\tilde{r}(k)}| \leq \bar{d}, \forall k \in \mathcal{M}, k > K. \tag{3.26}$$

Assumption 3.7. *Provided that the conditions in* (3.25) *and* (3.26) *are satisfied, we further require that the interference between UEs of the same class is controlled via sufficient separation:*

$$|\mathbf{x}_l - \mathbf{x}_{\tilde{r}(k)}| \geq (1+\Delta)|\mathbf{x}_k - \mathbf{x}_{\tilde{r}(k)}|, \forall k, l \in \mathcal{M}, k \leq K, l \leq K, l \neq k, \text{ and} \tag{3.27}$$
$$|\mathbf{x}_{l'} - \mathbf{x}_{\tilde{r}(k)}| \geq (1+\Delta')|\mathbf{x}_k - \mathbf{x}_{\tilde{r}(k)}|, \forall k, l' \in \mathcal{M}, k > K, l' > K, l' \neq k, \tag{3.28}$$

where $\Delta \in \mathbb{R}_+$ and $\Delta' \in \mathbb{R}_+$ denote some deployment-specific control parameters.

Assumption 3.8. *Moreover, the cross-interference due to the reuse of cellular resources in the D2D underlay must be controlled as well:*

$$|\mathbf{x}_{l'} - \mathbf{x}_{\tilde{r}(k)}| \geq (1+\xi')|\mathbf{x}_{l'} - \mathbf{x}_{\tilde{r}(l')}|, \forall k \in \mathcal{M}, k \leq K, l' \in \mathcal{M}, l' > K, \text{ and} \tag{3.29}$$
$$|\mathbf{x}_l - \mathbf{x}_{\tilde{r}(k)}| \geq \left(1-\frac{1}{\xi}\right)|\mathbf{x}_l - \mathbf{x}_{\tilde{r}(l)}|, \forall k \in \mathcal{M}, k > K, l \in \mathcal{M}, l \leq K, \tag{3.30}$$

where $\xi \in \mathbb{R}_+$ and $\xi' \in \mathbb{R}_+$ denote some deployment-specific control parameters.

Hence, under the location-based model, cellular and D2D transmissions are both received successfully when all of the inequalities (3.25) - (3.30) are fulfilled.

Theorem 3.2. *If* (3.25)-(3.30) *are satisfied, the MPUTC for the considered two-tier network under the location-based model is bounded*

- *in the primary network as:*

$$\lambda \leq \begin{cases} \frac{6}{\Delta\delta} W \frac{C}{K}, & if K >> C, \\ \frac{6}{\Delta\delta} W \frac{C}{K} \sqrt{\frac{C}{K}}, & otherwise, \end{cases} \tag{3.31}$$

- *and in the D2D underlay as:*

$$\lambda' \leq \begin{cases} 0, & if\ C \geq \left\lfloor \frac{\delta^2}{\pi \xi'^2 \bar{d}^2} \right\rfloor, \\ \sqrt{\frac{16 - 16\pi C \xi'^2 \bar{d}^2 - 4\left(1-\frac{1}{\xi}\right)^2 \delta^2}{\pi \Delta'^2 \bar{d}^2}} \frac{W}{\sqrt{L}}, & if\ C < \left\lfloor \frac{\delta^2}{\pi \xi'^2 \bar{d}^2} \right\rfloor, K >> C, \\ \sqrt{\frac{16 - 16\pi C \xi'^2 \bar{d}^2 - 4\frac{K}{C}\left(1-\frac{1}{\xi}\right)^2 \delta^2}{\pi \Delta'^2 \bar{d}^2}} \frac{W}{\sqrt{L}}, & if\ C < \left\lfloor \frac{\delta^2}{\pi \xi'^2 \bar{d}^2} \right\rfloor, K << C, \end{cases} \tag{3.32}$$

where $\delta > 0$ denotes some constant.

Proof. To start the proof, first consider the primary network, i.e., the case of $k \leq K$. In accordance to the system model, its performance should not be severely degraded by D2D communication. Hence, the two network layers can be considered separately under the location-based model, where stricter constraints are imposed on the D2D underlay. Ensuring that sufficient separation between eNBs and V-UEs is always enforced, the implications due to the reuse of resources in the D2D underlay can be considered as non-existent in the analysis of the MPUTC in the primary network. Note that this approach has severe implications on the per-user transport capacity in the D2D underlay, as it will be shown later in the proof. By applying the triangle inequality to the constraints for successful communication under the location-based model (i.e., (3.25) and (3.27)), it follows that

$$|\mathbf{x}_{\tilde{r}(l)} - \mathbf{x}_{\tilde{r}(k)}| \geq |\mathbf{x}_l - \mathbf{x}_{\tilde{r}(k)}| - |\mathbf{x}_l - \mathbf{x}_{\tilde{r}(l)}|, \tag{3.33}$$

$$|\mathbf{x}_{\tilde{r}(l)} - \mathbf{x}_{\tilde{r}(k)}| \geq |\mathbf{x}_k - \mathbf{x}_{\tilde{r}(l)}| - |\mathbf{x}_k - \mathbf{x}_{\tilde{r}(k)}|. \tag{3.34}$$

By definition, the right-hand side (RHS) in the above equations is positive, as the distance from a transmitting C-UE to any eNB other than its serving (i.e., closest) one is greater than the distance to said serving eNB. Adding (3.33) and (3.34) and applying condition (3.27) results in:

$$|\mathbf{x}_{\tilde{r}(l)} - \mathbf{x}_{\tilde{r}(k)}| \geq \frac{\Delta}{2} \left(|\mathbf{x}_k - \mathbf{x}_{\tilde{r}(k)}| + |\mathbf{x}_l - \mathbf{x}_{\tilde{r}(l)}| \right). \tag{3.35}$$

Hence, simultaneous cellular UL transmissions are successfully received at the respective eNBs when disks of radius $\frac{\Delta}{2}$ times the link range centered at the eNB are disjoint from radio resource perspective. In other words, each cellular UL transmission has an associated *guard* area and such guard areas should not intersect in order to enable successful communication[3].

[3]Note that, as a result, a eNB can only receive one UL transmission in a given time- and frequency-slot since two disks with the same origin cannot be disjoint. This is a reflection of the assumed eNB capabilities.

Furthermore, allowing for edge effects at the domain boundary and considering that the link range is at most equal to the domain radius, it is guaranteed that at least a quarter of each guard disk is within the domain [GK00].

Again, consider the abbreviation $d_{k,\tilde{r}(k)} = |\mathbf{x}_k - \mathbf{x}_{\tilde{r}(k)}|$ and the fact that not all of the K C-UEs may be supported at the same time, where $\mathcal{K}_{\text{active}}$ denotes the set of active ones. Hence, the above inequalities only need to hold for the elements of $\mathcal{K}_{\text{active}}$. Further consider that each guard area has a surface of $\pi\frac{\Delta^2}{4}d_{k,\tilde{r}(k)}^2$. Since at least a quarter of these disjoint guard areas is within the unit area domain, it follows that

$$\sum_{k\in\mathcal{K}_{\text{active}}} \frac{\pi\Delta^2}{16} d_{k,\tilde{r}(k)}^2 \leq 1 \equiv \sum_{k\in\mathcal{K}_{\text{active}}} d_{k,\tilde{r}(k)}^2 \leq \frac{16}{\pi\Delta^2}. \tag{3.36}$$

By the Cauchy-Schwarz inequality [RW00], the following holds:

$$\sum_{k\in\mathcal{K}_{\text{active}}} d_{k,\tilde{r}(k)} \leq \sqrt{\sum_{k\in\mathcal{K}_{\text{active}}} d_{k,\tilde{r}(k)}^2 \sum_{k\in\mathcal{K}_{\text{active}}} 1^2}, \tag{3.37}$$

where $\sum_{k\in\mathcal{K}_{\text{active}}} 1^2 = \sum_{k\in\mathcal{K}_{\text{active}}} 1 = n_{\text{sim}}$ is the number of simultaneous transmissions in the primary network. Substituting (3.36) in (3.37) results in

$$\sum_{k\in\mathcal{K}_{\text{active}}} d_{k,\tilde{r}(k)} \leq \sqrt{\frac{16}{\pi\Delta^2} n_{\text{sim}}}. \tag{3.38}$$

Considering a total of λKT bits to be transmitted in the primary network, the instantaneous transport capacity must satisfy

$$\lambda KT \sum_{k\in\mathcal{K}_{\text{active}}} d_{k,\tilde{r}(k)} \leq \sqrt{\frac{16}{\pi\Delta^2} n_{\text{sim}}} CWT, \tag{3.39}$$

where CWT again denotes the system capacity of the primary network. Evaluating the sum on the LHS (for sufficiently large n_{sim}) yields

$$\lambda KT n_{\text{sim}} \bar{d}_{k,\tilde{r}(k)} \leq \sqrt{\frac{16}{\pi\Delta^2} n_{\text{sim}}} CWT, \tag{3.40}$$

where $\bar{d}_{k,\tilde{r}(k)}$ again denotes the mean distance between a C-UE and its respective receiving eNB. Following the same assumptions as in the proof regarding the results for the CSI-based model, it follows that $\bar{d}_{k,\tilde{r}(k)} = \frac{2r(C)}{3} = \frac{2\delta}{3\sqrt{\pi C}}$ for some constant $\delta > 0$. Plugging this in (3.40) and rearranging yields

$$\lambda \leq \frac{6}{\Delta\delta} \frac{WC\sqrt{C}}{K\sqrt{n_{\text{sim}}}}. \tag{3.41}$$

Again, substituting

$$n_{\text{sim}} = \begin{cases} C, & \text{if } K >> C, \\ K, & \text{otherwise}, \end{cases} \tag{3.42}$$

concludes the proof of the first part of the theorem.

Next, consider the D2D underlay, i.e., the case of $k > K$. Similarly to the case of cellular communication, using the triangle inequality and applying (3.28), it follows that

$$|\mathbf{x}_{\tilde{r}(l')} - \mathbf{x}_{\tilde{r}(k)}| \geq \frac{\Delta'}{2} \left(|\mathbf{x}_k - \mathbf{x}_{\tilde{r}(k)}| + |\mathbf{x}_{l'} - \mathbf{x}_{\tilde{r}(l')}| \right). \tag{3.43}$$

As the assumed V2X transmissions in the D2D underlay are required to be received by all V-UEs within the intended broadcast range, $|\mathbf{x}_k - \mathbf{x}_{\tilde{r}(k)}| = \bar{d}$, $\forall k = K+1, \ldots, L$, can be set. Hence, successful reception in the D2D underlay necessitates a guard area around each worst-case receiver with a radius of $\frac{\Delta'}{2}\bar{d}$. As in the case of cellular communication, at least a quarter of these guard areas is within the domain [GK00], i.e.,

$$\sum_{k=K+1}^{M} \frac{\pi \Delta'^2}{16} \bar{d}^2 \leq 1. \tag{3.44}$$

In contrast to the case of cellular communication, however, the collective of the guard areas cannot span across the entire domain. From (3.29) and the triangle inequality, it follows that

$$|\mathbf{x}_{\tilde{r}(k)} - \mathbf{x}_{\tilde{r}(l)}| \geq \xi' \bar{d}. \tag{3.45}$$

Hence, additional guard areas of radius $\xi'\bar{d}$ around each eNB are necessary in order to protect cellular UL transmissions from harmful cross-interference. The portion of the domain where D2D communication can take place is therefore no longer the entire unit area disk. Instead, it is disrupted by 'holes' due to the said *cross-interference guard areas*. Note that this could render the entire domain restricted for D2D communication allowing for 0 bits to be transmitted in the underlay. This is the case when the entire coverage area of an eNB is contained by the cross-interference guard area, i.e., when

$$\xi' \bar{d} \geq r(C) \equiv \xi' \bar{d} \geq \frac{\delta}{\sqrt{\pi C}} \equiv C \geq \left\lfloor \frac{\delta^2}{\pi \xi'^2 \bar{d}^2} \right\rfloor. \tag{3.46}$$

Moreover, in order to protect the received D2D signal from the harmful cross-interference due to cellular UL transmissions, the condition in (3.30) must be satisfied. Hence, the cross-interference guard areas further include disks of radius $\left(1 - \frac{1}{\xi}\right) |\mathbf{x}_l - \mathbf{x}_{\tilde{r}(l)}|$, $\forall l \in \mathcal{K}_{\text{active}}$, around each active C-UE. Considering all of the 'holes' in the domain where D2D communication is restricted, the expression in (3.44) is modified to the following tighter bound:

$$\sum_{k=K+1}^{M} \frac{\pi \Delta'^2}{16} \bar{d}^2 \leq 1 - C\pi \left(\xi' \bar{d}\right)^2 - \sum_{l \in \mathcal{K}_{\text{active}}} \pi \left(1 - \frac{1}{\xi}\right)^2 |\mathbf{x}_l - \mathbf{x}_{\tilde{r}(l)}|^2, \tag{3.47}$$

which can be expressed (for sufficiently large $n_{\text{sim}} = |\mathcal{K}_{\text{active}}|$) as

$$\sum_{k=K+1}^{M} \frac{\pi \Delta'^2}{16} \bar{d}^2 \leq 1 - C\pi \left(\xi' \bar{d}\right)^2 - n_{\text{sim}} \pi \left(1 - \frac{1}{\xi}\right)^2 \frac{r(C)^2}{4}. \tag{3.48}$$

This is due to the application of the Cauchy-Schwarz inequality [RW00] as

$$\sum_{l \in \mathcal{K}_{\text{active}}} \pi \left(1 - \frac{1}{\xi}\right)^2 |\mathbf{x}_l - \mathbf{x}_{\tilde{r}(l)}|^2 \geq \frac{\pi}{n_{\text{sim}}} \left(1 - \frac{1}{\xi}\right)^2 \left(\sum_{l \in \mathcal{K}_{\text{active}}} |\mathbf{x}_l - \mathbf{x}_{\tilde{r}(l)}| \right)^2 \tag{3.49}$$

and $\left(\sum_{l\in\mathcal{K}_{\text{active}}} |\mathbf{x}_l - \mathbf{x}_{\tilde{r}(l)}|\right)^2 = n_{\text{sim}}^2 \frac{r(C)^2}{4}$ for sufficiently large n_{sim}. Following similar reformulation steps as for the case of cellular communication, (3.48) can be expressed as

$$\sum_{k=K+1}^{M} \bar{d} \leq \sqrt{\frac{16 - 16C\pi\left(\xi'\bar{d}\right)^2 - 4n_{\text{sim}}\pi\left(1-\frac{1}{\xi}\right)^2 r(C)^2}{\pi\Delta'^2} n'_{\text{sim}}}, \tag{3.50}$$

where n'_{sim} denotes the number of simultaneous transmissions in the D2D underlay. Hence, considering a total of $\lambda' LT$ bits to be transmitted by the V-UEs, the instantaneous transport capacity must satisfy

$$\lambda' LT n'_{\text{sim}}\bar{d} \leq \sqrt{\frac{16 - 16C\pi\left(\xi'\bar{d}\right)^2 - 4n_{\text{sim}}\pi\left(1-\frac{1}{\xi}\right)^2 r(C)^2}{\pi\Delta'^2} n'_{\text{sim}} n'_{\text{sim}}} WT, \tag{3.51}$$

where $n'_{\text{sim}}WT$ denotes the capacity of the D2D underlay. Assuming full duplex capabilities at the V-UEs, $n'_{\text{sim}} = L$ can be selected. In the case of half duplex operation, it would only be reasonable that at least one receiver listens to each transmission. Hence, $n'_{\text{sim}} = \frac{L}{2}$ might be selected. Nevertheless, this scalar factor has little influence on the asymptotic behavior of the MPUTC. Therefore, the final result in (3.32) considers the full duplex option. As previously discussed, it also considers the limitation on the number of parallel transmissions in the primary network (cf. (3.42)) and the evaluation of $r(C)$ for large C. □

3.4 Discussion

3.4.1 RRM Design Implications

Figure 3.2 illustrates the behavior of the derived MPUTC bounds in the primary network, while Figure 3.3 focuses on the D2D underlay. Both of these figures consider some arbitrary system parameters, as the general implications of the bounds are more important than the absolute values. Hereby, the $K >> C$ operation regime has been chosen for the primary network, as the opposite case is unreasonable from economical point of view. The goal of this analysis is to investigate the influence of cross-interference and the respective counter-measures taken in both RRM approaches.

Primary network

As it can be seen in Figure 3.2, the upper bound of the MPUTC in the primary network is not affected by the increasing number of V-UEs under the location-based model. This is due to the fact that this approach imposes a direct prioritization of the cellular links and a strict limit on the cross-interference from V-UEs. In trade, the location-based model imposes severer restrictions on the D2D underlay, as it will be seen below. On the other hand, the CSI-based model allows for "softer" resource sharing and the MPUTC decreases with the increasing number of V-UEs, as further cross-interference is added to the wireless system. The main limiting factor under both models, however, is the number of C-UEs that needs to be served. The MPUTC in the primary network decreases the fastest in this parameter. Increasing the number of eNBs can help boost the MPUTC in the primary network, and at

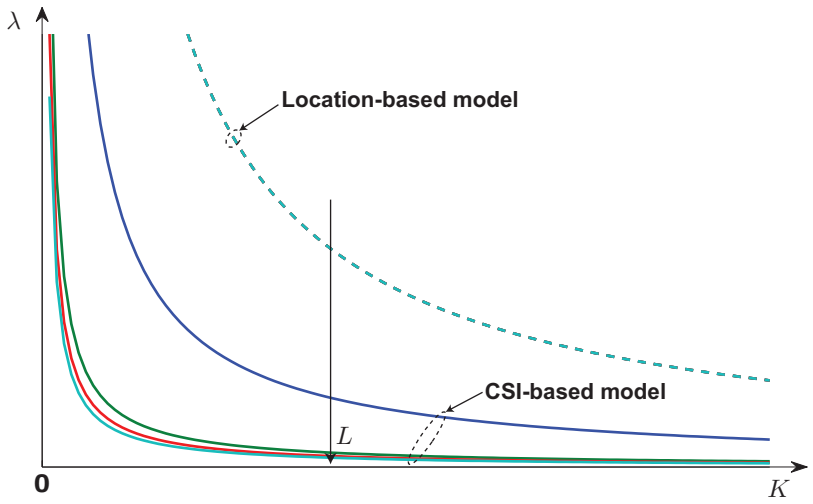

Figure 3.2: Mean per-user transport capacity scaling behavior in the primary network under both RRM models for some arbitrary control parameters, increasing L, and a fixed $C, C << K$.

the same time reduce the influence of the cross-interference due to the D2D underlay. This is most evident under the location-based model, where the upper bound of the MPUTC in the primary network grows with the square of C, but a high enough number of eNBs would prohibit direct communication. Under the CSI-based model, on the other hand, the growth with C is limited to a power of at most $\frac{3}{2}$. A similar result has been derived in [ZKF12] for regular cellular networks. Hence, we consider that the D2D underlay in the investigated wireless system can be added without severe negative impact on the primary network.

D2D underlay

In correspondence to the strict limits imposed on direct communication in the location-based model, the MPUTC in the D2D underlay is generally lower as compared to the CSI-based model. This is again due to its more conservative approach to the resource reuse problem. Depending on the value of α, the CSI-based model has the further advantage of possible slower decline of the MPUTC with increasing number of transmitting V-UEs, although the decline with increasing number of eNBs (and C-UEs) is more severe. Regardless, both models would eventually not allow for D2D communication when the density of eNBs and C-UEs is high enough[4]. Hence, although a dense deployment of eNBs will help to increase the capacity of the primary network, taking this to the extreme (referred to as ultra-dense networks [MFP+14]) might hinder the adoption of underlay D2D communication. This is especially the case when the services running in the D2D underlay are associated with strict requirements on the communication range. The coexistence of D2D services and cellular services would be infeasible as the network infrastructure density reaches a certain threshold (cf. Theorem 3.2). Hence, the trade-off between the added cellular capacity and the possibility to allow for D2D communication should be carefully investigated when designing future networks.

Moreover, as the primary network is to be prioritized, the attempts to avoid cross-interference from the D2D underlay will prohibit direct communication when a higher number of C-UEs is

[4]Note that, under reasonable system parameters, this may be the case sooner under the location-based model.

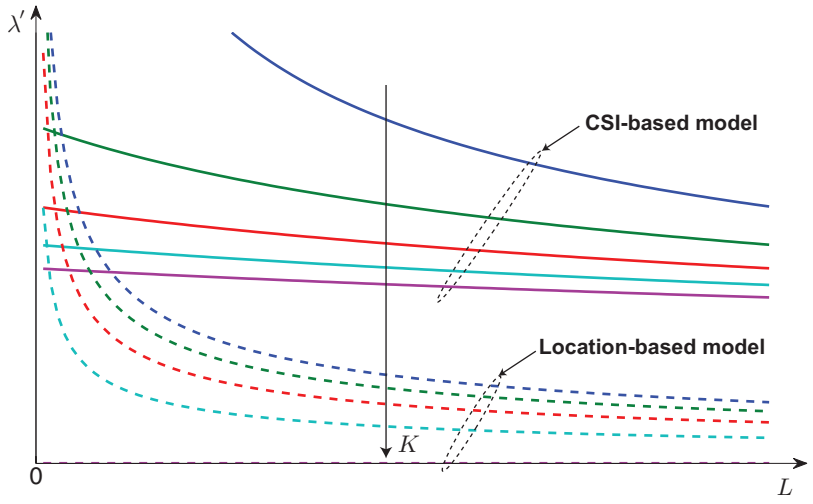

Figure 3.3: Mean per-user transport capacity scaling behavior in the D2D underlay under both RRM models for some arbitrary control parameters, increasing K, and $\frac{C}{K} = \text{const}, C << K$.

active. It should be considered that direct communication is likely to present a more resource-efficient channel. Hence, the overall performance of a future two-tier network can benefit from an acceptable reduction in the cellular throughput that allows for services based on the D2D paradigm to be implemented. To this end, the prioritization of services needs to be revised.

The demonstrated results indicate that a reasonable implementation of a cellular network with a D2D underlay can be achieved. It should be noted, however, that the derived MPUTC bounds have no implications on their achievability or the instantaneous QoS for individual users. Nevertheless, it is worth to invest more effort in the design of RRM schemes that enable C-ITS applications by means of underlay D2D communication. This motivates the contributions described in Chapter 4 and Chapter 5.

3.4.2 Reuse of DL Resources

The reuse of DL resources will not be investigated explicitly in the context of the CSF, as no new insight can be won from such an investigation. Although the roles of eNBs and C-UEs are swapped (i.e., eNBs become transmitters and C-UEs become receivers) on the cellular links, following the outline of the provided proof will lead to the same results under the CSI-based model (cf. Theorem 3.1). Under the location-based model, this swapping leads to the opposite interpretation of the cross-interference guard areas, i.e., the ones centered at eNBs protect receiving V-UEs from the interference due to cellular DL transmissions, and the ones centered at C-UEs provide protection against the interference due to direct transmissions. With this, it is likely that the environment-dependent control parameters would take different values as compared to the case of UL resource reuse. Nevertheless, the upper bound on the MPUTC will retain the same form (cf Theorem 3.2). In practical deployments, the transmit power of eNBs is typically higher than the transmit power of C-UEs. Hence, it is likely that the guard areas centered at the eNBs are larger in the case of DL resource reuse and the MPUTC is limited to zero sooner (with the growing C) as compared to the case of UL resource reuse.

Chapter 4

Resource Allocation Based on Channel State Information

Encouraged by the scaling of the upper bounds on the asymptotic MPUTC both in the primary network and in the D2D underlay under the CSI-based model, this chapter is devoted to developing a feasible RRM scheme for the considered deployment scenario. In particular, we aim at designing algorithms for the assignment of RBs and the allocation of transmit powers to users such that the QoS requirements of all of the transmitting C-UEs and V-UEs are met. Hereby, we consider the cases of perfect and imperfect CSI. The results of this work are published in [BSF15a, BSF16c, BSF16a].

4.1 Preliminaries

The interference is one of the major limiting factors in contemporary wireless networks [Uts16]. It is a common practice to consider the so-called interference coupling matrix to capture the impact of interference between different users [SWB09].

Definition 4.1 (Interference Coupling Matrix)**.** *If all users are assigned to a single RB, then the interference coupling matrix* $\mathbf{A}^{(s)} \in \mathbb{R}_{\geq 0}^{M \times M}$ *(associated with the considered RB* $s \in \mathcal{S}$*) is defined to be*

$$\mathbf{A^{(s)}} = \begin{pmatrix} 0 & a_{12}^{(s)} & \dots & a_{1M}^{(s)} \\ a_{21}^{(s)} & 0 & \dots & a_{2M}^{(s)} \\ \vdots & & \ddots & \vdots \\ a_{M1}^{(s)} & \dots & a_{MM-1}^{(s)} & 0 \end{pmatrix}, \tag{4.1}$$

where the (effective) interference power gains $a_{kl}^{(s)} \geq 0$ *are defined as*

$$a_{kl}^{(s)} = \begin{cases} \frac{|h_{kl}^{(s)}|^2}{|h_{kk}^{(s)}|^2} = \frac{d_{kl} z_{kl}^{(s)}}{d_{kk} z_{kk}^{(s)}}, & if k \neq l, \\ 0, & if k = l, \end{cases} \quad \forall k, l \in \mathcal{M}. \tag{4.2}$$

These matrices are grouped in the following block diagonal matrix to describe the interference couplings in the entire system bandwidth (if users are assigned to orthogonal RBs):

$$\mathbf{A} = \operatorname{diag}\big(\mathbf{A}^{(1)}, \dots, \mathbf{A}^{(S)}\big) \in \mathbb{R}_{\geq 0}^{MS \times MS}. \tag{4.3}$$

Definition 4.2 (Allocation Matrix). *The allocation matrix* $\mathbf{\Pi} \coloneqq (\pi_{ks}) \in \mathcal{P} \subseteq \{0,1\}^{M \times S}$ *is defined to be*

$$\pi_{ks} = \begin{cases} 1, & \text{if user } k \text{ is assigned to RB } s, \\ 0, & \text{otherwise}, \end{cases} \quad \forall k \in \mathcal{M}, s \in \mathcal{S}. \tag{4.4}$$

Here, $\mathcal{P}$ *denotes the set of feasible resource allocations.*

In general, the set of feasible resource allocations can be limited to the family of allocation matrices which correspond to the usage of only continuous subsets of RBs by C-UEs in the UL (i.e., $\mathcal{P} \subseteq \big\{\{0,1\}^{M \times S} : \text{ if } \pi_{ks} = 1 \cap \pi_{k(s+1)} = 0, \text{ for some } s \in \mathcal{S}, \text{ then } \pi_{ks'} = 0, \forall s' \in \mathcal{S}, s' > s, k \in \mathcal{M}, k \leq K\big\}$ can be selected). Such a restriction is relevant in practical scenarios in order to enable the lower peak-to-average power ratio associated with the Single-Carrier Frequency Division Multiple Access (SC-FDMA) scheme used in the LTE UL [3GP10].

The allocation matrix $\mathbf{\Pi}$ describes the utilization of the available RBs. Hence, it determines the active links in the system and, as such, the effective interference couplings. This is captured by an (interference) activation matrix defined as follows.

Definition 4.3 (Interference Activation Matrix). *Given an arbitrary assignment matrix* $\mathbf{\Pi} \in \mathcal{P}$*, the interference activation matrix associated with RB* $s \in \mathcal{S}$ *is defined as* $\mathbf{E}^{(s)} \coloneqq \mathbf{E}^{(s)}(\mathbf{\Pi}) \coloneqq (e_{kl}^{(s)}) \in \{0,1\}^{M \times M}$*, where*

$$e_{kl}^{(s)} = \begin{cases} 0, & \text{if } k = l, \\ \pi_{ks} \cdot \pi_{ls}, & \text{if } k \neq l, \end{cases} \forall k, l \in \mathcal{M}. \tag{4.5}$$

Moreover, the following block diagonal matrix describes the interference activation in the entire system bandwidth:

$$\mathbf{E} \coloneqq \mathbf{E}(\mathbf{\Pi}) \coloneqq \operatorname{diag}\big(\mathbf{E}^{(1)}, \ldots, \mathbf{E}^{(S)}\big) \in \{0,1\}^{MS \times MS}. \tag{4.6}$$

By definition, we have $e_{kl}^{(s)} = e_{lk}^{(s)}$, which is equal to 1 if and only if both users k and l are allocated to RB s; otherwise it is zero. This is intuitive, since two users have to be assigned to the same RB in order to interfere with each other.

Definition 4.4 (Effective Interference Coupling Matrix). *With the above in hand, the actual interference structure for the entire multi-band communication system, as determined by the RB allocation, is captured by the effective interference coupling matrix*

$$\mathbf{G} \coloneqq \mathbf{G}(\mathbf{\Pi}) \coloneqq \mathbf{A} \circ \mathbf{E}(\mathbf{\Pi}) = \operatorname{diag}(\mathbf{A}^{(1)} \circ \mathbf{E}^{(1)}, \ldots, \mathbf{A}^{(S)} \circ \mathbf{E}^{(S)}). \tag{4.7}$$

4.2 Non-fading Channels

Before proceeding with the more realistic case of imperfect CSI, we consider first the perfect knowledge of all channel gains in the wireless network. It is assumed that the channels are non-fading from the perspective of RRM. This can be taken into account in the considered system model by setting $z_{kl}^{(s)} = 1$, $\forall k, l \in \mathcal{M}, s \in \mathcal{S}$, and assuming that the distance/location-dependent components $d_{kl}^{(s)}$, $\forall k, l \in \mathcal{M}, s \in \mathcal{S}$ can be acquired instantaneously and without errors. Under this assumption, the interference coupling matrix $\mathbf{A}$ and the derived effective interference coupling matrix $\mathbf{G}$ are deterministic matrices.

4.2.1 Problem formulation

In the considered scenario, the main challenge is to allocate wireless resources (transmit powers and RBs) to the users while ensuring that their QoS requirements (expressed in terms of SINR requirements, as discussed in Section 2.3) are satisfied. In this regard, let the vectors $\boldsymbol{\gamma}^{(s)} \coloneqq (\gamma_1^{(s)}, \ldots, \gamma_M^{(s)}) \in \mathbb{R}_{\geq 0}^{MS}$, where $\gamma_k^{(s)} \coloneqq \gamma_k \cdot \pi_{ks}$, collect the respective SINR targets of all users in RB $s \in \mathcal{S}$. Hereby, we consider the SINR targets of users that are not assigned to transmit in RB s to be zero. It is well-known [SWB09] (references therein) that given any fixed allocation matrix $\boldsymbol{\Pi} \in \mathcal{P}$, a necessary and sufficient condition for the feasibility of the SINR requirements of all of the allocated users is

$$\rho\big(\boldsymbol{\Gamma}\mathbf{G}\big) < 1. \tag{4.8}$$

Here, $\rho(\mathbf{X})$ is used to denote the spectral radius [Mey00, p. 497] of any quadratic matrix $\mathbf{X}$, $\mathbf{G}$ is defined in (4.7), and

$$\boldsymbol{\Gamma} \coloneqq \boldsymbol{\Gamma}(\boldsymbol{\Pi}) \coloneqq \operatorname{diag}(\boldsymbol{\gamma}^{(1)}, \ldots, \boldsymbol{\gamma}^{(S)}) \in \mathrm{R}_{\geq 0}^{MS \times MS}. \tag{4.9}$$

The condition in (4.8) can be interpreted as follows: if the condition is satisfied for some RB allocation, then there exists a power assignment such that the SINR requirement of each user is satisfied [SWB09]. It should be noted, however, that said power assignment does not necessarily satisfy any power constraints that may be in place [SWB09]. In this regard, let the vector

$$\mathbf{q} \coloneqq (\mathbf{p}^{(1)}, \ldots, \mathbf{p}^{(S)}) \in \mathbb{R}_{\geq 0}^{MS} \tag{4.10}$$

contain the transmit powers of all users in all RBs, where $\mathbf{p}^{(s)} \coloneqq \left(p_1^{(s)}, \ldots, p_M^{(s)}\right)$ denotes the power vector associated with RB $s \in \mathcal{S}$. Considering this interpretation, a power vector satisfying the SINR requirements is given by

$$\mathbf{q}\left(\boldsymbol{\Pi}\right) = \sigma^2\Big(\mathbf{I} - \alpha_{\mathrm{pow}}\boldsymbol{\Gamma}\mathbf{G}\big(\boldsymbol{\Pi}\big)\Big)^{-1}\boldsymbol{\Gamma}\mathbf{1} \tag{4.11}$$

for some $\alpha_{\mathrm{pow}} \in [1, 1/\rho(\boldsymbol{\Gamma}\mathbf{G}(\boldsymbol{\Pi})))$ and any $\boldsymbol{\Pi} \in \mathcal{P}$ if (4.8) is satisfied [SWB09]. Clearly, any reasonable solution must fulfill the condition that a user does not invest transmit power in RBs in which it is not assigned to transmit, i.e.,

$$p_k^{(s)} = 0 \Leftarrow \pi_{ks} = 0, \, \forall k \in \mathcal{M}, s \in \mathcal{S}, \tag{4.12}$$

in addition to the power constraints in (2.1). Note, however, that (4.12) is always satisfied under the proposed approach, since $\gamma_k^{(s)} = 0$ if $\pi_k^{(s)} = 0$ (cf. (4.9)). Hence, if $\mathbf{q}$ satisfies (2.1) and (4.8) holds, then we consider $\boldsymbol{\Pi} \in \mathcal{P}$ to be a feasible allocation matrix.

A promising approach to the resource allocation problem at hand is to find a RB allocation that minimizes the spectral radius in (4.8), as it is a metric which characterizes the mutual interference between the scheduled transmissions. Formally, this is written as

$$\boldsymbol{\Pi}^* \in \arg\min_{\boldsymbol{\Pi} \in \mathcal{P}} \rho\left(\boldsymbol{\Gamma}\mathbf{G}(\boldsymbol{\Pi})\right), \tag{4.13}$$

where the dependence of $\mathbf{G}$ on the allocation matrix $\boldsymbol{\Pi} \in \mathcal{P}$ is explicitly emphasized. Hereby, the set of feasible allocation matrices $\mathcal{P}$ may be restricted to only allow realizations of $\boldsymbol{\Pi}$, where all users are allocated at least one RB and the corresponding power vectors $\mathbf{q}\left(\boldsymbol{\Pi}\right)$

satisfy (2.1). Since this problem is of combinatorial nature and its complexity increases very fast with the number of RBs and users, an exhaustive search is not feasible in large-scale networks. Moreover, there is no other general approach to reach optimality in similar problems, as the scheduling problem has been shown to be NP-complete [Ull75, SMS06, BR07, CTV11]. Therefore, the solutions available in the literature are strongly dependent on the considered utility metric and communications system. Some heuristic algorithms for classical OFDM-based wireless networks, such as LTE, can be found in [SL05, WOM09, CPG+13], among others.

In this regard, finding an algorithm that minimizes the interference in the considered wireless system by solving (4.13) in feasible time is highly unlikely, as it is difficult to derive useful properties of the spectral radius $\rho\left(\mathbf{\Gamma G}(\mathbf{\Pi})\right)$ that would allow for the definition of an efficient algorithm. Moreover, an additional layer of complexity is added due to the considered system model (and the broadcast nature of V2X communication, in particular). As discussed in Section 2.2, the relevant worst-case links to a D2D receiver are determined by the RB allocation. As the spectral radius $\rho\left(\mathbf{\Gamma G}(\mathbf{\Pi})\right)$ quantifies the interference in the wireless system, the selection of the worst-case receivers can be formulated as finding the channels which maximize it, i.e.,

$$h_{kl}^{(s)} = \underset{h_{kl}^{(s)} \in \left\{ h_{kl}^{(s,r)} : r \in \mathfrak{R}(l) \right\}}{\arg\max} \rho\left(\mathbf{\Gamma G}\left(\mathbf{\Pi}\right)\right), \forall k, l \in \mathcal{M}, s \in \mathcal{S}, \tag{4.14}$$

where $h_{kl}^{(s,r)}$ denotes the channel coefficient for the link between transmitter k and the receiver r associated with transmission l in RB s. Hence, the channel coefficients for the (worst-case) links can be considered as a function of $\mathbf{\Pi}$, i.e., $h_{kl}^{(s)} = h_{kl}^{(s)}\left(\mathbf{\Pi}\right)$ and with it, $\mathbf{A} = \mathbf{A}\left(\mathbf{\Pi}\right)$. For convenience, these dependencies will be dropped from the notation.

It should be noted, however, that the minimization of the interference in the wireless system is not the primary objective of RRM in the context of this work. Its goal is to ensure that the QoS requirements of all allocated users are met, while maximizing the number of such allocated users. Hence, a heuristic algorithm for the construction of a feasible allocation matrix $\overline{\mathbf{\Pi}}$ under the considered assumption of perfect CSI knowledge is proposed in the following.

4.2.2 Resource Allocation with Spectral Radius Feasibility Check

Based on the above considerations, we define the Resource Allocation algorithm with a Spectral Radius Feasibility Check (RASRFC), as summarized in Algorithm 4.1. Its goal is to maximize the number of allocated V-UEs in the D2D underlay, while satisfying the SINR requirements of all of the allocated users. Starting from an empty allocation (i.e., no users are allowed to transmit in the system), the algorithm iteratively attempts to enable service for one more user in each step. Hereby, the condition in (4.8) is used as a feasibility test in order to determine if the resulting interference environment would allow for reliable communication.

The SINR requirements of all users that are to be served by the wireless system (i.e., $\gamma_k, \forall k \in \mathcal{M}$), and the channel coefficients for all of the potential links (i.e., $h_{kl}^{(s,r)}, \forall r \in \mathfrak{R}\left(l\right), k, l \in \mathcal{M}$) are the required input, whereas the output of RASRFC is a feasible allocation matrix $\overline{\mathbf{\Pi}}$. Due to the orthogonality of RBs, the allocation of each individual RB can be considered independently, from the perspective of interference feasibility[1]. This intuitive

[1] The allocation of RBs is subject to power constraints as well. Their effect is taken into account by a second stage feasibility check, which is discussed later on.

result can also be derived analytically from the condition in (4.8). Per definition (cf. Section 4.1), the matrix $\mathbf{\Gamma G}(\mathbf{\Pi})$ represents the normal form of a reducible matrix [Var09] with the mutually independent matrices

$$\mathbf{V}^{(s)} \coloneqq \operatorname{diag}\left(\boldsymbol{\gamma}^{(s)}\right)\left(\mathbf{A}^{(s)} \circ \mathbf{E}^{(s)}\right) \in \mathbb{R}_{\geq 0}^{M \times M}, s \in \mathcal{S}, \tag{4.15}$$

on the diagonal and zeros in the remaining entries. As a consequence the following holds [Var09]:

$$\rho(\mathbf{\Gamma G}(\mathbf{\Pi})) = \max_{s} \rho\left(\mathbf{V}^{(s)}\right). \tag{4.16}$$

In other words, provided that $\rho\left(\mathbf{V}^{(s)}\right) < 1, \forall s \in \mathcal{S}$, holds, the condition in (4.8) holds as well. Hence, each RB is treated individually in RASRFC, as reflected by the loop starting in line 3 in Algorithm 4.1.

In a first step, the algorithm attempts to allocate a C-UE in the considered RB s, in accordance with the primary application of the radio resources. Hereby, it identifies the C-UE that would cause the least interference to any V-UE in the D2D underlay, as reflected by the interference coupling coefficients $a_{k,l}^{(s)}, \forall k, l \in \mathcal{M}, k \leq K, l > K$, specified in Definition 4.1. These coefficients are to be evaluated under the assumption that only the individual users k and l are transmitting simultaneously. Provided that it will not lead to a violation of the sum power constraints that may be in place or some predefined Mobile Network Operator (MNO) policies, RB s is allocated to the considered C-UE (cf. lines 7–16). The former is ensured by verifying that the resulting power vector is member of the family of feasible power assignments denoted as $\mathfrak{P} \coloneqq \left\{\mathbf{q} : \sum_{s=1}^{S} p_k^{(s)} \leq P_k, \right\}$. This set is defined to reflect the sum power constraints in (2.1). The latter check is denoted by the boolean function policy $(\mathbf{\Pi})$ which returns a true value if the considered allocation matrix is deemed feasible. This function can be used to enforce, for example, SC-FDMA properties in the cellular UL allocation or fairness among users by restricting the set of feasible resource allocations $\mathcal{P}$ accordingly. Note that a spectral radius feasibility check is not required in this step since users are allocated orthogonal resources, which does not increase the spectral radius of $\mathbf{\Gamma G}(\overline{\mathbf{\Pi}})$. Due to the definition of the effective interference coupling matrix, the allocation of a single user in a given RB $s \in \mathcal{S}$ results in an all zeros matrix $\mathbf{V}^{(s)}$ with $\rho\left(\mathbf{V}^{(s)}\right) = 0$. Hence, the property in (4.16) guarantees that the spectral radius of $\mathbf{\Gamma G}(\overline{\mathbf{\Pi}})$ will not increase.

In the second step, the considered RB s is also allocated to V-UE(s) in order to realize the reuse gain. To this end, the V-UEs are sorted according to the interference they would cause to the already allocated C-UE, as reflected by the interference coupling coefficients $a_{k,l}^{(s)}, \forall k, l \in \mathcal{M}, k > K, l \in \mathcal{K}_{\text{active}}$. Hereby, the set $\mathcal{K}_{\text{active}}$ denotes the index of the already allocated C-UE, and the coefficients are to be evaluated under the assumption that the individual users k and l are transmitting simultaneously. Starting with the one causing the least interference, RASRFC tests if the allocation of s to an additional V-UE would cause a violation of the condition in (4.8). If this is not the case, and provided that the resulting power vector is feasible, and any MNO policies that may be in place are not violated, s is allocated to the considered V-UE. In case the spectral radius check is not passed, s is considered overloaded and no more V-UEs can reuse it. This is due to the structure of the matrix $\mathbf{\Gamma G}(\mathbf{\Pi})$, and the properties of its spectral radius, which can only grow with the increasing number of non-zero elements, i.e., $\rho(\mathbf{A}) \leq \rho(\mathbf{B})$ if $\mathbf{A}, \mathbf{B} \in \mathbb{R}^{MS \times MS} : \mathbf{A} \leq \mathbf{B}$ [Mey00, p. 619]. Here, the inequality is to be applied element-wise. In case no C-UE was allocated in the considered RB

Algorithm 4.1 Heuristic resource allocation algorithm based on a spectral radius feasibility check.

Input: SINR requirements $\gamma_k, \forall k \in \mathcal{M}$, Channel coefficients $h_{kl}^{(s,r)}, \forall r \in \mathfrak{R}(l), k, l \in \mathcal{M}$
Output: Feasible allocation matrix $\overline{\mathbf{\Pi}}$

$\overline{\mathbf{\Pi}} = 0^{M \times S}$;
$\mathfrak{P} \coloneqq \left\{ \mathbf{q} \in \mathbb{R}_{\geq 0}^{MS} : \sum_{s=1}^{S} p_k^{(s)} \leq P_k, \forall k \in \mathcal{M} \right\}$;
for $s = 1 : S$ **do**
  $\mathcal{K}_{\text{active}}^{(s)} = \{K+1, \ldots, M\}$;
  //first allocate a favorable cellular user in resource s
  $\mathbf{idx} = \mathbf{sort}\left(a_{k,l}^{(s)} | \pi_{ks} = \pi_{ls} = 1, \forall k, l \in \mathcal{M}, k \leq K, l > K \cap \pi_{k's} = 0, \forall k' \in \mathcal{M} \setminus \{k, l\} \right)$;
  for $i = 1 : K$ **do**
    $\mathbf{\Pi} = \overline{\mathbf{\Pi}}$;
    $\pi_{\mathbf{idx}(i) \to k, s} = 1$;
    $\mathbf{q} = \sigma^2 \left(\mathbf{I} - \alpha \mathbf{\Gamma G}(\mathbf{\Pi}) \right)^{-1} \mathbf{\Gamma 1}$;
    if policy $(\mathbf{\Pi})$ && $\mathbf{q} \in \mathfrak{P}$ **then**
      $\overline{\mathbf{\Pi}} = \mathbf{\Pi}$;
      $\mathcal{K}_{\text{active}}^{(s)} = \{k\}$;
      break;
    end if
  end for
  //then allocate D2D user(s) in reuse mode
  $\mathbf{idx} = \mathbf{sort}\left(a_{k,l}^{(s)} | \pi_{ks} = 1, \forall k \in \mathcal{M}, k > K \cap \pi_{k's} = \overline{\pi}_{k's}, \forall k' \in \mathcal{M} \setminus k, l \in \mathcal{K}_{\text{active}}^{(s)} \right)$;
  for $i = 1 : M - K$ **do**
    $\mathbf{\Pi} = \overline{\mathbf{\Pi}}$;
    $\pi_{\mathbf{idx}(i) \to k, s} = 1$;
    $\mathbf{q} = \sigma^2 \left(\mathbf{I} - \alpha \mathbf{\Gamma G}(\mathbf{\Pi}) \right)^{-1} \mathbf{\Gamma 1}$;
    if $\rho(\mathbf{\Gamma G}(\mathbf{\Pi})) < 1$ **then**
      if policy $(\mathbf{\Pi})$ && $\mathbf{q} \in \mathfrak{P}$ **then**
        $\overline{\mathbf{\Pi}} = \mathbf{\Pi}$;
      end if
    else
      break;
    end if
  end for
end for

in the first step (e.g., since all of the active C-UEs were already satisfied in a previous step), it can still be used for D2D communication. To this end, the V-UEs are sorted with regards to the interference coupling coefficients which describe the interference between V-UEs only. Starting from the one which would cause the weakest interference to any other, RB s is then allocated to as many V-UEs as possible, until the spectral radius feasibility check fails.

Note that Algorithm 4.1 summarizes the general concept of RASRFC. Practical imple-

mentations may benefit from the exclusion of users for which it is a-priori known that they cannot be allocated (e.g., due to depleted transmit power budget, or policy constraints) at a certain step. Moreover, some computations can be simplified using (4.16). Since changes are only applied to $\mathbf{V}^{(s)}$ in each step, it suffices to calculate $\rho\left(\mathbf{V}^{(s)}\right)$ instead of the spectral radius of the complete matrix $\boldsymbol{\Gamma}\mathbf{G}(\boldsymbol{\Pi})$. It should be further noted, that a similar two-stage framework was used in [EE04] for the joint scheduling and power control for wireless ad-hoc networks under the consideration of a different feasibility metric and time-division multiple access.

4.3 Fading Channels

The above RASRFC is well suited to the case of propagation environments where the channel gains can be predicted/known, as it can be seen in the performance evaluation in Chapter 6. However, the assumption of instantaneously available CSI (i.e., exactly knowing the values of $|h_{kl}|^2$) is too optimistic in wireless networks, where the signal propagation is subjected to random fading. In this regard, consider the random channel component to originate from multipath-induced fading following the Rayleigh distribution [Gol05] with variance σ_{kl}^2 for the link between transmitter k and an intended (worst-case) receiver for transmitter l. Hence, $z_{kl}^{(s)} \sim \exp\left(z; \frac{1}{2\sigma_{kl}^2}\right)$ [Gol05] can be assumed throughout the current section. In such scenarios, the best one can hope for is CDI, i.e., being able to measure or predict the constant components d_{kl} and being able to approximate the distributions of the random gains z_{kl}. Hence, enabling reliable (D2D and cellular) communication becomes quite challenging in such scenarios. To this end, we propose a resource allocation algorithm relying on a resource allocation feasibility metric, which projects the condition in (4.8) to the domain of random channel gains.

4.3.1 Resource Allocation Feasibility Metric

Considering $|h_{kl}|^2$, $\forall k, l \in \mathcal{M}$, to be random renders the effective interference coupling matrix $\mathbf{G}\left(\boldsymbol{\Pi}\right)$ random, in which case the spectral radius $\rho\left(\boldsymbol{\Gamma}\mathbf{G}\left(\boldsymbol{\Pi}\right)\right)$ is a random variable itself. Hence, it is not possible to determine its value with absolute certainty. However, the condition in (4.8) can be extended to the domain of random variables by imposing

$$\Pr\left(\rho(\boldsymbol{\Gamma}\mathbf{G}(\boldsymbol{\Pi})) \geq 1\right) \leq r_{\text{th}} \tag{4.17}$$

for a fixed probability threshold $r_{\text{th}} \in (0, 1]$, which defines an acceptable error in the estimation of the spectral radius. Building upon the previous results for non-fading channels, this condition can be interpreted as follows: if (4.17) is satisfied for some RB allocation, then there exists a power assignment (with a probability of at least $1 - r_{\text{th}}$) such that the SINR requirements of each user are satisfied. To add to the problem, $\rho\left(\boldsymbol{\Gamma}\mathbf{G}\left(\boldsymbol{\Pi}\right)\right)$ is difficult to express as an explicit function of the allocation matrix, as per Abel's theorem [Haz88, p. 7] there is no general algebraic formula for the solution of the characteristic polynomial of degree of five or higher. Hence, we propose an alternative condition for the feasibility of a given allocation matrix based on an upper bound of $\rho\left(\boldsymbol{\Gamma}\mathbf{G}\left(\boldsymbol{\Pi}\right)\right)$ that allows for an easier derivation of a scheduling algorithm.

Corollary 4.1 (Bound on the spectral radius using traces)**.** *Let* $\mathbf{A}$ *be a* $M \times M$ *complex matrix whose eigenvalues are not necessarily all real. Then the following holds:*

$$\rho(\mathbf{A}) \leq \left|\frac{\operatorname{Tr}\mathbf{A}}{M}\right| + \sqrt{\left(\frac{\operatorname{Tr}\mathbf{A}^*\mathbf{A}}{M} - \left|\frac{\operatorname{Tr}\mathbf{A}}{M}\right|^2\right)(M-1)}.$$

An equality only holds if $\mathbf{A}$ *is normal, its greatest eigenvalue* $\lambda_1 = c\frac{\operatorname{Tr}\mathbf{A}}{M}$ *for some scalar* $c \geq 1$ *and its remaining eigenvalues are all equal, i.e.,* $\lambda_2 = \lambda_3 = \cdots = \lambda_M$*.*

Proof. The corollary follows directly from [WS80, Theorem 3.1]. □

Theorem 4.1 (Upper Bound on the Spectral Radius)**.** *The upper bound* $\overline{\rho}(\mathbf{\Gamma G}(\mathbf{\Pi})) \geq \rho(\mathbf{\Gamma G}(\mathbf{\Pi}))$*, can be expressed as*

$$\overline{\rho}(\mathbf{\Gamma G}(\mathbf{\Pi})) \coloneqq \max_s \sqrt{\frac{M-1}{M}\sum_{k=1}^{M}\sum_{\substack{l=1,\\ l\neq k}}^{M}\left(\gamma_k \pi_{ks} a_{kl}^{(s)}\right)^2}. \tag{4.18}$$

Proof. To begin the proof, again consider that the matrix $\mathbf{\Gamma G}(\mathbf{\Pi})$ represents the normal form of a reducible matrix [Var09] with the matrices $\mathbf{V}^{(s)}, \forall s \in \mathcal{S}$, on the diagonal and zeros in the remaining entries, and that (4.16) holds. Hereby, we consider that the matrices $\mathbf{V}^{(s)}, \forall s \in \mathcal{S}$ are real and non-negative, and have an all-zeros diagonal per definition (cf. (4.15)), but are not necessarily symmetric. Therefore, they may have complex eigenvalues [Mey00, p. 492]. Applying Corollary 4.1, an upper bound of $\rho\left(\mathbf{V}^{(s)}\right)$ can be expressed as follows:

$$\rho\left(\mathbf{V}^{(s)}\right) \leq \sqrt{\frac{M-1}{M}\operatorname{Tr}\left(\mathbf{V}^{(s)\mathrm{T}}\mathbf{V}^{(s)}\right)}. \tag{4.19}$$

Expressing the trace as a sum and plugging (4.19) into (4.16) yields the formula in Theorem 4.1. □

The above defined upper bound is an explicit function of the resource allocation and can be used to determine the feasibility of a given allocation matrix as a sufficient condition (instead of the actual spectral radius). The effectiveness of such an approach, however, depends on the gap between the upper bound and the actual spectral radius. Hereby, as stated in Corollary 4.1, the equality $\overline{\rho}(\mathbf{\Gamma G}(\mathbf{\Pi})) = \rho(\mathbf{\Gamma G}(\mathbf{\Pi}))$ is only achieved when the matrices $\mathbf{V}^{(s)}$ are normal (i.e., when $\mathbf{V}^{(s)\mathrm{T}}\mathbf{V}^{(s)} = \mathbf{V}^{(s)}\mathbf{V}^{(s)\mathrm{T}}$), the $M-1$ smallest eigenvalues of each of the matrices $\mathbf{V}^{(s)}, \forall s \in \mathcal{S}$ are equal, and $\rho(\mathbf{\Gamma G}(\mathbf{\Pi})) = \frac{\operatorname{Tr}(\mathbf{\Gamma G}(\mathbf{\Pi}))}{MS} = 0$. None of the above conditions are guaranteed to be satisfied due to the definition of $\mathbf{V}^{(s)}$. Moreover, $\rho(\mathbf{\Gamma G}(\mathbf{\Pi})) = 0$ represents a trivial case with no interference in the system and is not of particular interest in the considered cellular network with D2D underlay. Hence, the case of $\overline{\rho}(\mathbf{\Gamma G}(\mathbf{\Pi})) > \rho(\mathbf{\Gamma G}(\mathbf{\Pi}))$ is likely. Figure 4.1 illustrates the cumulative distribution function (cdf) of the gap $\overline{\rho}(\mathbf{\Gamma G}(\mathbf{\Pi})) - \rho(\mathbf{\Gamma G}(\mathbf{\Pi}))$ for $M = 20, K = 1, S = 1$, and under different numbers of allocated users (i.e., ones in the allocation matrix $\mathbf{\Pi}$) to share this resource in the cell. Hereby, arbitrary (but specific and fixed) interference coupling coefficients are used to illustrate the behavior of the proposed upper bound in the considered application. As it can be seen, the gap to the actual spectral radius is quite small when only 2 users are allocated in the available RB, but grows with the number of allocated transmissions.

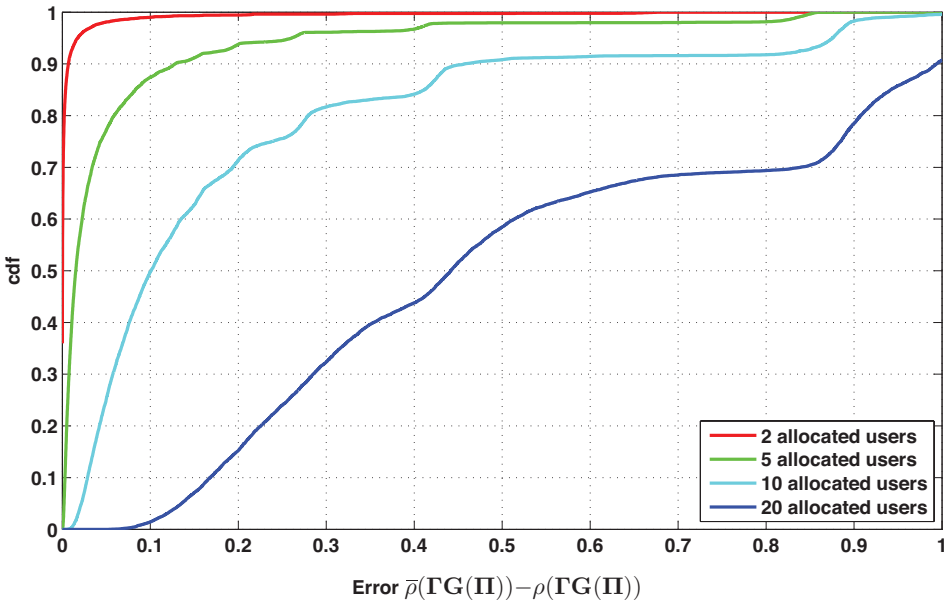

Figure 4.1: Cumulative distribution function of the gap between the derived upper bound the the actual spectral radius for arbitrary interference coupling coefficients.

Number of allocated users	2	5	10	20
Portion of feasible allocation matrices considered infeasible [%]	0	5×10^{-4}	1.76	30.13

Table 4.1: Portion of feasible allocation matrices rendered infeasible due to the consideration of the upper bound on the spectral radius.

In accordance, Table 4.1 summarizes the occurrence of 'false negatives', i.e., situations where $\overline{\rho}(\mathbf{\Gamma G}(\mathbf{\Pi})) \geq 1$, but $\rho(\mathbf{\Gamma G}(\mathbf{\Pi})) < 1$, in the considered experiments. In other words, it summarizes the portion of feasible allocation matrices rendered infeasible should

$$\overline{\rho}(\mathbf{\Gamma G}(\mathbf{\Pi})) < 1 \tag{4.20}$$

be considered as a feasibility condition instead of (4.8). Formally, this portion can be expressed as $\Pr\left(\overline{\rho}(\mathbf{\Gamma G}(\mathbf{\Pi})) \geq 1 | \rho(\mathbf{\Gamma G}(\mathbf{\Pi})) < 1\right)$. As it can be seen, using (4.20) as a feasibility criterion does not lead to any false negatives, if only 2 users are allocated to the available RB. Increasing the number of allocated transmissions, however, leads to an increase in the gap between the actual spectral radius and its upper bound. If all 20 users are allocated to reuse the available RB, this renders $\approx 30\%$ of the otherwise feasible allocation matrices infeasible. It should be noted, however, that allocating the same RB to such a large number of users within the same cell, is likely to be infeasible in realistic scenarios (cf. the results in Chapter 6). Hence, considering the lower occurrence of false negatives in scenarios with less users allocated to the same RB, the condition in (4.20) is deemed a good approximation of the original requirement in (4.8) (in reasonable scenarios) and can be used instead.

However, $\overline{\rho}(\mathbf{\Gamma G}(\mathbf{\Pi}))$ is still a random variable and its value cannot be determined with absolute certainty. Nevertheless, the probability with which it takes a value in a certain range, provided that the distributions of the random channel gains are known, can be controlled.

Corollary 4.2. *From Theorem 4.1 follows that* $\Pr\left(\rho(\mathbf{\Gamma G}(\mathbf{\Pi})) \geq 1\right) \leq \Pr\left(\overline{\rho}(\mathbf{\Gamma G}(\mathbf{\Pi})) \geq 1\right)$. *Hence, it suffices to set* $\Pr\left(\overline{\rho}(\mathbf{\Gamma G}(\mathbf{\Pi})) \geq 1\right) \leq r_{th}$ *in order to ensure that* $\Pr\left(\rho(\mathbf{\Gamma G}(\mathbf{\Pi})) \geq 1\right) \leq r_{th}$.

Corollary 4.3. *The inequality* $\overline{\rho}(\mathbf{\Gamma G}(\mathbf{\Pi})) \geq 1$ *can equivalently be expressed as* $\max_s \frac{M-1}{M} \sum_{k=1}^{M} \sum_{\substack{l=1,\\ l\neq k}}^{M} \left(\gamma_k \pi_{ks} a_{kl}^{(s)}\right)^2 \geq 1$.

For brevity, let

$$\tilde{\rho} \coloneqq \max_s \frac{M-1}{M} \sum_{k=1}^{M} \sum_{\substack{l=1,\\ l\neq k}}^{M} \left(\gamma_k \pi_{ks} a_{kl}^{(s)}\right)^2. \tag{4.21}$$

The above two corollaries build the foundation for the formulation of a condition for the feasibility of a certain allocation matrix in random fading channels. To this end, we still require an expression for $\Pr\left(\tilde{\rho} \geq 1\right)$, which we derive in the following, based on the probability density function (pdf) of $\tilde{\rho}$. We first consider the 'random' part of the addends consisting of $Z_{kl}^{(s)} = \frac{z_{kl}^{(s)2}}{z_{kk}^{(s)2}}$ (part of the multiplier $a_{kl}^{(s)2}$, cf. Definition 4.1).

Theorem 4.2. *The pdf of* $Z_{kl}^{(s)}$ *can be expressed as:*

$$f_{Z_{kl}^{(s)}}(z) = \frac{\sigma_{kl}^2 \sigma_{kk}^2}{2\sigma_{kk}^4 z\sqrt{z} + 4\sigma_{kl}^2 \sigma_{kk}^2 z + 2\sigma_{kl}^4 \sqrt{z}}, z > 0. \tag{4.22}$$

Proof. Consider $Z_{kl}^{(s)} = \left(\frac{z_{kl}^{(s)}}{z_{kk}^{(s)}}\right)^2 = X^2$ and $z_{kl}^{(s)} \sim f_{z_{kl}^{(s)}}(z) \coloneqq \exp\left(z; \frac{1}{2\sigma_{kl}^2}\right)$, according to the assumed system model. As a consequence, X represents the quotient of two exponentially distributed random variables, and its pdf can be derived using the quotient distribution rule [Cur41, Theorem 3.1]:

$$f_X(x) = \int_{-\infty}^{+\infty} |y| f_{z_{kl}^{(s)}}(xy)\, f_{z_{kk}^{(s)}}(y)\, \mathrm{d}y \tag{4.23}$$

$$= \int_{0}^{+\infty} \frac{1}{2\sigma_{kl}^2} \mathrm{e}^{-\frac{xy}{2\sigma_{kl}^2}} \frac{1}{2\sigma_{kk}^2} \mathrm{e}^{-\frac{y}{2\sigma_{kk}^2}} \mathrm{d}y = \frac{1}{4\sigma_{kl}^2 \sigma_{kk}^2} \int_{0}^{+\infty} \mathrm{e}^{-\left(\frac{x}{2\sigma_{kl}^2} + \frac{1}{2\sigma_{kk}^2}\right) y} \mathrm{d}y \tag{4.24}$$

$$= \frac{\sigma_{kl}^2 \sigma_{kk}^2}{\left(\sigma_{kk}^2 x + \sigma_{kl}^2\right)^2}, x > 0. \tag{4.25}$$

Finally, considering $Z_{kl}^{(s)} = g(X) = X^2$ and $g^{-1}(z) = \sqrt{z}$, and $\frac{\mathrm{d}g^{-1}(z)}{\mathrm{d}z} = \frac{1}{2\sqrt{z}}$, the following holds ('change of variables' with monotonic transformation function [Bon13]):

$$f_{Z_{kl}^{(s)}}(z) = f_X\left(g^{-1}(z)\right) \left|\frac{\mathrm{d}g^{-1}(z)}{\mathrm{d}z}\right| = \frac{\sigma_{kl}^2 \sigma_{kk}^2}{\left(\sigma_{kk}^2 x + \sigma_{kl}^2\right)^2} \frac{1}{2\sqrt{z}} \tag{4.26}$$

$$= \frac{\sigma_{kl}^2 \sigma_{kk}^2}{2\sigma_{kk}^4 z\sqrt{z} + 4\sigma_{kl}^2 \sigma_{kk}^2 z + 2\sigma_{kl}^4 \sqrt{z}}, z > 0. \tag{4.27}$$

□

Note that $f_{z_{kl}^{(s)}}$ will take different forms in non-Rayleigh environments (i.e., in environments where the random fading components follow a different distribution). Moreover, a closed-form expression is not guaranteed to exist. In such cases, the pdf can be approximated numerically. Whatever the case may be, the following results, derived for (4.22), can be adapted by plugging in any valid $f_{z_{kl}^{(s)}}$.

Corollary 4.4. *Now, consider* $I_{kl}^{(s)} = \gamma_k^2 \pi_{ks} \frac{d_{kl}^2}{d_{kk}^2} Z_{kl}^{(s)} = c_{kl} Z_{kl}^{(s)}$. *This random variable is the product of* $Z_{kl}^{(s)}$ *and a real positive constant and its pdf can, hence, be expressed as [Bon13]:*

$$f_{I_{kl}^{(s)}}(z) = \frac{\sigma_{kl}^2 \sigma_{kk}^2 \sqrt{c_{kl}}}{2\sigma_{kk}^4 z\sqrt{z} + 4\sigma_{kl}^2 \sigma_{kk}^2 \sqrt{c_{kl}} z + 2\sigma_{kl}^4 c_{kl} \sqrt{z}}, z > 0. \tag{4.28}$$

It should be noted, however, that if $\pi_{ks} = 0$ *for some* $k \in \mathcal{M}, s \in \mathcal{S}$ *(i.e., when user* k *is not allocated for transmission in RB* s*),* $I_{kl}^{(s)} = 0, \forall l \in \mathcal{M}$*, is reduced to a constant. Hence, the above definition of the pdf needs to be extended as follows:*

$$f_{I_{kl}^{(s)}}(z) = \begin{cases} \frac{\sigma_{kl}^2 \sigma_{kk}^2 \sqrt{c_{kl}}}{2\sigma_{kk}^4 z\sqrt{z} + 4\sigma_{kl}^2 \sigma_{kk}^2 \sqrt{c_{kl}} z + 2\sigma_{kl}^4 c_{kl} \sqrt{z}}, z > 0, & c_{kl} \neq 0, \\ \delta(0), & c_{kl} = 0, \end{cases} \tag{4.29}$$

where $\delta(\cdot)$ *denotes the Dirac delta function [Dir81, p. 58].*

Theorem 4.3 (Resource Allocation Feasibility Metric)**.** *With Corollaries 4.2-4.4 the following holds:*

$$r(\mathbf{\Pi}) \coloneqq \Pr(\tilde{\rho} \geq 1) \leq \sum_{s=1}^{S} \int_{\frac{M}{M-1}}^{\infty} \overset{M}{\underset{k=1}{(*)}} \overset{M}{\underset{\substack{l=1,\\ l\neq k}}{(*)}} f_{I_{kl}^{(s)}}(z)\, \mathrm{d}z, \tag{4.30}$$

where $(*)$ *denotes the convolution operator for a multitude of functions (i.e.,* $\overset{X}{\underset{x=1}{(*)}} f_x(z) = f_1(z) * f_2(z) * \cdots * f_X(z)$*) and* $r(\mathbf{\Pi})$ *shall hereinafter be referred to as resource allocation feasibility metric (or feasibility metric in short).*

Proof. Consider the S independent events $E_s \coloneqq \left(\frac{M-1}{M} \sum_{k=1}^{M} \sum_{\substack{l=1,\\ l\neq k}}^{M} I_{kl}^{(s)} \geq 1 \right), s \in \mathcal{S}$. Hence,

$$\Pr(\tilde{\rho} \geq 1) = \Pr(\text{at least one of the } S \text{ events } E_s \text{ occurs}) \tag{4.31}$$

$$= \sum_{s=1}^{S} \Pr(E_s) - \sum_{s=1}^{S-1} \sum_{s'=s+1}^{S} \Pr(E_s \cap E_{s'}) \tag{4.32}$$

$$+ \sum_{s=1}^{S-2} \sum_{s'=s+1}^{S-1} \sum_{s''=s'+1}^{S} \Pr(E_s \cap E_{s'} \cap E_{s''}) - \dots,$$

where (4.32) yields from the Poincaré formula [RW00, p. 407] and has S terms in total, following the established scheme. The upper bound of the RHS (i.e., the union bound $\sum_{s=1}^{S} \Pr(E_s)$),

is nevertheless a particularly good approximation thereof, if the probability of each E_s is small. Hence, it can be used to reduce the computational complexity. In addition, substituting

$$\Pr(E_s) = \Pr\left(\sum_{k=1}^{M}\sum_{\substack{l=1,\\ l\neq k}}^{M} I_{kl}^{(s)} \geq \frac{M}{M-1}\right) = \int_{\frac{M}{M-1}}^{\infty} \underset{k=1}{\overset{M}{(*)}} \underset{\substack{l=1,\\ l\neq k}}{\overset{M}{(*)}} f_{I_{kl}^{(s)}}(z)\,\mathrm{d}z, \tag{4.33}$$

as the pdf of the sum of independent random variables is the convolution of the individual pdfs [Ibe11], yields the final result in Theorem 4.3. □

4.3.2 Analysis

The proposed feasibility metric $r(\mathbf{\Pi})$ for CDI-based resource allocation can be interpreted as an extension of the condition for CSI-based resource allocation in (4.8) and quantifies the interference environment under the considered allocation matrix. As such, $1 - r(\mathbf{\Pi})$ gives a (lower bound on the) probability with which a power assignment exists such that all of the allocated users' SINR requirements can be met (although it does not need to satisfy all power constraints that are in place).

As the density of V-UEs can be extremely high, especially in inner city scenarios, an additional objective of RRM allocation for D2D-based V2X communication is to allow for the highest possible reuse of radio resources. Maximizing both $1 - r(\mathbf{\Pi})$ and the number of supported users, is a combinatorial problem with very high complexity, similar to the problem of CSI-based resource allocation (cf. Section 4.2.1). It should be noted that the wireless system is supposed to exhibit consistent and predictable behavior in order to enable C-ITS applications. Therefore, maximizing $1 - r(\mathbf{\Pi})$ plays a secondary role compared to guaranteeing a certain baseline performance. In consequence, a reasonable approach to the problem of finding a feasible allocation matrix $\mathbf{\Pi}$ is to keep $r(\mathbf{\Pi})$ below a certain tolerable threshold r_{th}, according to the desired performance, while maximizing the number of UEs utilizing each RB. In fact, this problem resembles the well known Knapsack problem [KPP04] which deals with filling a knapsack with a collection of items from a given set. Hereby, each item is associated with a weight and a value, and a selected collection is said to be optimal when the total weight is less than or equal to a given limit and the total value is as large as possible. Considering that our goal is to enable transmissions with guaranteed QoS, the value in our problem can be measured by the number of allocated users. Allocating an additional user (or packing one more user in the knapsack), however leads to an additional non-negative addend in $r(\mathbf{\Pi})$ per definition. This non-decreasing metric can be thought of as the weight of the knapsack. Further, let us consider r_{th} as the knapsack's capacity (as it denotes the tolerable bound on the resource allocation feasibility metric). With this, we can formulate the problem at hand as

$$\max_{\mathbf{\Pi}\in\mathcal{P}} \mathbf{1}_M^{\mathrm{T}} \mathbf{\Pi} \mathbf{1}_S \quad \text{subject to} \tag{4.34a}$$

$$r(\mathbf{\Pi}) \leq r_{\mathrm{th}}, \tag{4.34b}$$

which is the general nonlinear Knapsack problem [KPP13, p. 409]. This problem has been shown to be NP-hard [Hoc07]. Therefore, finding an optimal allocation matrix $\mathbf{\Pi}$ (in the sense of maximizing the allocated users while $r(\mathbf{\Pi}) \leq r_{\mathrm{th}}$) is not possible in polynomial time. A satisfactory solution can be found, however, by a greedy approximation algorithm.

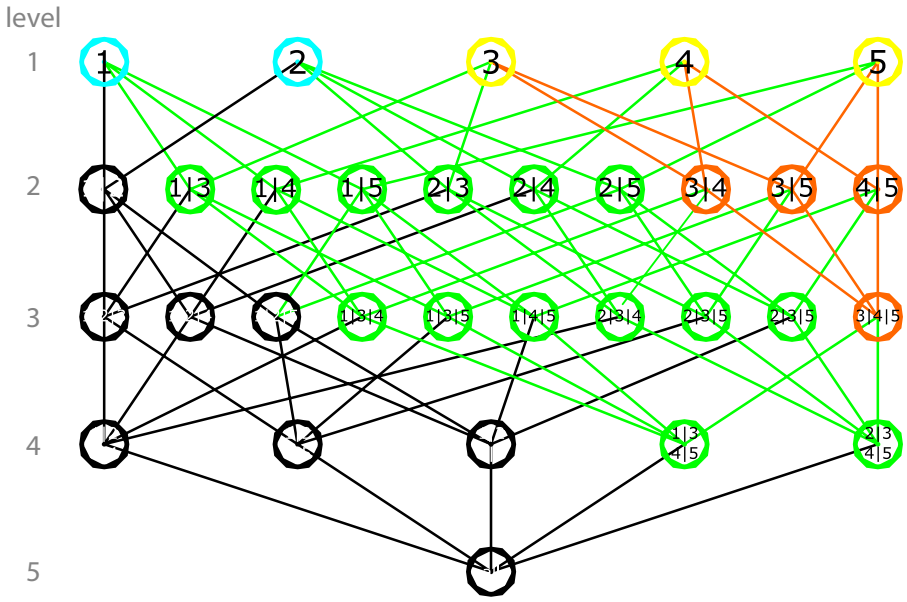

Figure 4.2: Exemplary allocation graph for a given RB s with $M = 5$ and $K = 2$.

To define such an algorithm, we consider the process of selecting users to be allocated to a specific RB s as a walk on an allocation graph, such as the one shown in Figure 4.2. For illustrative purposes, we consider $M = 5$ users in total, the first two of which are C-UEs. The vertices, as indicated by their indices, suggest distinct options for reusing a RB (e.g., '1|4|5' indicates that all three of the stated users simultaneously utilize the considered RB) and, hence, correspond to different allocation matrices. Therefore, each vertex is further associated with a different value of the resource allocation feasibility metric. A desirable allocation matrix is one which is associated with a vertex in the higher levels of the allocation graph, as these correspond to a higher number of allocated users.

The edges in the graph indicate a connection between the respective feasibility metric values, i.e., the feasibility metric value of a higher level vertex is a function of the feasibility metric values of all of the connected lower level vertices. Hereby, higher level vertices can never have a lower value of the feasibility metric than any of the connected lower level vertices. This is due to the definition of r ($\mathbf{\Pi}$) and can be understood intuitively as allowing for one more user to reuse the same RB cannot improve the interference situation and, hence, cannot improve the feasibility metric value. Moreover, starting from the second level by selecting the vertex with lowest feasibility metric value and following the edges to the next connected vertex with lowest feasibility metric value (unless it violates the set threshold r_{th}) is guaranteed to lead the walk on the graph to the *locally* highest level vertex with a minimal feasibility metric. The term 'locally' in this context is used to emphasize the fact that there may be another higher (or equal) level vertex in the graph with a lower value of the feasibility metric. The globally optimal vertex (i.e., the highest level vertex with feasible and minimal feasibility metric among all other vertices of the same level) can be found by starting the walk on the highest level and following the respective edges that leads to the steepest decrease in the value of the feasibility metric. This approach, however, is equivalent to an exhaustive search (as the feasibility metrics of all of the vertices in the graph need to be determined due to their functional dependencies) and is not applicable in large scale networks due to the extremely

high computational complexity. Moreover, it should be noted that attempting to allocate a relatively high number of RBs to a high number of users generates diversity effects that are likely to lead the simple walk to a vertex on the graph that matches the level of the globally optimal one closely. As previously stated, this is the main priority with regards to the allocation of RBs to users.

It should be noted that the first level of the allocation graph reflects the allocation of a single user and per definition leads to $r(\mathbf{\Pi}) = 0$ (for $S = 1$, or no increase in the feasibility metric for $S > 1$). Hence, the allocation of at least one user in each RB is always possible under lack of power constraints. Furthermore, the graph can be divided into different regions which can be useful in reducing the complexity of the walk. For example, the paths highlighted in black in Figure 4.2 consider allocating two C-UEs in the same RB which is guaranteed to lead to a violation of their SINR requirements in a system where the serving eNB has only a single receive antenna at its disposal. Hence, these paths need not be considered by the allocation algorithm in such a system. Additionally, the green marked paths correspond to allocation matrices where a C-UE is allocated in the considered RB. This might be imposed as a prerequisite for V-UEs to reuse spectrum primarily intended for cellular communication. As a consequence, the orange marked paths, which correspond to the allocation of V-UEs only, could also be ignored. The combination of green and orange marked paths needs to be considered in a reversed scenario, where the C-UEs reuse spectrum primarily intended for C-ITS applications or when serving the most V-UEs is prioritized by the MNO.

4.3.3 CDI-based Resource Allocation Algorithm

Based on the above properties of the feasibility metric (and the insights obtained in Section 4.2.2), a heuristic method is defined in the following to find a satisfactory allocation matrix with reasonable effort. Algorithm 4.2 summarizes this proposition for the composition of an assignment matrix that allows for the SINR requirements of all of the allocated users to be satisfied. Its goal is to maximize the number of allocated V-UEs in each RB. Each RB is again treated separately since there is no interference between users assigned to different resources due to the considered orthogonality (cf. Section 4.2.2 and the definition of the feasibility metric in Theorem 4.3). In a first step, the algorithm identifies a pair of users that causes the least increase in the feasibility metric if allocated to simultaneously utilize RB s. Hereby, the allocation of s to the considered UEs must not lead to a violation of the feasibility constraints (i.e., $r(\mathbf{\Pi}^*) < r_{\text{th}}$), their power constraints (i.e., the resulting power vector must be contained in the family of feasible power vectors $\mathfrak{P}$), or some predefined MNO policies (as indicated, again, by the policy check function $\text{policy}(\mathbf{\Pi})$). These MNO policies may include, for example, the constraint that (for as long as there are unsatisfied C-UEs) one of the users in the allocated pair is a C-UE (i.e., following the green paths in Figure 4.2). A method for retrieving the power vector $\mathbf{q}$ that allows for the SINR requirements of all allocated users to be satisfied is presented in Section 4.3.4.

Once the considered RB s is assigned to a pair of users, the algorithm proceeds to check if additional V-UEs can be accommodated in the same radio resources. To this end, the search for a feasible allocation matrix is sequentially extended to the domain of allocating $i > 3, i \in \mathbb{N}$ users denoted as $\mathcal{P}^{(i)}$. Starting with the one causing the smallest increase in the feasibility metric, the CDI-based Resource Allocation Algorithm (CDI-bRAA) tests if the allocation of s to an additional V-UE causes a violation of the feasibility, power, or policy constraints. If all of these constraints are met, the additional V-UE is allocated and the search continues

Algorithm 4.2 CDI-based resource allocation algorithm.

Input: SINR requirements $\gamma_k, \forall k \in \mathcal{M}$, CDI (i.e., $d_{kl}^{(r)}, \forall r \in \mathfrak{R}(l), k, l \in \mathcal{M}$ and pdf of $z_{kl}^{(s,r)}, \forall r \in \mathfrak{R}(l), k, l \in \mathcal{M}$)

Output: Feasible allocation matrix $\overline{\mathbf{\Pi}}$

$\mathfrak{P} = \left\{ \mathbf{q} \in \mathbb{R}_{\geq 0}^{MS} : \sum_{s=1}^{S} p_k^{(s)} \leq P_k, \forall k \in \mathcal{M} \right\}$;
$\overline{\mathbf{\Pi}} = 0^{M \times S}$;
for $s = 1 : S$ **do**
  $\mathcal{P} = \left\{ \mathbf{\Pi} \in \{0,1\}^{M \times S} : \pi_{ks'} = \pi_{ks'}, \forall s' \in \mathcal{S} \setminus s, \sum_{k=1}^{M} \pi_{ks} = 2 \right\}$;
  $\mathbf{\Pi}^* = \arg\min_{\mathbf{\Pi} \in \mathcal{P}} r(\mathbf{\Pi})$,
  if $r(\mathbf{\Pi}^*) < r_{\text{th}} \cap \mathbf{q}(\mathbf{\Pi}^*) \in \mathfrak{P} \cap \text{policy}(\mathbf{\Pi}^*)$ **then**
    $\overline{\mathbf{\Pi}} = \mathbf{\Pi}^*$;
    for $i = 3 : M - K + 1$ **do**
      $\mathcal{P}^{(i)} = \left\{ \mathbf{\Pi} \in \{0,1\}^{M \times S} : \pi_{ks'} = \pi_{ks'}, \forall s' \in \mathcal{S} \setminus s, \right.$
        $\left. \pi_{k's} = 1, \forall k' \in \mathcal{M} : \pi_{k's} = 1, \sum_{k=1}^{M} \pi_{ks} = i \right\}$;
      do
        $\mathbf{\Pi}^* = \arg\min_{\mathbf{\Pi} \in \mathcal{P}^{(i)}} r(\mathbf{\Pi})$;
        if $r(\mathbf{\Pi}^*) < r_{\text{th}} \cap \mathbf{q}(\mathbf{\Pi}^*) \in \mathfrak{P} \cap \text{policy}(\mathbf{\Pi}^*)$ **then**
          $\mathbf{\Pi} = \mathbf{\Pi}^*$;
          break;
        else if $r(\mathbf{\Pi}^*) < r_{\text{th}}$ **then**
          $\mathcal{P}^{(i)} = \mathcal{P}^{(i)} \setminus \mathbf{\Pi}^*$;
        end if
      while $r(\mathbf{\Pi}^*) < r_{\text{th}} \cap \mathcal{P}^{(i)} \neq \emptyset$
    end for
  else
    $\mathbf{\Pi}^* = \mathbf{\Pi}; \pi^*_{\arg\max_k \{U(k)\} s} = 1$;
    if $\mathbf{q}(\mathbf{\Pi}^*) \in \mathfrak{P} \cap \text{policy}(\mathbf{\Pi}^*)$ **then**
      $\overline{\mathbf{\Pi}} = \mathbf{\Pi}^*$;
    end if
  end if
end for

by adding one more user to the potential allocation assignment, i.e. $i \to i + 1$. Otherwise, if the feasibility constraint is not violated (but at least one of the other constraints is) the search continues for the current i while the last tested allocation is excluded from the explored domain. In case the feasibility constraint is violated, the RB s is considered to be overloaded and no more users can reuse it.

If it is impossible to allocate at least one pair of users in the first place, only a single user

is appointed to utilize RB s. It is chosen according to an urgency metric[2] $U(k), \forall k \in \mathcal{M}$, and its allocation must not violate any power constraints that are in place. Note that such an allocation will not increase the feasibility metric. Hence, there is no need to pass the feasibility check.

Furthermore, as discussed earlier (cf. Section 2.2 and Section 4.2.1), the RB allocation determines the worst-case receiving V-UE for each D2D transmission. Formally, the evaluation of the feasibility metric needs to consider the tuples

$$\left\{d_{kl}, z_{kl}^{(s)}\right\} = \underset{\left\{d_{kl}, z_{kl}^{(s)}\right\} \in \left\{\left\{d_{kl}^{(r)}, z_{kl}^{(s,r)}\right\} : r \in \mathfrak{R}(l)\right\}}{\arg\max} r(\mathbf{\Pi}), \forall k, l \in \mathcal{M}. \tag{4.35}$$

4.3.4 Power Control

Problem Formulation

The aim of power control in the context of CDI-bRAA is to allow for the SINR targets of all of the allocated users (for a given allocation matrix $\mathbf{\Pi}$) to be met with a certain probability $r_{\mathrm{p,th}}$, while minimizing the transmission power. We consider the following form of the SINR experienced by the worst-case receiver of each transmission (cf. Section 2.3):

$$\mathrm{SINR}_k^{(s)} = \frac{d_{kk} z_{kk}^{(s)} p_k^{(s)}}{\sum\limits_{\substack{l \neq k, \\ \pi_{ls} \neq 0}} d_{lk} z_{lk}^{(s)} p_l^{(s)} + \eta_{ks}}, \forall k, s : \pi_{ks} = 1, \tag{4.36}$$

where the distance/location-dependent and random fading components of each channel gain are determined according to (4.35). Different noise powers for each user and RB, denoted as η_{ks}, are considered. Taking the SINR requirements of the allocated users into account, it is required to ensure that $\mathrm{SINR}_k^{(s)} \geq \gamma_k^{(s)}$ with high probability. Hence, the problem of Stochastic Power Control (SPC) can be formulated as

$$\min_{\mathbf{q} \in \mathbb{R}_{\geq 0}^{MS}} \mathbf{q}\mathbf{1}_{MS}^{\mathrm{T}} \quad \text{subject to} \tag{4.37a}$$

$$\Pr\left(\mathrm{SINR}_k^{(s)} < \gamma_k^{(s)}\right) \leq r_{\mathrm{p,th}}, \forall k, s : \pi_{ks} = 1, \tag{4.37b}$$

$$\mathbf{q} \geq 0. \tag{4.37c}$$

Solving this optimization problem (OP), however, requires some more knowledge on the form of the constraints in (4.37b).

Theorem 4.4. *Under the consideration of Rayleigh-fading channels, the constraints in* (4.37b) *can be equivalently expressed as*

$$\frac{\gamma_{ks}\eta_{ks}}{2\sigma_{kk}^2 d_{kk} p_k^{(s)}} + \sum_{\substack{l \neq k, \\ \pi_{ls} \neq 0}} \ln\left(1 + \gamma_{ks} \frac{\sigma_{lk}^2 d_{lk} p_l^{(s)}}{\sigma_{kk}^2 d_{kk} p_k^{(s)}}\right) + \ln(1 - r_{p,th}) \leq 0, \forall k, s : \pi_{ks} = 1. \tag{4.38}$$

[2]The remaining delay budget for the users' transmissions is a simple example for such a metric. More sophisticated metrics can also be defined, reflecting the MNO's preferences.

Proof. First, we consider the following reformulation by substituting (4.36) in (4.37b) :

$$\Pr\left(\mathrm{SINR}_k^{(s)} < \gamma_k^{(s)}\right) = \Pr\left(\frac{d_{kk} z_{kk}^{(s)} p_k^{(s)}}{\gamma_{ks}} < \sum_{\substack{l \neq k, \\ \pi_{ls} \neq 0}} d_{lk} z_{lk}^{(s)} p_l^{(s)} + \eta_{ks}\right) \tag{4.39}$$

$$= 1 - \Pr\left(t_k \geq \sum_{\substack{l \neq k, \\ \pi_{ls} \neq 0}} t_l + \eta_{ks}\right), \tag{4.40}$$

where t_x denote exponential random variables with a mean equal to λ_x, respectively. The probability of an exponential random variable being greater than the sum of independent exponential random variables can be expressed as [KB02]:

$$\Pr\left(t_k \geq \sum_{\substack{l \neq k, \\ \pi_{ls} \neq 0}} t_l + \eta_{ks}\right) = \mathrm{e}^{-\lambda_k \eta_{ks}} \prod_{\substack{l \neq k, \\ \pi_{ls} \neq 0}} \frac{1}{1 + \frac{\lambda_k}{\lambda_l}}. \tag{4.41}$$

Hence, by substituting the respective means, (4.38) can be evaluated as

$$1 - \Pr\left(t_k \geq \sum_{\substack{l \neq k, \\ \pi_{ls} \neq 0}} t_l + \eta_{ks}\right) = 1 - \mathrm{e}^{-\lambda_k \eta_{ks}} \prod_{\substack{l \neq k, \\ \pi_{ls} \neq 0}} \frac{1}{1 + \frac{\lambda_k}{\lambda_l}} \tag{4.42}$$

$$= 1 - \mathrm{e}^{-\frac{\gamma_{ks}\eta_{ks}}{2\sigma_{kk}^2 d_{kk} p_k^{(s)}}} \prod_{\substack{l \neq k, \\ \pi_{ls} \neq 0}} \frac{1}{1 + \gamma_{ks} \frac{2\sigma_{lk}^2 d_{lk} p_l^{(s)}}{2\sigma_{kk}^2 d_{kk} p_k^{(s)}}}. \tag{4.43}$$

Bounding this probability from above by $r_{p,\mathrm{th}}$ and reformulating by taking the natural logarithm, yields the result in Theorem 4.4. □

Considering Theorem 4.4, the OP at hand consists of a linear objective function and non-linear constraints. The constraints, however, are not convex as their Hessian matrix is not defined on the entire feasible set. Hence, the problem cannot be solved by using standard tools for convex programming. Nevertheless, numerical results can be retrieved by employing interior point methods or sequential quadratic programming [NW06]. Dealing with an akin problem, [DE03] further proposes an iterative fix-point method. These solutions, however, are computationally intensive in a large-scale network. Furthermore, CDI-bRAA requires multiple executions of the power control function per iteration and, hence, higher computational complexity may violate the real-time constraints of the resource allocation (i.e., a feasible resource and power assignment for each user needs to be retrieved within a transmission time interval). As a consequence, simplifying the above OP by means of a linear approximation of the constraints is hugely beneficial in practical applications.

Linear Approximation

Consider the following reformulation:

$$\Pr\left(\mathrm{SINR}_k^{(s)} < \gamma_k^{(s)}\right) = \Pr\left(\sum_{\substack{l\neq k,\\ \pi_{ls}\neq 0}} d_{lk} z_{lk}^{(s)} p_l^{(s)} > \frac{d_{kk} z_{kk}^{(s)} p_k^{(s)}}{\gamma_k^{(s)}} - \eta_{ks}\right) \tag{4.44}$$

and the event

$$E_{l_1} \coloneqq \left(d_{l_1 k} z_{l_1 k}^{(s)} p_{l_1}^{(s)} > \underbrace{\overbrace{\frac{d_{kk} z_{kk}^{(s)} p_k^{(s)}}{\gamma_k^{(s)}}}^{a} - \eta_{ks} - \sum_{\substack{l\neq k, l_1,\\ \pi_{ls}\neq 0}} d_{lk} z_{lk}^{(s)} p_l^{(s)}}_{b_1}\right) \tag{4.45}$$

for some arbitrary $l_1 \neq k : \pi_{l_1 s} = 1$. We have

$$\Pr\left(E_{l_1}\right) = \int_{b_1}^{\infty} \frac{1}{2\sigma_{l_1 k}^2 d_{l_1 k} p_{l_1}^{(s)}} \mathrm{e}^{-\frac{x}{2\sigma_{l_1 k}^2 d_{l_1 k} p_{l_1}^{(s)}}} \,\mathrm{d}x = \mathrm{e}^{-\frac{b_1}{2\sigma_{l_1 k}^2 d_{l_1 k}}}. \tag{4.46}$$

Bounding the probability of this undesired event by some given threshold r_p yields

$$\mathrm{e}^{-\frac{b_1}{2\sigma_{l_1 k}^2 d_{l_1 k} p_{l_1}^{(s)}}} \leq r_\mathrm{p} \Leftrightarrow b_1 \geq \ln\left(\frac{1}{r_\mathrm{p}}\right) 2\sigma_{l_1 k}^2 d_{l_1 k} p_{l_1}^{(s)}. \tag{4.47}$$

Defining E_{l_2} as the event of (4.47) not holding true, i.e.,

$$E_{l_2} \coloneqq \left(b_1 < \ln\left(\frac{1}{r_\mathrm{p}}\right) 2\sigma_{l_1 k}^2 d_{l_1 k}\right) = \left(d_{l_2 k} z_{l_2 k}^{(s)} p_{l_2}^{(s)} > b_2\right), \tag{4.48}$$

where $b_2 = a - \sum\limits_{\substack{l\neq k, l_1, l_2\\ \pi_{ls}\neq 0}} d_{lk} z_{lk}^{(s)} p_l^{(s)} - \ln\left(\frac{1}{r_\mathrm{p}}\right) 2\sigma_{l_1 k}^2 d_{l_1 k} p_{l_1}^{(s)}$, and bounding its probability yields:

$$\mathrm{e}^{-\frac{b_2}{2\sigma_{l_2 k}^2 d_{l_2 k} p_{l_2}^{(s)}}} \leq r_\mathrm{p} \Leftrightarrow b_2 \geq \ln\left(\frac{1}{r_\mathrm{p}}\right) 2\sigma_{l_2 k}^2 d_{l_2 k} p_{l_2}^{(s)}. \tag{4.49}$$

Repeating this procedure for the $N-1$ interferers to user k, where $N \coloneqq \sum\limits_{k=1}^{M} \pi_{ks}$, eventually yields

$$a \geq \sum_{\substack{l\neq k,\\ \pi_{ls}\neq 0}} \ln\left(\frac{1}{r_\mathrm{p}}\right) d_{lk} p_l^{(s)} 2\sigma_{lk}^2 \Leftrightarrow d_{kk} z_{kk}^{(s)} p_k^{(s)} \geq b_k, \tag{4.50}$$

where $b_k = \gamma_k^{(s)} \left(\sum\limits_{\substack{l\neq k,\\ \pi_{ls}\neq 0}} \ln\left(\frac{1}{r_\mathrm{p}}\right) d_{lk} p_l^{(s)} 2\sigma_{lk}^2 + \eta_{ks}\right)$. Note that the dependency of N on s is dropped from the notation for convenience. Finally, by defining E_k as the event of (4.50) not holding true, i.e.,

$$E_k \coloneqq \left(d_{kk} z_{kk}^{(s)} p_k^{(s)} < b_k\right), \tag{4.51}$$

and bounding its probability, it follows:

$$\Pr\left(E_k\right) = 1 - \mathrm{e}^{-\frac{b_k}{2\sigma_{kk}^2 d_{kk} p_k^{(s)}}} \leq r_\mathrm{p}. \tag{4.52}$$

From this, it follows that setting

$$p_k^{(s)} \geq \gamma_{ks} \frac{\sum\limits_{\substack{l \neq k, \\ \pi_{ls} \neq 0}} \ln\left(\frac{1}{r_\mathrm{p}}\right) d_{lk} p_l^{(s)} 2\sigma_{lk}^2 + \eta_{ks}}{\ln\left(\frac{1}{1-r_\mathrm{p}}\right) d_{kk} 2\sigma_{kk}^2} \tag{4.53}$$

will satisfy the SINR requirement of user k in RB s with a probability of

$$1 - \Pr\left(E_{l_1} \cup E_{l_2} \cup \cdots \cup E_{l_{N-1}} \cup E_k\right).$$

Calculating $0 \leq r_\mathrm{p} < 1$ such that $\Pr\left(E_{l_1} \cup E_{l_2} \cup \cdots \cup E_{l_{N-1}} \cup E_k\right) \leq r_{\mathrm{p,th}}$, however, is not possible in the general case, since the relations between these events are unknown. For the case that a given RB is only used by one UE, it can easily be seen that setting $r_\mathrm{p} = r_{\mathrm{p,\,th}}$ leads to the desired behavior (cf. Theorem 4.4). Knowing the statistics of the channel realizations, an appropriate value for r_p in all other possible scenarios in the considered system can be retrieved by applying the Monte Carlo method [Fis13]. In particular, the value of r_p is tuned to all of the deemed feasible resource allocations (according to the feasibility metric from Theorem 4.3) in a huge amount of experiments over different channel realizations such that the resulting overall probability of a SINR target violation is below the set target $r_{\mathrm{p,th}}$. Table 6.2 offers an excerpt of some of the resulting values for the communications environment considered in the performance evaluation (cf. Section 6.1). Hereby, the value of r_p shows a dependency on the total number of users sharing a specific RB s (i.e., N).

By using (4.53), the OP in (4.37) can be reformulated as

$$\min_{\mathbf{q} \in \mathbb{R}_{\geq 0}^{MS}} \mathbf{q}\mathbf{1}_{MS}^\mathrm{T} \quad \text{subject to} \tag{4.54a}$$

$$p_k^{(s)} \geq \gamma_{ks} \frac{\sum\limits_{\substack{l \neq k, \\ \pi_{ls} \neq 0}} \ln\left(\frac{1}{r_\mathrm{p}(N)}\right) d_{lk} p_l^{(s)} 2\sigma_{lk}^2 + \eta_{ks}}{\ln\left(\frac{1}{1-r_\mathrm{p}(N)}\right) d_{kk} 2\sigma_{kk}^2}, \; \forall k, s : \pi_{ks} \neq 0 \tag{4.54b}$$

$$\mathbf{q} \geq 0. \tag{4.54c}$$

The so formulated OP can be classified as a linear program [NW06] in the taxonomy of optimization and can be solved efficiently with the well established simplex or interior-point methods [NW06]. Note that as there is no dependency between the different RBs in this formulation, the problem of power control can be split into S smaller subproblems. As a consequence, the workload in each stage of CDI-bRAA (cf. Algorithm 4.2) can be reduced by only solving one of these subproblems. It should be further noted that due to the linearization of the constraints in (4.54a), the resulting power vectors are expected to display a gap to the feasible power assignment with minimal total power according to the original constraints (cf. Theorem 4.4). Further analysis in this direction is, however, omitted as power efficiency plays a secondary role to satisfying the reliability of the individual transmissions in the scope of this work. A further drawback of the proposed approximation is the need to calibrate r_p for the considered deployment.

4.4 Additional Aspects

4.4.1 Multicell Deployments

The proposed RASRFC and CDI-bRAA are directly applicable[3] in multicell deployments under the assumption that a central RRM entity can be used to make the scheduling decisions for the entire relevant area. This assumption, however, might be too optimistic in practical implementations. A single entity is unlikely to be able to allocate resources to all of the users in an unbounded area in real-time due to limited processing power. Furthermore, the coordination effort associated with such a centralized approach (i.e., collecting all of the required CDI and distributing the scheduling decisions) might take too long and create difficulties in meeting the delay requirements of C-ITS applications. Hence, a distributed approach, where each eNB determines the resource allocation to its served users, is preferable. It must be ensured, however, that users from neighboring cells do not cause high mutual interference. To this end, RASRFC and CDI-bRAA can be paired with distributed interference alignment techniques [MDV13], which have been extensively studied in the context of two-tier networks consisting of macro and micro cells. This can be done by defining policy constraints in Algorithm 4.1 and Algorithm 4.2, respectively, that ensure tolerable inter-cell interference levels. In the considered system model, the users that potentially suffer the most from inter-cell interference are V-UEs near the cell borders. Hence, an effective interference alignment technique can be as simple as avoiding the allocation of V-UEs near the cell border in the same RBs. To this end, a disjoint subset of the available RBs is to be chosen by each eNB to serve the affected users. A user can be deemed to be near a cell border when the Received Signal Strength (RSS) for other eNBs is within a certain margin from the RSS for its serving eNB. Note that more sophisticated techniques are applicable as well. However, herein, the performance of the proposed algorithms (cf. Chapter 6) is evaluated under the assumption of a central RRM entity.

4.4.2 Signaling and CSI/CDI Acquisition

It is clear that introducing a vehicular D2D underlay generates additional complexity as compared to conventional cellular systems. Hence, it is important to quantify the additional effort required to enable V2X communication based on the D2D paradigm, in terms of the required SMOH. Media access control protocols established in current 4G networks (although refinements can be expected in 5G) are used as a baseline for the following analysis. In particular, the considered V-UE transmissions can be thought of as UL transmissions, where the receiver is not the serving eNB. Hence, MAC concepts for the LTE UL can be projected to the considered D2D-enabled network. Figure 4.3 summarizes the resulting RB allocation protocol and the associated SMOH.

Scheduling Request

An essential condition for a V-UE to be granted radio resources for a transmission is the awareness at the serving eNB of the available data to be transmitted. Such awareness is achieved in LTE by means of Buffer Status Reports (BSRs), which are triggered when new data arrives in previously empty buffers [STB11]. In an effort to reduce the signaling overhead,

[3] Small modifications are needed to lift the restriction of allocating only one C-UE in each RB, and allow for C-UEs served by different eNBs to reuse radio resources.

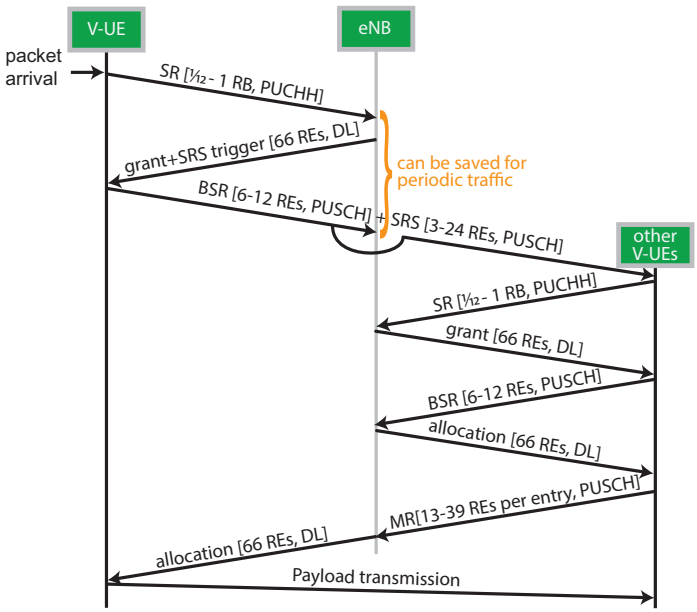

Figure 4.3: Signaling protocol and required resources for the operation of RASRFC/CDI-bRAA for general and periodic traffic.

LTE groups data buffers into four groups for reporting (although more buffer categories may exist on the UE side). By modifying one of these groups to refer to C-ITS messages, a BSR containing the corresponding identification will unambiguously identify D2D traffic. In such a case, using the so-called short BSR, which refers to a single buffer group (i.e., the D2D buffer in the considered deployment), is more beneficial, rather than the long BSR which contains the status of all four. With their size of 1 byte [3GP16], short BSRs are better suited as they introduce lower overhead and C-ITS messages are likely to be prioritized over any other types of traffic, rendering the contents of other buffers irrelevant for the time being. The first two bits identify the buffer group, and the remaining six bits quantify the size of the data stored in it. Hereby, the 64 possible values indicate that the data size is within a corresponding interval within the range of an empty buffer all the way up to above 150 kB (cf. [3GP16, Table 6.1.3.1-1]). Messages related to C-ITS applications, are expected to be much smaller and of discrete size. Hence, some of the identifiers used for greater amounts of data can be modified to refer to the exact size of a particular message in the buffer, by linking to its category. In this manner, a single BSR can accurately describe the demand for radio resources in order to transmit a specific message without the need for periodical updates. Furthermore, some C-ITS applications may generate periodic messages of regular size and, hence, predictable buffer status. Hence, by means of linking such categories to a specific buffer size indicator, the transmission of BSRs might not be required prior to each payload transmission. Instead, the scheduler can anticipate V-UEs, which have previously reported such traffic, as willing to transmit in the respective pre-configured intervals.

In the likely case that a V-UE does not have any UL transmissions scheduled for the instance when a BSR with regards to C-ITS traffic is triggered, it first requires to obtain radio resources for the transmission of the report. Assuming that V-UEs can constantly maintain a connected state and by using protocol designs from the LTE UL, this can be done by sending a Scheduling Request (SR) on pre-configured resources in the Physical Uplink

Control CHannel (PUCCH) [STB11]. Each RB assigned for such purpose can carry up to 12 UEs' SRs, multiplexed by means of code division. Once an eNB recognizes a specific UE's SR, it answers this request by allocating resources for the transmission of the BSR on the Physical Uplink Shared CHannel (PUSCH) [STB11]. Signaling this grant (which consists of 132 bits of coded control information for a system bandwidth of 20 MHz) takes up 66 REs in a downlink control channel, while the transmission of the BSR requires 6 to 12 REs in the PUSCH, depending on the chosen MCS. Once the eNB determines the amount of resources needed for the transmission (for a certain MCS), and the scheduling algorithm determines which RBs are to be used, another scheduling grant is sent to the considered UE, describing the RB allocation.

Channel Gain Measurement

In order to determine this RB allocation, CSI/CDI-based schedulers, such as RASRFC and CDI-bRAA, require knowledge over the relevant channel gains. In LTE, C-UEs are required to periodically transmit a Sounding Reference Signal (SRS) in the PUSCH for the purpose of channel quality estimation [STB11]. This concept can be extended to the considered network by instructing V-UEs to transmit such signals. These pilot signals occupy the last symbol in every second subcarrier (within the configured bandwidth) in a frame configured for SRS transmission. A minimum of 4 RBs are considered in this regard, which is also the best suited setting for the considered system. On the one hand, using the minimal bandwidth allows for higher power concentration (and, hence, more accurate channel estimation [Ber11]) and higher coverage distance (i.e., more UEs can be reached by the SRS). On the other hand, occupying less resources would allow for more V-UEs to simultaneously transmit SRSs. Hereby, up to 16 UEs may be multiplexed on the same RB by means of code division. However, the channel gain measurement is more accurate, if the noise contribution can be estimated. For this purpose, [Ber11] proposes to reserve certain windows for accurate noise estimation, hence, effectively reducing the maximum supported number of multiplexed UEs per RB to 14.

As information about every potential link in the system is required (cf. Algorithm 4.1 and Algorithm 4.2), all potential receivers in the system need to estimate the channels to every potential transmitter. The transmission of an SRS can be triggered by using a respective field in the scheduling request grant for the transmission of BSRs, while the actual configuration can be carried out in advance (e.g., when a UE establishes a connection) [STB11]. Hence, no further signaling overhead is considered for the transmission of a SRS in this analysis. Under these assumptions, non-transmitting V-UEs need to monitor the entire PUSCH bandwidth and attempt to identify power contributions by testing all possible SRS sequences, as they are not aware which exactly are to be expected. Under high load, this would, nevertheless, be the case even if the exact SRS configurations were known at the potential receivers.

Once the channel gain measurements are carried out at each non-transmitting V-UE, their results need to be forwarded to the eNB. In the case of CDI-bRAA, only the distance/location-dependent contribution, which can be extracted from the measurements by means of further processing is required to be transmitted. From a signaling point of view, one[4] channel gain value accompanied by a contributor identification needs to be forwarded to the eNB. In order to do so, each V-UE (that has measurements to report) first needs to obtain resources for this transmissions, by means of a SR. The Measurement Report (MR) can be considered to

[4]Note that other CSI-based schemes may require information about each of the 4 RBs (or more) in which a specific UE transmits, thus increasing the overhead further.

contain 14 bits to describe the channel gain (sufficient to represent the range of −163.83 dB to 0 dB with two decimals) and 12 bits to identify the starting RB, the comb, and cyclic shift of the measured SRS. Using this information, the eNB can unambiguously identify the considered channel. A V-UE needs to transmit a corresponding set of data for each identified SRS contribution (including SRSs transmitted by C-UEs). Not receiving a MR entry from a specific V-UE about a given triggered SRS is to be interpreted by the eNB to mean that the respective channel is too weak. The complete report size depends on the number of nearby active UEs and needs to be forwarded to the eNB by means of a BSR such that an adequate amount of resources can be allocated for its transmission.

4.4.3 Reuse of DL Resources

The proposed RASRFC and CDI-bRAA require no further extension with respect to the reuse of DL resources. The inversion of the roles of C-UEs and eNBs on the cellular links leads solely to a different interpretation of the CSI (or CDI, respectively), while the established notations are still applicable.

Chapter 5

Resource Allocation Based on Location Information

Many of the state-of-the-art RRM schemes for D2D underlay communication, as well as the RASRFC and CDI-bRAA proposed in Chapter 4, rely on some form of CSI. Its complete acquisition, however, is associated with a vast amount of signaling (cf. Section 4.4.2 and Section 6.3.2) and therefore significantly reduces the efficiency of the cellular network. This is especially the case when considering broadcast transmissions in the D2D underlay, as in the communications scenario of interest in this work. Moreover, fast moving terminals (such as vehicles) induce shorter channel coherence times. For example, a link from a static eNB/UE to a V-UE traveling at a speed of 50 km/h with a carrier frequency of 2 GHz has a coherence time of [Rap02]

$$T_{\mathrm{coh}} \approx \frac{0.423}{f_{\mathrm{D,50\,km/h}}} \approx 4.5\,\mathrm{ms}, \tag{5.1}$$

where $f_{\mathrm{D,50\,km/h}}$ stands for the maximal Doppler shift at the said velocity. The coherence time for a link between two V-UEs, both traveling with 50 km/h in opposite directions (i.e., resulting in a relative speed of 100 km/h), is only half of the above value. Such a short time interval may be insufficient for the complete CSI acquisition, the processing according to an arbitrary RRM scheme, and the distribution of the RB and power allocation in many practically relevant deployments. Hence, by the time the scheduling and power control decisions are made, the acquired CSI is likely to be outdated, thus compromising the network performance.

Motivated by the above mentioned short-comings of CSI-based RRM in the context of the considered communications scenario, we explore an alternative approach to the problem at hand. Encouraged by the behavior of the upper bounds on the asymptotic MPUTC both in the primary network and in the D2D underlay under the location-based model (cf. Section 3.3), this chapter proposes a corresponding feasible RRM scheme for practical deployments. The results of this work are published in [Bot13, BKKF14, BSF15a, BKKF15, BSF16a].

5.1 Basic Concept and Preliminary Work

The basic concept of the Location Dependent Resource Allocation Scheme (LDRAS) was previously introduced in the author's Master's thesis [Bot13] considering only non-fading channels and simpler communication scenarios, and is briefly summarized in the current section. More

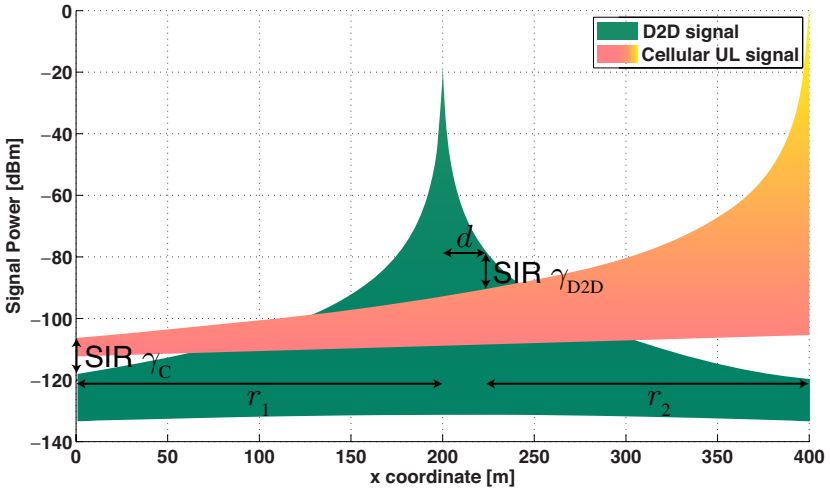

Figure 5.1: Spatial distribution of the signal power radiated by two transmitters occupying the same radio resources.

detailed explanations, considering specific aspects of the scheme, are provided in the following sections, which constitute the contributions of this work beyond the state of the art.

Motivated by the properties of wireless channels (and the location-based RRM model presented in Section 3.3), LDRAS defines a resource reuse strategy based on sufficient separation between C-UEs, V-UEs, and eNBs (affected by transmissions that reuse the same RBs). Figure 5.1 illustrates the idea behind it with a simple example of reuse of UL radio resources between one C-UE and one V-UE. Consider an eNB located at $x = 0\,\text{m}$ to be the receiver of a transmission by a C-UE located at $x = 400\,\text{m}$. Moreover, consider a V-UE located at $x = 200\,\text{m}$ that broadcasts a transmission to any other V-UE within the relevant distance of d. While the transmit power of the C-UE ($P_{\text{C-UE}}$) is determined by the comparatively large separation from the eNB (and bounded by hardware limitations), the transmit power of the V-UE ($P_{\text{V-UE}}$) can be chosen significantly lower, as the relevant distance d is generally much smaller. For given transmit powers for both UEs, it is possible to achieve predefined SINR targets for (a) cellular communication γ_{C} and (b) D2D communication γ_{D2D} by maintaining a certain minimum distance between the eNB and the interfering V-UE (r_1), and between the V-UE and the interfering C-UE (r_2).

Such separation between UEs and eNBs affected by the reuse of given RBs is enforced in LDRAS by means of cell partitioning. The considered cellular network is split on sub-cellular level into a total of Z spatially disjoint zones, whose dimensions are determined by r_1 and r_2. The available radio resources in each cell are then split into Y RB subsets $\mathcal{RB}_y$ ($y \in \mathcal{Y} = \{1, \ldots, Y\}$) and for each zone $z \in \mathcal{Z} = \{1, \ldots, Z\}$, a specific set of RBs is reserved for D2D communication. The same RB sets $\mathcal{RB}_y$ are then also reused within the primary network. However, here the sets are only allowed to be reused in zones with sufficient spatial separation, as given by r_2, in order to limit the interference caused by C-UEs to the D2D underlay to a given threshold. Hence, from resource management point of view, a zone is fully described by the tuple $\left(z, \mathcal{RB}_{\text{D2D},z} \subset \{\mathcal{RB}_y\}_{y=1}^{Y}, \mathcal{RB}_{\text{C},z} \subset \{\mathcal{RB}_y\}_{y=1}^{Y}\right)$ constructed by the zone index z, the reserved RB sets for D2D communication $\mathcal{RB}_{\text{D2D},z}$, and the reserved RB sets for cellular communication $\mathcal{RB}_{\text{C},z}$. Note that a V-UE transmitting within a distance of r_1 from an eNB will cause high interference to any UL transmission in the same RBs. Hence, the

subset of RBs reserved for D2D communication in such zones around each eNB cannot be reused by any C-UE within the same cell.

Under the simpler assumptions in [Bot13] (i.e., non-fading channels and simple communication scenario with only one cross-interferer), two sources of interference need to be considered in the cell partitioning: (a) the interference caused at the eNB by transmitting V-UEs in the D2D underlay and (b) the interference caused at the D2D receivers from the UL signals of the C-UEs in the primary network. With this, the guard distances r_1 and r_2 are determined as a function of the SINR target γ_{C} (in dB), the SINR target γ_{D2D} (in dB), and the required transmission range d (in m) between communicating V-UEs. Assuming that the power of the interference signal at the eNB is much higher than the noise power, the SINR target γ_{C} is satisfied by setting

$$r_1 \geq \overline{PL}^{-1}\left(\gamma_{\mathrm{C}} - R_0 + P_{\text{V-UE}} + G_0\right), \tag{5.2}$$

where R_0 denotes a certain target RSS at the eNB (in dBm), $P_{\text{V-UE}}$ the transmit power of V-UE (in dBm), and G_0 the maximum antenna gain at the receiving eNB (in dBi). Moreover, $\overline{PL}\,(.)$ denotes a specific path loss model for the link between the interfering V-UE and the eNB, which maps a distance in meter to a path loss value in dB.

In order to satisfy the minimum SINR threshold γ_{D2D}, a minimum distance r_2 between zones (or equivalently, between V-UEs and C-UEs) that spatially reuse the same resources $\mathcal{RB}_z$ has to be maintained such that

$$r_2 \geq PL^{-1}\left(\gamma_{\mathrm{D2D}} - P_{\text{V-UE}} + PL\,(d) + P_{\text{C-UE}}\right). \tag{5.3}$$

Here, an isotropic, zero dBi gain antenna is assumed at the receiving V-UEs. Furthermore, note that $PL\,(.)$ denotes a specific path loss model for the link between the interfering C-UE and the receiving V-UE as well as for the link between two V-UEs.

The conditions in (5.2) and (5.3) are used to derive a zone topology that guarantees the required separations for reliable cellular and D2D communication. Figure 5.2 illustrates an arbitrary example for cell partitioning with generic zone design (as well as a corresponding resource reservation) for a single isolated sector of a three-sector LTE deployment in an urban environment. Hereby, some arbitrary channel models and arbitrary values for the relevant control parameters (i.e., the parameters on the RHS in (5.2) and (5.3)) are used to evaluate $r_1 = 100\,\mathrm{m}$ and $r_2 = 200\,\mathrm{m}$, satisfying the conditions in (5.2) and (5.3). Based on these design parameters, the cell is split into a total of $Z = 11$ zones. Polygonal zone shapes are chosen in this example, since they allow for a simple map representation of the zone topology with just a few points in space. Assuming a uniform user distribution, the number of reserved RBs for each zone is selected proportional to its size. This allows for splitting the set $\mathcal{RB}_{10}$ into two halves to be used for cellular communication in the smaller zones $z = 1$ and $z = 5$. Again, note that this is a simple example to illustrate the concept of LDRAS. The selection of channel models and control parameters (along with further details on the scheme's mechanics) is explained and justified once it is extended and applied to the scenario of interest in this work.

Once the zone topology and resource reservation are defined, the allocation of radio resources is determined as follows. Since the zone topology does not change over time, it is stored in the memory of each V-UE, which uses its built-in positioning system in order to track its location. Hence, each V-UE can signal its corresponding zone index z to the eNB, along with its SR. The eNB then assigns a subset of RBs from the set $\mathcal{RB}_{\mathrm{D2D},z}$ to the requesting V-UE. Note that the size of the subset depends on the data rate requirements of the

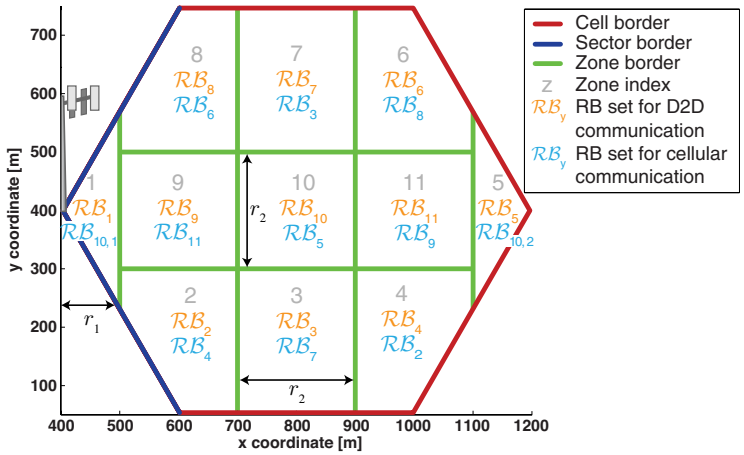

Figure 5.2: Example of cell partitioning, zone design and resource assignment for a single urban cell.

corresponding V2X service and on the RB availability. In the primary network the resources are assigned to C-UEs according to the network operator's scheduling policy, with the additional constraint that only RBs of the set which has been assigned to the respective zone for cellular communication can be allocated. In this manner, the need of full CSI knowledge at the eNB is eliminated and thus the necessity for extensive channel measurements and signaling overhead. Further details and enhancement of the resource allocation mechanism under LDRAS are presented in Section 5.5.

The described basic concept fails to consider fading channels, multiple interference sources, and heterogeneous propagation environments. These issues are addressed in Section 5.2 of this work. Moreover, a clustering approach for the definition of the zone topology is presented in Section 5.3, while Section 5.4 is devoted to a graph coloring approach to determine the RB reservation such that transmissions in neighboring zones do not cause harmful mutual interference.

5.2 Spatial Resource Reuse Scheme

5.2.1 Homogeneous Propagation Environment

The first task in applying the initial LDRAS concept is the derivation of appropriate guard distances. To this end, we extend the conditions in (5.2) and (5.3) to take the considered channel model (cf. Section 2.2) into account. In this regard, consider first the case of a homogeneous propagation environment (i.e., the distance/location-dependent portion of the channel gains only depend on the link distance and are consistent across different locations in the network).

Since it is desired to avoid the need for complete instantaneous CSI/CDI, LDRAS may not use such information to determine the allocation matrix and the power vector for the active users in the system. Nevertheless, all of the allocated transmissions still need to satisfy the imposed QoS requirements. Hence, with the instantaneous propagation conditions unknown, the resource reuse scheme in LDRAS is built around the presumption of a permanently occurring worst-case scenario.

Assumption 5.1. *As the (cross-) interference in this location-based scheme is controlled via the spatial separation of the affected UEs/eNBs, we assume that all of the (relevant) interferers are at the same minimal tolerable distance from an affected receiver and transmit at their maximum power in the worst-case scenario.*

In this regard, we consider some simplifications to the SINR model for the derivation of the guard distances. Based on the worst-case presumption, there is no need to consider the SINR of individual transmissions. However, differentiation between cellular and D2D transmissions is beneficial.

Assumption 5.2. *We assume that the interference contributions originating from C-UEs, which are more than half the cell range away from the receiving V-UE are negligible (in the sum-interference).*

Definition 5.1 (Simplified SINR Model for Direct Links)**.** *Consider the following model for the worst-case SINR in the D2D underlay:*

$$SINR_{D2D} = \frac{P_{V\text{-}UE} h\left(d\right) g}{\sum\limits_{i=1}^{6} P_{C\text{-}UE} h\left(r_2\right) g_i + \sum\limits_{j=1}^{3} P_{V\text{-}UE} h\left(r_2\right) g_j}, \tag{5.4}$$

where $h\left(\cdot\right)$ denotes the distance-dependent component of the channel gain at the respective distance for direct links and g denotes the random power gain due to fading.

Hereby, the above definition considers interference-dominated SINR, where the noise power can be ignored in the calculations. Moreover, it is based on the practical observation that the relevant cross-interferers (i.e., C-UEs) are at most six in count. Figure 5.3 illustrates the considered constellation. In typical cellular deployments, interference due to transmissions in neighboring cells add to the interference caused by users within the same cell. In this regard, transmissions associated with UEs near the cell edge are known to suffer the most from this *inter-cell interference*. Hence, receiving V-UEs near the border between cells are expected to be affected the most by UL transmissions originating at C-UEs outside the cell they reside in. According to Assumption 5.2, there are at most six relevant close cells. As per the system model, each of the six cells may only support one UL transmission in a given RB each. According to Assumption 5.1, all of the six relevant cross-interferers contribute with an equally strong constant interference component (i.e., transmit with their maximum transmit power and are located at the same distance from the affected receiving V-UE). Similarly, only the three strongest interfering V-UEs are considered in the simplified SINR model. This is due to the expected much lower transmit power in the D2D underlay. Moreover, for the sake of simplicity, the interfering V-UEs are to be separated from the considered receiving V-UE by the same guard distance as the C-UEs (i.e., r_2).

Considering the fading nature of the channels, reaching a given SINR target for D2D communication cannot be guaranteed in all cases even under the above simplified model. However, the probability that the SINR target is violated can be determined as a function of the guard distance r_2. Again, assuming Rayleigh-fading for all of the links in the network with the same[1] variance σ^2_{D2D} for the direct ones, the power gains follow an exponential distribution [Gol05,

[1] The same variance on all links is chosen for the sake of simpler expressions. The results can be extended for different variance values at the cost.

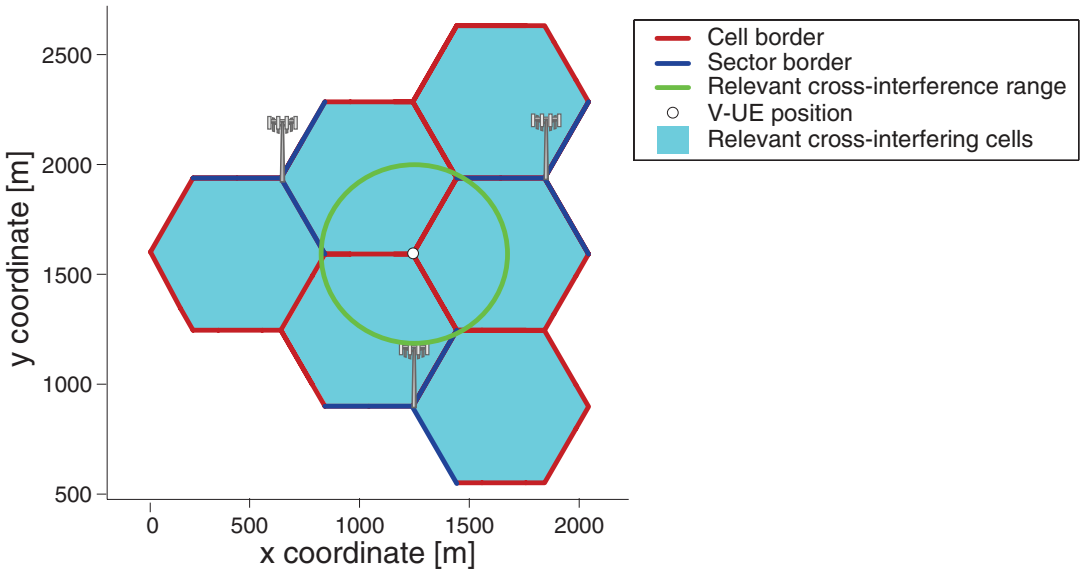

Figure 5.3: Illustration of the relevant cross-interference sources considered in the simplified SINR model for direct links under LDRAS.

p. 74], i.e., $g \sim \exp\left(\frac{1}{2\sigma^2_{\mathrm{D2D}}}\right)$, $g_i \sim \exp\left(\frac{1}{2\sigma^2_{\mathrm{D2D}}}\right)$, and $g_j \sim \exp\left(\frac{1}{2\sigma^2_{\mathrm{D2D}}}\right), \forall i = 1, \ldots, 6, j = 1, 2, 3$.

Theorem 5.1 (Outage Probability for Direct Links). *Under the simplified SINR model, the probability with which a given SINR target for D2D communication γ_{D2D} is violated is given by*

$$\Pr\left(SINR_{D2D} < \gamma_{D2D}\right) \coloneqq \beta_1^6 \beta_2^3 \Bigg[\frac{1}{\beta^3}\left(\frac{1}{(\alpha\gamma_{D2D}+\beta_1)^6} - \frac{1}{\beta_1^6}\right) + \frac{3}{\beta^4}\left(\frac{1}{(\alpha\gamma_{D2D}+\beta_1)^5} - \frac{1}{\beta_1^5}\right) \tag{5.5}$$

$$+ \frac{6}{\beta^5}\left(\frac{1}{(\alpha\gamma_{D2D}+\beta_1)^4} - \frac{1}{\beta_1^4}\right) + \frac{10}{\beta^6}\left(\frac{1}{(\alpha\gamma_{D2D}+\beta_1)^3} - \frac{1}{\beta_1^3}\right) \tag{5.6}$$

$$+ \frac{15}{\beta^7}\left(\frac{1}{(\alpha\gamma_{D2D}+\beta_1)^2} - \frac{1}{\beta_1^2}\right) + \frac{21}{\beta^8}\left(\frac{1}{(\alpha\gamma_{D2D}+\beta_1)} - \frac{1}{\beta_1}\right) \tag{5.7}$$

$$- \frac{1}{\beta^6}\left(\frac{1}{(\alpha\gamma_{D2D}+\beta_2)^3} - \frac{1}{\beta_2^3}\right) + \frac{6}{\beta^7}\left(\frac{1}{(\alpha\gamma_{D2D}+\beta_2)^2} - \frac{1}{\beta_2^2}\right) \tag{5.8}$$

$$- \frac{21}{\beta^8}\left(\frac{1}{(\alpha\gamma_{D2D}+\beta_2)} - \frac{1}{\beta_2}\right) \Bigg], \tag{5.9}$$

where $\alpha \coloneqq \frac{1}{2P_{V\text{-}UE}h(d)\sigma^2_{D2D}}, \beta_1 \coloneqq \frac{1}{2P_{C\text{-}UE}h(r_2)\sigma^2_{D2D}}, \beta_2 \coloneqq \frac{1}{2P_{V\text{-}UE}h(r_2)\sigma^2_{D2D}}$, *and* $\beta \coloneqq \beta_1 - \beta_2$.

Proof. To begin the proof, note that the nominator and denominator in (5.4) consist of (sums) of scaled exponentially distributed random variables. Let $Z_{\mathrm{S}} \coloneqq P_{\mathrm{V\text{-}UE}} h\left(d\right) g$ denote the

random variable in the nominator. Applying the rule for changing variables [Bon13], its pdf can be expressed as:

$$f_{Z_{\mathrm{S}}}(z) = \frac{1}{P_{\text{V-UE}} h(d)} f_g\left(\frac{z}{P_{\text{V-UE}} h(d)}\right) = \frac{1}{2P_{\text{V-UE}} h(d)\,\sigma^2_{\text{D2D}}} \mathrm{e}^{-\frac{z}{2P_{\text{V-UE}} h(d)\sigma^2_{\text{D2D}}}} = \alpha \mathrm{e}^{-\alpha z}. \quad (5.10)$$

Hence, Z_{S} is again an exponentially distributed random variable with variance α (as defined in Theorem 5.1). Moreover, let $Z_{\mathrm{I}} \coloneqq \sum_{i=1}^{6} P_{\text{C-UE}} h(r_2)\, g_i + \sum_{j=1}^{3} P_{\text{V-UE}} h(r_2)\, g_j$. With the above results, each individual addend is an exponentially distributed random variable with variance β_1 or β_2, respectively. Applying the results in [AM97], the pdf of Z_{S} can, hence, be expressed as:

$$f_{Z_{\mathrm{I}}}(z) = \beta_1^6 \beta_2^3 \mathcal{L}^{-1}\left\{\left(\frac{1}{\iota+\beta_1}\right)^6 \left(\frac{1}{\iota+\beta_2}\right)^3\right\}(z), \quad (5.11)$$

where $\mathcal{L}^{-1}$ denotes the reverse Laplace transform with respect to ι. Evaluating the RHS yields

$$f_{Z_{\mathrm{I}}}(z) = \beta_1^6 \beta_2^3 \left(-\frac{z^5 \mathrm{e}^{-\beta_1 z}}{120\beta^3} - \frac{z^4 \mathrm{e}^{-\beta_1 z}}{8\beta^4} - \frac{z^3 \mathrm{e}^{-\beta_1 z}}{\beta^5} - \frac{5z^2 \mathrm{e}^{-\beta_1 z}}{\beta^6}\right. \quad (5.12)$$

$$\left. + \frac{z^2 \mathrm{e}^{-\beta_2 z}}{2\beta^6} - \frac{15z \mathrm{e}^{-\beta_1 z}}{\beta^7} - \frac{21 \mathrm{e}^{-\beta_1 z}}{\beta^8} - \frac{21 \mathrm{e}^{-\beta_2 z}}{\beta^8}\right). \quad (5.13)$$

Hence, using the quotient distribution rule [Cur41], the pdf of $SINR_{\mathrm{D2D}} = \frac{Z_{\mathrm{S}}}{Z_{\mathrm{I}}}$ is given by:

$$f_{SINR_{\mathrm{D2D}}}(x) = \int_{-\infty}^{+\infty} |z| f_{Z_{\mathrm{S}}}(xz)\, f_{Z_{\mathrm{I}}}(z)\,\mathrm{d}z \tag{5.14}$$

$$= \alpha\beta_1^6\beta_2^3 \int_0^{+\infty} z\mathrm{e}^{-\alpha xz}\left(-\frac{z^5\mathrm{e}^{-\beta_1 z}}{120\beta^3} - \frac{z^4\mathrm{e}^{-\beta_1 z}}{8\beta^4} - \frac{z^3\mathrm{e}^{-\beta_1 z}}{\beta^5} - \frac{5z^2\mathrm{e}^{-\beta_1 z}}{\beta^6}\right. \tag{5.15}$$

$$\left. + \frac{z^2\mathrm{e}^{-\beta_2 z}}{2\beta^6} - \frac{15z\mathrm{e}^{-\beta_1 z}}{\beta^7} - \frac{21\mathrm{e}^{-\beta_1 z}}{\beta^8} - \frac{21\mathrm{e}^{-\beta_2 z}}{\beta^8}\right)\mathrm{d}z \tag{5.16}$$

$$= \alpha\beta_1^6\beta_2^3 \left(- \int_0^{+\infty} \frac{z^6\mathrm{e}^{-(\alpha x+\beta_1)z}}{120\beta^3}\,\mathrm{d}z - \int_0^{+\infty} \frac{z^5\mathrm{e}^{-(\alpha x+\beta_1)z}}{8\beta^4}\,\mathrm{d}z - \int_0^{+\infty} \frac{z^4\mathrm{e}^{-(\alpha x+\beta_1)z}}{\beta^5}\,\mathrm{d}z \right. \tag{5.17}$$

$$- 5\int_0^{+\infty} \frac{z^3\mathrm{e}^{-(\alpha x+\beta_1)z}}{\beta^6}\,\mathrm{d}z + \int_0^{+\infty} \frac{z^3\mathrm{e}^{-(\alpha x+\beta_2)z}}{2\beta^6}\,\mathrm{d}z - 15\int_0^{+\infty} \frac{z^2\mathrm{e}^{-(\alpha x+\beta_1)z}}{\beta^7}\,\mathrm{d}z \tag{5.18}$$

$$\left. -21\int_0^{+\infty} \frac{z\mathrm{e}^{-(\alpha x+\beta_1)z}}{\beta^8}\,\mathrm{d}z + 21\int_0^{+\infty} \frac{z\mathrm{e}^{-(\alpha x+\beta_2)z}}{\beta^8}\,\mathrm{d}z \right) \tag{5.19}$$

$$= \alpha\beta_1^6\beta_2^3 \left(- \frac{6}{\beta^3(\alpha x+\beta_1)^7} - \frac{15}{\beta^4(\alpha x+\beta_1)^6} - \frac{24}{\beta^5(\alpha x+\beta_1)^5} - \frac{30}{\beta^6(\alpha x+\beta_1)^4} \right. \tag{5.20}$$

$$\left. + \frac{3}{\beta^6(\alpha x+\beta_2)^4} - \frac{30}{\beta^7(\alpha x+\beta_1)^3} - \frac{21}{\beta^8(\alpha x+\beta_1)^2} + \frac{21}{\beta^8(\alpha x+\beta_2)^2} \right). \tag{5.21}$$

Finally, evaluating $\Pr(SINR_{\mathrm{D2D}} < \gamma_{\mathrm{D2D}}) = \int_0^{\gamma_{\mathrm{D2D}}} f_{SINR_{\mathrm{D2D}}}(x)\,\mathrm{d}x$ yields the result in the theorem. □

Based on the above theorem, an appropriate value for the guard distance r_2 can be derived for a given (feasible) targeted outage probability $p_{\mathrm{out,D2D}}$ (and for fixed maximal transmit powers and desired broadcast distance), such that

$$\Pr(SINR_{\mathrm{D2D}} < \gamma_{\mathrm{D2D}}) \leq p_{\mathrm{out,D2D}} \tag{5.22}$$

holds. A similar condition for the guard distance r_1, which ensures that

$$\Pr(SINR_{\mathrm{C}} < \gamma_{\mathrm{C}}) \leq p_{\mathrm{out,C}} \tag{5.23}$$

for some (feasible) targeted outage probability $p_{\mathrm{out,C}}$ is derived below.

The location-dependent resource allocation scheme can use conventional scheduling strategies for the cellular links and, hence, is able to use the already available cellular CSI in order to facilitate inter-cell interference coordination for the cellular transmissions (see Section 5.5 for details). The role of the guard distance r_1 is to protect the UL transmissions from the unknown cross-interference due to direct transmissions and it can be derived independent of the cellular inter-cell interference.

Definition 5.2 (Simplified SINR Model for Cellular UL Transmissions)**.** *Consider the following model for the worst-case SINR in the cellular UL for the purpose of parametrization of the spatial resource reuse scheme in LDRAS:*

$$SINR_C = \frac{R_0 g'}{\sum_{j=1}^{3} P_{V\text{-}UE} h'(r_1)\, g'_j}. \tag{5.24}$$

Here, $h'(\cdot)$ denotes the constant power gain at the considered distance for a link to the respective eNB and g' denotes the power gain due to random fading.

Again, we only consider the three strongest interfering V-UEs to contribute significantly to the cross-interference and it is assumed that the SINR is dominated by the interference power. Moreover, $g' \sim \exp\left(\frac{1}{2\sigma_{\mathrm{C}}^2}\right)$ and $g'_j \sim \exp\left(\frac{1}{2\sigma_{\mathrm{C}}^2}\right), \forall j = 1,2,3$, are independent according to our system model. Hereby, σ_{C}^2 denotes the variance on the links to an eNB.

Theorem 5.2 (Outage Probability for Cellular Links)**.** *Under the simplified SINR model, the probability with which a given SINR target for cellular communication γ_C is violated can be expressed as*

$$\Pr\left(SINR_C < \gamma_C\right) \coloneqq 1 - \frac{1}{\left(\alpha'\beta'\gamma_C + 1\right)^3}, \tag{5.25}$$

where $\alpha' = \frac{1}{2R_0\sigma_C^2}$, and $\beta' = \frac{1}{2P_{V\text{-}UE}h'(r_1)\sigma_C^2}$.

Proof. First, consider that the nominator and denominator in (5.24) consist of (sums) of scaled exponentially distributed random variables. Let $Z'_{\mathrm{S}} \coloneqq R_0 g'$ denote the random variable in the nominator. Applying the rule for changing variables [Bon13], its pdf is given by:

$$f_{Z'_{\mathrm{S}}}(z') = \frac{1}{R_0} f_g\left(\frac{z'}{R_0}\right) = \frac{1}{2R_0\sigma_{\mathrm{C}}^2} \mathrm{e}^{-\frac{z'}{2R_0\sigma_{\mathrm{C}}^2}} = \alpha' \mathrm{e}^{-\alpha' z'}. \tag{5.26}$$

Hence, Z'_{S} is again an exponentially distributed random variable with variance α' (as defined in Theorem 5.2). Moreover, let $Z'_{\mathrm{I}} \coloneqq \sum_{j=1}^{3} P_{\mathrm{V\text{-}UE}} h'(r_1)\, g'_j$. Again, each individual addend is an exponentially distributed random variable with variance β'. Applying the results in [AM97], the pdf of Z'_{I} can be expressed as:

$$f_{Z'_{\mathrm{I}}}(z') = \frac{\beta'^3}{2} z'^3 \mathrm{e}^{-\beta' z'}, \tag{5.27}$$

where β' is defined in Theorem 5.2. Hence, the pdf of $SINR_{\mathrm{C}} = \frac{Z'_{\mathrm{S}}}{Z'_{\mathrm{I}}}$ results from the quotient distribution rule [Cur41] as follows:

$$f_{SINR_{\mathrm{C}}}(x) = \int_{-\infty}^{+\infty} |z'| f_{Z'_{\mathrm{S}}}(xz')\, f_{Z'_{\mathrm{I}}}(z')\, \mathrm{d}z' = \frac{\alpha'\beta'^3}{2} \int_{0}^{+\infty} z'^3 \mathrm{e}^{-(\alpha' x + \beta')z'}\, \mathrm{d}z' = \frac{3\alpha'\beta'^3}{(\alpha' x + \beta')^4}. \tag{5.28}$$

The final result is obtained from the evaluation of $\Pr\left(SINR_{\mathrm{C}} < \gamma_{\mathrm{C}}\right) = \int_0^{\gamma_{\mathrm{C}}} f_{SINR_{\mathrm{C}}}(x)\, \mathrm{d}x$. □

It should be noted that the outage probabilities for direct and cellular links can take different forms in non-Rayleigh propagation environments. However, the following framework can still be applied by plugging in appropriate expressions.

5.2.2 Parameter Selection

Using Theorem 5.1 and Theorem 5.2, we can derive appropriate guard distances for some fixed control parameters (i.e., $P_{\text{C-UE}}, P_{\text{V-UE}}, d, R_0, \gamma_{\text{D2D}}, \gamma_{\text{C}}$), such that reliable D2D and cellular communication is possible. Note that unfavorable propagation environments can result in infeasible guard distances.

While d is defined by the corresponding D2D application in the vehicular underlay, $P_{\text{C-UE}}$ is fixed due to hardware constraints. Furthermore, R_0 is determined by the imposed power control strategy (cf. [3GP12]), and γ_{D2D} and γ_{C} are given by the SINR requirements on the direct and cellular links. However, there is some freedom in the selection of $P_{\text{V-UE}}$. Hence, there is more than one tuple $(P_{\text{V-UE}}, r_1, r_2)$ which satisfies the conditions in (5.22) and (5.23). Consider again the simple example in Figure 5.1. It is obvious that, increasing $P_{\text{V-UE}}$ in relation to $P_{\text{C-UE}}$ allows for a lower separation between the considered C-UE and V-UE at the cost of a higher required separation between the V-UE and the eNB. In contrast, decreasing $P_{\text{V-UE}}$ in relation to $P_{\text{C-UE}}$ reduces r_1 at the cost of higher r_2. This trade-off affects the dimensions of the zones in LDRAS and, therefore, the reuse of radio resources.

The efficiency of LDRAS can be measured in terms of the mean frequency with which RBs can be reused throughout the considered deployment. This is determined by the result of the resource reservation due to graph coloring (cf. Section 5.4) and the zone formation (cf. Section 5.3). Hence, it is difficult to find an explicit expression that relates the efficiency of LDRAS to its tunable parameters (i.e., $P_{\text{V-UE}}, r_1$, and r_2). A closer observation of the scheme reveals that the potential to reuse RBs more often grows with Z, if sufficient separation between the zones is given. In turn, Z grows with decreasing guard distances. Hence, a promising approach to the problem of optimizing the performance of LDRAS is to jointly minimize r_1 and r_2.

In this regard, consider the coverage area of an eNB as an ideal circle with radius R and assume that each eNB serves three cells in a typical three sector deployment. Furthermore, consider partitioning this area into squares of size $r_2 \times r_2$, with the exception of disks around each eNB with radius r_1 that protect the eNBs from interference due to V-UEs. The number of zones can be approximated as $Z \sim \frac{C}{3}\pi\frac{\left(R^2-r_1^2\right)}{r_2^2} + C$. Thus, the problem of maximizing Z can be expressed as

$$\min_{P_{\text{V-UE}}, r_1, r_2} \frac{r_2^2}{R^2 - r_1^2}, \quad \text{subject to} \tag{5.29a}$$

$$\Pr\left(SINR_{\text{C}} < \gamma_{\text{C}}\right) \leq p_{\text{out,C}}, \tag{5.29b}$$

$$\Pr\left(SINR_{\text{D2D}} < \gamma_{\text{D2D}}\right) \leq p_{\text{out,D2D}}, \tag{5.29c}$$

$$0 \leq P_{\text{V-UE}} \leq \overline{P_{\text{V-UE}}}, \tag{5.29d}$$

$$0 \leq r_1 \leq \overline{r_1}, \tag{5.29e}$$

$$0 \leq r_2 \leq \overline{r_2}. \tag{5.29f}$$

Here, $\overline{P_{\text{V-UE}}} \in \mathbb{R}_{\geq 0}, \overline{r_1} \in \mathbb{R}_{\geq 0}$, and $\overline{r_2} \in \mathbb{R}_{\geq 0}$ denote the upper bounds on the respective LDRAS parameter.

With (5.25) and (5.9), it is obvious that the constraints in the above OP are nonlinear, in addition to the objective function. Sequential Quadratic Programming (SQP) [NW06] is one of the efficient tools available for solving such OPs. In particular, inequality-constrained QP [NW06], which iteratively minimizes a quadratic approximation of the original problem, and then uses the minimizer of the current subproblem to define a new iterate can be applied. It is worth noting that this method demonstrates good performance in small- to mid-scale problems such as the one above, but tends towards local minima [NW06]. A good starting point is required to initiate the first iteration, in order to find the optimal tuple $(P_{\text{V-UE}}, r_1, r_2)$. It should be noted that the OP at hand is relatively simple, with effectively only one strictly constrained variable $P_{\text{V-UE}}$ (as r_1 and r_2 are functions of $P_{\text{V-UE}}$). Moreover, it only needs to be solved in an initial planning step in LDRAS and does not affect its performance in terms of the computational complexity during scheduling. A brute force approach to finding the globally optimal tuple, i.e., testing the outcome of the SQP with different starting points and sweeping the feasible region given by the constraints (5.29d)-(5.29f), can be adopted without a performance penalty.

5.2.3 Heterogeneous Propagation Environment

The above stated optimization is suited to retrieve the control parameters for LDRAS in homogeneous propagation environments. In heterogeneous environments, however, the mappings h and h' are likely to be surjective (i.e., distance- and location-dependent). For example, consider the signal propagation in the open space of a street compared to propagation through a wall. Although both transmissions may travel the same distance, the power gains differ due to the additional penetration loss in the latter case. The framework in Section 5.2.1 and Section 5.2.2 can, nevertheless, be applied by considering the worst-case scenario in reference to the respective propagation environment. In other words, the OP in (5.29) needs to be solved taking the most pessimistic realization of $h(d)$, and the most optimistic realizations of $h(r_2)$ and $h'(r_1)$ into account. This simple approach is wasteful, however. The reuse of resources between UEs in zones formed considering the pessimistic values for r_1 and r_2 may be prohibited unnecessarily. This potential inefficiency in heterogeneous propagation environments is, however, easy to circumvent, as it will be shown in Section 5.3.2.

5.3 Zone Topology Formation

As previously mentioned, LDRAS ensures that the guard distances required by the proposed resource reuse scheme are always enforced by means of cell partitioning. On the one hand, this avoids the need for accurate location information and, hence, reduces the data privacy problem of tracking the movement of UEs. On the other hand, such an approach allows for lower management overhead and requires simpler allocation algorithms. For the purpose of forming the zone topology, consider the network area as a discrete grid of $U \times V$ pixels $(U, V \in \mathbb{N})$ defined by sampling the 2D space in regular distances $d_{\text{samp}} \in \mathbb{R}_+$. Grouping these locations into zones can be seen as a problem in the domain of cluster analysis [JD88].

5.3.1 Similarity Metric and Hierarchical Clustering

One suitable method to solve the problem of defining zones is commonly referred to as *hierarchical clustering* [JD88]. In this approach, individual elements (denoted as pixels) are grouped

in accordance to a similarity metric. The process is initiated by considering each individual element as a cluster. Then, iteratively, pairs of clusters that show the strongest similarity (averaged among their members) are merged, until a single cluster is built or the process is terminated according to stopping criteria (considering the number of clusters or a similarity threshold). In order to apply hierarchical clustering in the context of LDRAS, we need to define an appropriate similarity metric. To this end, consider first the case of a homogeneous propagation environment.

Definition 5.3. *Let the set of matrices* $\{\mathfrak{M}^{(w)} \in \{0,1\}^{U\times V}\}_{w=1}^{UV}$ *describe the locations, where another transmitter is allowed to transmit in the same RBs as a V-UE at location* w*, according to the resource reuse strategy. In other words,*

$$\mathfrak{m}_{u,v}^{(w)} \coloneqq \begin{cases} 0, & \text{if } \exists w' : \mathfrak{e}\left(w,w'\right) \leq \frac{d}{d_{samp}} \cap \mathfrak{e}\left(u+(v-1)\,U,w'\right) \leq \frac{r_2}{d_{samp}}, \\ 1, & \text{otherwise}, \end{cases} \tag{5.30}$$

where

$$\mathfrak{e}\left(w,w'\right) \coloneqq \sqrt{\left(\left\lfloor\frac{w}{U}\right\rfloor - \left\lfloor\frac{w'}{U}\right\rfloor\right)^2 + \left(((w-1) \bmod U) - ((w'-1) \bmod U)\right)^2} \tag{5.31}$$

denotes the Euclidean distance between location w *and location* w' *on the grid, and* $a \bmod b$ *denotes the remainder of the Euclidean division of integer* a *and* b*.*

Definition 5.4. *Let the set of matrices* $\{\mathfrak{M}'^{(c)} \in \{0,1\}^{U\times V}\}_{c=1}^{C}$*, describe the locations, where a V-UE may reuse the radio resources occupied by a cellular UL transmission, i.e.,*

$$\mathfrak{m}'^{(c)}_{u,v} \coloneqq \begin{cases} 0, & \text{if } \mathfrak{e}\left(u+(v-1)\,U,\mathrm{loc}\left(c\right)\right) \leq r_1, \\ 1, & \text{otherwise.} \end{cases} \tag{5.32}$$

Here, $\mathrm{loc}\left(c\right)$ *denotes the location of eNB* c *on the grid.*

These matrices can be seen as images with 'light' and 'dark' pixels that quantify each location with respect to the prospect of hosting transmitters which reuse the same RBs. Hence, they serve as input to asses the similarity of the different locations in the context of LDRAS. The physical proximity of the locations needs to be considered as well, as it is required to have spatially continuous zones.

Definition 5.5 (Similarity Matrix)**.** *We define the overall similarity matrix as* $\mathfrak{S} \in \mathbb{R}_{\geq 0}^{UV\times UV}$*, where*

$$\mathfrak{s}_{w,w'} \coloneqq \frac{\mathfrak{e}\left(w,w'\right)}{1-\mathfrak{h}\left(\mathfrak{M}^{(w)},\mathfrak{M}^{(w')}\right)} + \left(\cup_c \mathfrak{m}'^{(c)}_{\left\lfloor\frac{w}{U}\right\rfloor+1,(w-1) \bmod U+1} \oplus \cup_c \mathfrak{m}'^{(c)}_{\left\lfloor\frac{w'}{U}\right\rfloor+1,(w'-1) \bmod U+1}\right). \tag{5.33}$$

Here, $\mathfrak{h}\left(\cdot,\cdot\right)$ *denotes the normalized Hamming distance between the respective binary matrices,* $\cup$ *denotes the binary or operator, and* $\oplus$ *denotes the binary xor operator. Note that small values of* $\mathfrak{s}_{w,w'}$ *indicate high similarity between the locations* w *and* w'*.*

The term on the RHS in the above definition increases the similarity if the locations are spatially close and share the similar properties (with respect to the remaining locations in the network which are allowed to host a secondary transmitter reusing the same RBs). The

second term decreases the similarity between locations where the reuse of resources is allowed and where dedicated resources should be used for D2D communication in order to protect the cellular UL transmissions from harmful cross-interference. Applying the hierarchical clustering method [JD88] by taking into account the relation between (clusters of) points with respect to this similarity metric yields the desired zone formation. Algorithm 5.1 summarizes our approach. Hereby, we sequentially search for the two most similar (clusters of) points at each iteration and group them. The stopping criterion is chosen to be the number of zones Z, where each resulting cluster is to be interpreted as a zone in the topology.

Algorithm 5.1 Bottom-up hierarchical clustering algorithm for the zone formation in LDRAS.

Input: Similarity matrix $\mathfrak{S}$
Output: Clusters of locations $\{\mathcal{O}_z\}_{z=1}^{Z}$

1: $i = UV$;
2: $\{\mathcal{O}_z\}_{z=1}^{i} = \{\{1\}, \{2\}, \ldots, \{i\}\}$; ▷ Initialization considering all locations as separate clusters
3: **while** $i > Z$ **do**
4: $(z, z') = \underset{\substack{z,z' \in \{1,\ldots,i\} \\ z \neq z'}}{\arg\min} \frac{1}{|\mathcal{O}_z| + |\mathcal{O}_{z'}|} \sum_{w \in \mathcal{O}_z} \sum_{w' \in \mathcal{O}_{z'}} \mathfrak{s}_{w,w'}$;
5: $\mathcal{O}_z = \mathcal{O}_z \cap \mathcal{O}_{z'}$;
6: $i = i - 1$;
7: Remove $\mathcal{O}_{z'}$ and re-enumerate the remaining clusters;
8: **end while**

5.3.2 Heterogeneous Propagation Environment

As mentioned in Section 5.2.3, the spatial resource reuse strategy in LDRAS considers the most pessimistic realizations of $h(r_2)$ and $h'(r_1)$ in order to derive the guard distances in heterogeneous propagation environments. Forming the zone topology based on these pessimistic values of r_1 and r_2 is wasteful in the cases where more favorable channel conditions occur. However, the environment models used to derive the guard distances can be exploited to mitigate this potential inefficiency. In other words, instead of defining the zone topology based on physical separation of the communicating terminals, we propose to do this based on their *channel separation*.

Let the set of matrices $\{H^{(w)} \in \mathbb{R}_{\geq 0}^{U \times V}\}_{w=1}^{UV}$ describe the constant power gain for potential direct transmissions originating from a transmitting V-UE at location w to all other locations in the considered network. Moreover, let $\{H'^{(c)} \in \mathbb{R}_{\geq} 0^{U \times V}\}_{c=1}^{C}$ denote the set of matrices holding the realizations of the constant power gain for the links between eNB c and all of the UV locations in the network. With this, the control parameters under LDRAS for each location w (i.e., $P_{\text{V-UE}}^{(w)}, r_1^{(w)}, r_2^{(w)}$) can be retrieved by solving (5.29) for

$$h^{(w)}(d) = \min \left\{ h_{u,v}^{(w)} : \sqrt{\left(u - \left\lfloor \frac{w}{U} \right\rfloor + 1\right)^2 + (v - (w-1) \bmod U + 1)^2} \leq \frac{d}{d_{\text{samp}}} \right\}. \quad (5.34)$$

We use the retrieved values for $r_1^{(w)}$ and $r_2^{(w)}$ in conjunction with the most pessimistic realizations of $h(\cdot)$ and $h'(\cdot)$ to determine the path loss thresholds $h\left(r_2^{(w)}\right)$ and $h'\left(r_1^{(w)}\right)$.

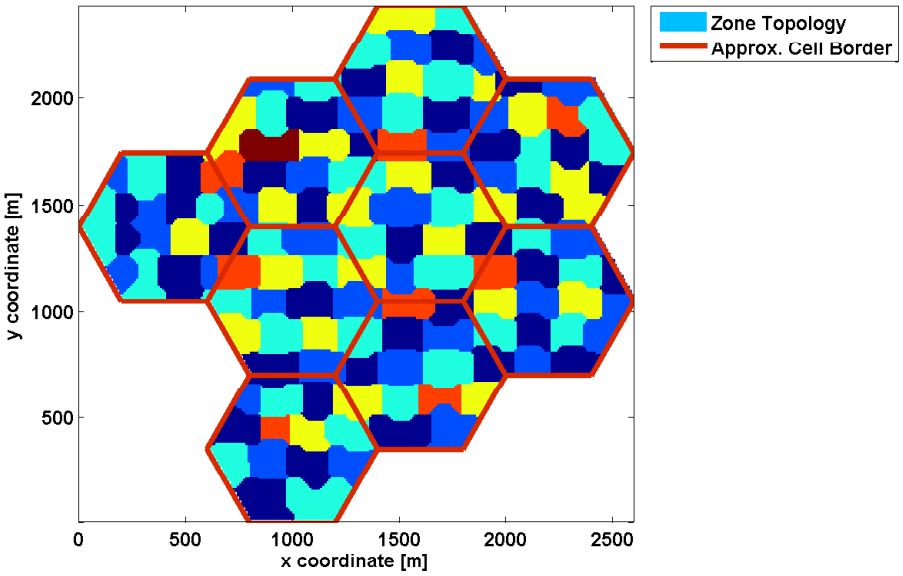

Figure 5.4: Example zone topology for an urban environment, retrieved by means of hierarchical clustering.

Again, note that the same path loss can (and will) be measured at lower distances when more favorable path loss models are applicable. This allows for lower separation between UEs reusing the same radio resources than the pessimistic bounds. In order to take this into account, we introduce a slight modification to the similarity metric's definition as follows:

$$\mathfrak{m}_{u,v}^{(w)} := \begin{cases} 0, & \text{if } \exists w' : h_{u,v}^{(w')} \geq h\left(r_2^{(w)}\right), \mathfrak{e}\left(w, w'\right) \leq \frac{d}{d_{\text{samp}}}, \\ 1, & \text{otherwise}, \end{cases} \tag{5.35}$$

and

$$\mathfrak{m}_{u,v}^{\prime(c)} := \begin{cases} 0, & \text{if } h_{u,v}^{\prime(c)} \geq h'\left(r_1^{(u+(v-1)U)}\right), \\ 1, & \text{otherwise}. \end{cases} \tag{5.36}$$

Plugging this into the definition of the similarity metric (cf. Definition 5.5) and applying Algorithm 5.1 yields the desired zone topology in heterogeneous propagation environments. Figure 5.4 shows an example retrieved for a network deployment according to the specifications in Section 6.1. The different colored patches indicate a distinct zone, where $Z = 126$ is specified as a stopping criterion for the clustering algorithm.

5.4 Resource Reservation

In addition to the definition of the zone topology, the spatial resource reuse scheme in LDRAS requires the reservation of (sets of) RBs for D2D and cellular communication in each zone. This reservation is carried out in order to minimize the complexity of the allocation algorithm. In this regard, each zone is fully described by the tuple $\left(z, \mathcal{RB}_{\text{D2D},z} \subset \{\mathcal{RB}_y\}_{y=1}^{Y}, \mathcal{RB}_{\text{C},z} \subset \{\mathcal{RB}_y\}_{y=1}^{Y}\right)$. In contrast to the interpretation of the set $\mathcal{RB}_{\text{C},z}$ in the preliminary work (cf.

Section 5.1), hereinafter, this set is to be interpreted as 'restricted for use by C-UEs in zone z'. This adjustment to LDRAS is made in order to preserve the frequency/multi-user diversity gain (cf. [RC00]) to a greater extent. Often the spatial resource reuse constraints allow for the C-UEs in a given zone to reuse the RBs used for D2D communication in more than one of the remaining zones. Hence, instead of appointing one fixed set for cellular communication in each zone, it is more beneficial to specify the sets of RBs restricted for UL transmissions. In this manner, C-UEs from different zones are allowed access to a wider pool of RBs and a better scheduling decisions can be made, (potentially) increasing the UL capacity as opposed to the former manner. Based on this interpretation, the RB reservation needs to satisfy

$$\mathcal{RB}_{\mathrm{D2D},z} \neq \emptyset, \forall z \in \mathcal{Z} \tag{5.37}$$

and

$$\mathcal{RB}_{\mathrm{C},z} \neq \left\{ \bigcup_{y=1}^{Y} \mathcal{RB}_y \right\}, \forall z \in \mathcal{Z}, \tag{5.38}$$

in the considered communications scenario[2]. Moreover, it needs to ensure that the resource reuse scheme is always enforced. In this regard, let

$$\mathcal{N}_z \coloneqq \left\{ z' | \exists w \in \mathcal{O}_z, w' \in \mathcal{O}_{z'} : \mathfrak{m}^{(w)}_{\left\lfloor \frac{w'}{U} \right\rfloor + 1, (w'-1) \bmod U + 1} = 0 \right\}, \forall z \in \mathcal{Z}, \tag{5.39}$$

denote the set of relevant neighbors of zone z, which impose restrictions on the sets of RBs that can be used for D2D transmissions. In other words, this set lists the zones whose reserved sets for D2D or cellular communication may not be reused for direct transmissions in z. Similarly, let

$$\mathcal{N}'_z \coloneqq \mathcal{N}_z \cup \left\{ z' | \exists w' \in \mathcal{O}_{z'}, c \in \mathcal{C}_z : \mathfrak{m}'^{(c)}_{\left\lfloor \frac{w'}{U} \right\rfloor + 1, (w'-1) \bmod U + 1} = 0 \right\}, \forall z \in \mathcal{Z}, \tag{5.40}$$

denote the set of relevant neighbors of zone z, which impose restrictions on the sets of RBs that can be used for cellular transmissions. In other words, this set lists the zones whose reserved sets for D2D communication may not be reused for UL transmissions in z. Hereby, the set $\mathcal{C}_z$ denotes the set of eNBs, which may serve users in zone z.

5.4.1 Graph Coloring Approach

The derivation of an appropriate RB reservation can be modeled as a problem in the domain of graph coloring [BM76]. To this end, consider the graph $\mathcal{G} = (\mathcal{V}, \mathcal{E})$ with the set of vertices $\mathcal{V} = \{\nu_1, \nu_2, ..., \nu_{2\mathrm{Z}}\}$. Hereby, each zone in the topology is reflected in this model twice, in order to consider both of the conditions in (5.37) and (5.38). The set of edges $\mathcal{E}$ contains a list of all pairs of (virtual) zones that are not allowed to use the same RBs and is defined as

$$\mathcal{E} \coloneqq \left\{ (\nu_z, \nu_{z'}), \nu_z, \nu_{z'} \in \mathcal{V} | z \in \mathcal{Z}, z' \in \mathcal{N}_z \right\} \cup \left\{ (\nu_{2z}, \nu_{z'}), \nu_z, \nu_{z'} \in \mathcal{V} | z \in \mathcal{Z}, z' \in \mathcal{N}'_z \right\}. \tag{5.41}$$

The task of graph coloring is to then assign a color to each vertex in the graph such that no two vertices connected by an edge share the same color. Interpreting the colors as disjoint

[2]Note that either of these conditions can be relaxed if, for some reason, D2D or cellular communication is not required in a given zone.

RB sets yields the desired resource reservation in LDRAS. Hereby, it is desired to obtain a reservation with the least amount of disjoint RB sets, as this allows for the most 'dense' reuse of RBs.

Finding an optimal solution to the graph coloring problem (i.e., a solution using the least possible colors) is NP-hard [SA89] and, hence, infeasible in practical implementations. In this regard, sequential graph coloring [Lei79] is one efficient method that can be applied in order to retrieve a color assignment with reasonable complexity. In this approach, all of the vertices are colored one after the other, with a color different than the colors of the previously colored connected vertices. Hereby, additional colors are dynamically added to the palette if necessary. The performance of this approach strongly depends on the order in which the vertices are processed. Its low computational complexity, however, allows for fast execution. Hence, satisfactory results can be achieved by selecting the color assignment as the one using the least colors from a finite amount of trials initiated with different permutations of the vertex set. We apply this approach to the considered reservation problem as summarized in Algorithm 5.2. A reservation with at most $Y = 14$ disjoint RB sets can be defined for the example topology in Figure 5.4 with $T_{\text{total}} = 5000$ trials. It should be noted that the color selection strategy (cf. Line 11) can be modified to assign, e.g., the least popular color (i.e., the one that has been used the least thus far) instead of the first feasible one in the palette. Considering a sufficiently large amount of trials, however, the effects of choosing different color selection strategies will be averaged out.

5.4.2 Load Dependency

The graph coloring algorithm constitutes an efficient way of determining the RB sets meant for D2D communication, and the sets restricted for cellular communication in each zone, with respect to the disjoint sets $\{\mathcal{RB}_y\}_{y=1}^{Y}$. In order to facilitate efficient communication, the available radio resources need to be distributed among these Y sets in a fair manner. Considering uniform D2D load distribution throughout the entire network deployment, the sets $\{\mathcal{RB}_y\}_{y=1}^{Y}$ need to be of (approximately) equal sizes. In the previous example with $Y = 14$ and a total number of 100 available RBs, this strategy leads to 12 sets of 7 RBs each, and 2 sets of 8 RBs. For networks with traffic hot-spots, however, a strategy that reserves more RBs for D2D communication in zones with higher load may be beneficial. Such a strategy can be implemented with slight modification to Algorithm 5.2, where each vertex in the graph is additionally associated with a weighting factor that is proportional to the number of colors that are to be assigned to it. In this case, each color is to be interpreted as an individual RB. A valid reservation is then obtained, if the number of used colors does not exceed the number of available RBs. In such a scenario, the resource reservation needs to be dynamically updated with the changing traffic conditions. As the performance evaluation of LDRAS is made under the assumption of uniform traffic (cf. Section 6.1), this approach is not pursued explicitly in this work.

5.5 Resource Allocation Mechanism

The appropriate cell partitioning and resource reservation for each zone ensure that the outage probabilities for the primary network and the D2D underlay are kept within the designed limits. As opposed to many of the state-of-the-art RRM schemes for D2D-enabled networks

Algorithm 5.2 Random ordered sequential graph coloring algorithm for the reservation of RB sets in the context of LDRAS.

Input: Graph (modeling the zone topology) $\mathcal{G}$, Total number of trials T_{total}
Output: RB sets reserved for D2D communication $\mathcal{RB}_{\text{D2D},z}$, RB sets restricted for cellular communication $\mathcal{RB}_{\text{C},z}$

$Y = \infty$;
for *trial*$=1 : T_{\text{total}}$ **do**
  $\mathfrak{C} = \{1\}$; ▷ Initialize the color palette with a single color
  Randomly permute the vertex indices without repeating previously tested permutations
  for $z = 1 : 2Z$ **do**
    $\mathfrak{C}' = \mathfrak{C} \setminus \left\{ \bigcup_{(\nu_z, \nu_{z'}) \in \mathcal{E}} \text{color}\left(\nu_{z'}\right) \right\}$;
    if $|\mathfrak{C}'| = 0$ **then**
      $\mathfrak{C} = \{\mathfrak{C} \cup \{|\mathfrak{C}| + 1\}\}$; ▷ Add one more color to the palette
      $\mathfrak{C}' = \{|\mathfrak{C}|\}$;
    end if
    $\text{color}\left(\nu_z\right) = \{\mathfrak{C}'\}_1$; ▷ Here, $\{\mathfrak{C}'\}_1$ denotes the first element in the set $\mathfrak{C}'$
  end for
  if $|\mathfrak{C}| < Y$ **then** ▷ Adopt more favorable solutions
    $Y = |\mathfrak{C}|$;
    Revert the current permutation to the original vertex order
    for $z = 1 : Z$ **do**
      $\mathcal{RB}_{\text{D2D},z} = \mathcal{RB}_{\text{color}(\nu_z)}$;
    end for
    for $z = 1 : Z$ **do**
      $\mathcal{RB}_{\text{C},z} = \left\{ \bigcup_{z' \in \mathcal{N}'_z} \mathcal{RB}_{\text{D2D},z'} \right\}$;
    end for
  end if
end for

(including RASRFC and CDI-bRAA), the need for (full) CSI knowledge at the eNB is eliminated with LDRAS; thus, also the need for the costly channel measurements. Moreover, the resource allocation mechanism can be shaped in simpler manner.

5.5.1 Resource Allocation for V-UEs

Centralized Approach

Since the zone topology remains unchanged once determined (unless changes in the network deployment occur), it can be stored in the memory of each V-UE. With respect to the envisioned context awareness of future vehicles, each V-UE will be able to use its built-in global navigation satellite system receiver to track its location within the topology. Based on this, we propose he following allocation mechanism: A V-UE reports the corresponding zone index z to its serving eNB upon entering a new zone, accompanied by its request for RBs. The eNB then assigns an arbitrary subset of $\mathcal{RB}_{\text{D2D},z}$ of appropriate size to the requesting V-UE. Hereby, this subset must be orthogonal to the RBs allocated to other V-UEs in the same zone

in the same TTI. The size of $\mathcal{RB}_{\mathrm{D2D},z}$ and the characteristics of the running V2X service, hence, determine how many V-UEs can be supported in the respective zone.

Decentralized Approach

Assuming a fixed (or at least rarely changing) RB reservation, the sets $\mathcal{RB}_{\mathrm{D2D},z}, \forall z \in \mathcal{Z}$, can be communicated to the V-UEs along with the topology description. This additional information enables support for mobile ad-hoc MAC protocols like Carrier Sense Multiple Access (CSMA) and its derivatives [BCGS04]. Therein, each V-UE needs to verify the absence of other traffic before transmitting in a given RB. Limiting the pool of RBs to select from to $\mathcal{RB}_{\mathrm{D2D},z}$ allows for retaining the control over the cross-interference according to the spatial resource reuse scheme in LDRAS. Ad-hoc MAC protocols, however, suffer from the *hidden node problem*: this problem arises if two transmitters that are outside each other's transmission range and cannot detect the competing medium access, simultaneously transmit in the same RBs. This then causes a collision at a receiver, which would otherwise have been able to successfully receive both messages. Hence, ad-hoc MAC protocols can be used as a fallback in areas without cellular coverage. However, these are less reliable than the centralized approach and will not be pursued explicitly in this work.

5.5.2 Resource Allocation for C-UEs

The proposed LDRAS fulfills its design goal of adding minimal additional complexity over conventional cellular networks. Resources can be allocated to C-UEs in the primary network based on the MNO's regular scheduling policy with the additional constraint that RBs from the restricted RB set $\mathcal{RB}_{\mathrm{C},z}$ cannot be allocated to C-UEs in the respective zone z. Assuming that, similar to the V-UEs, the C-UEs also report their zone index upon entering a new zone or it can be determined by means of network-based positioning, this can be accommodated through a simple modification to the scheduling algorithm. Many of the practically relevant approaches are based on some form of metric which characterizes the incentive of allocating a given RB to a specific C-UE [AATSH14]. For instance, a proportional fair (PF) scheduler [LPM+09] leverages information about the channel conditions in order to determine the ratio of the potentially achievable throughput in a given RB and the historical average throughput of the considered C-UE. This ratio (modified according to fairness criteria) builds the PF metric. In this regard, let κ_{ks} denote the PF metric associated with C-UE k and RB s. The scheduling decisions are then taken such that each RB is allocated to the C-UE which maximizes the value of the PF metric.

The additional restrictions on the usage of RBs due to LDRAS can be adopted in such a setting by modifying the PF metric to take an infeasible value in the restricted RBs, i.e., $\kappa_{ks} = -\infty, \forall s \in \mathcal{RB}_{\mathrm{C},z(k)}$, where $z(k)$ denotes the current zone of C-UE k. These restrictions, naturally, only need to be enforced for RBs which are assigned to a V-UE in the zones listed in $\mathcal{N}'_{z(k)}$ in the considered TTI. In this manner, it can be ensured that another user in the cell will always be preferred in the affected RBs and that C-UEs, which would cause strong cross-interference, are not allocated. A minimalistic example of the behavior of such modified scheduler is summarized in Table 5.1. Similar modifications can be introduced to any other scheduling algorithm.

	$z(k)$	RB1	RB2	RB3	RB4
C-UE1	1	κ_{11}	$-\infty$	$-\infty$	κ_{14}
C-UE2	2	κ_{21}	d	$-\infty$	$-\infty$
C-UE3	1	κ_{31}	$-\infty$	$-\infty$	κ_{34}
Allocation		C-UE1	C-UE2	-	C-UE1

Table 5.1: Example behavior of LDRAS-modified PF scheduler for 3 C-UEs in 2 zones with $\mathcal{RB}_{\mathrm{C},1} = \{\mathrm{RB1}, \mathrm{RB2}, \mathrm{RB3}\}, \mathcal{RB}_{\mathrm{C},2} = \{\mathrm{RB3}, \mathrm{RB4}\}$, PF-metric values $\kappa_{11} > \kappa_{14} > \cdots > \kappa_{34}$, and under the assumption that RB1 is not used in the D2D underlay in the considered TTI.

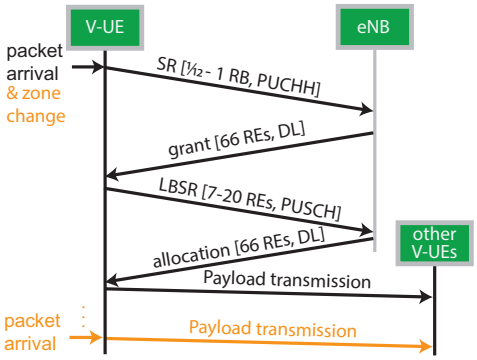

Figure 5.5: Signaling protocol and required resources for the operation of LDRAS for general and periodic traffic.

5.6 Additional Aspects

5.6.1 Signaling and Location Information Acquisition

As opposed to CSI-based RRM, LDRAS does not require knowledge over the channel gains and, hence, avoids the previously discussed measurement overhead. Based on an LTE system, Figure 5.5 illustrates an appropriate protocol for the scheme. According to the proposed resource allocation mechanism, the eNB only needs to know the zone index associated with a specific V-UE and the amount of data it needs to transmit. As discussed in Section 4.4.2, a BSR is used to report the size of the payload to be transmitted. We propose adding location information to this message; a (local) zone index in the case of LDRAS should not take up more than 5 bits, since an eNB is unlikely to cover more than 32 zones. In order to transmit this Location and Buffer Status Report (LBSR), a UE first needs to retrieve resources on the PUSCH using the SR procedure (similar as in the case of the BSR for CSI-based RRM). In the case of LDRAS, however, the eNB is able to directly respond to the LBSR with an appropriate resource allocation for the transmission of the actual payload, as all of the required data has already been acquired. For periodic traffic, a simplification that enables the eNB to anticipate the demand for radio resources of each V-UE without explicit signaling is again applicable. In such a case, the allocation is accompanied by a periodicity indicator, stating in which time intervals the affected V-UE can reuse its allocated RBs without explicit authorization by the serving eNB. Hence, the LBSR and allocation need to be updated only after a zone change.

Distributing the information on the resource reservation allows also for a CSMA-based implementation, where the V-UEs can claim RBs in the D2D underlay autonomously to reduce

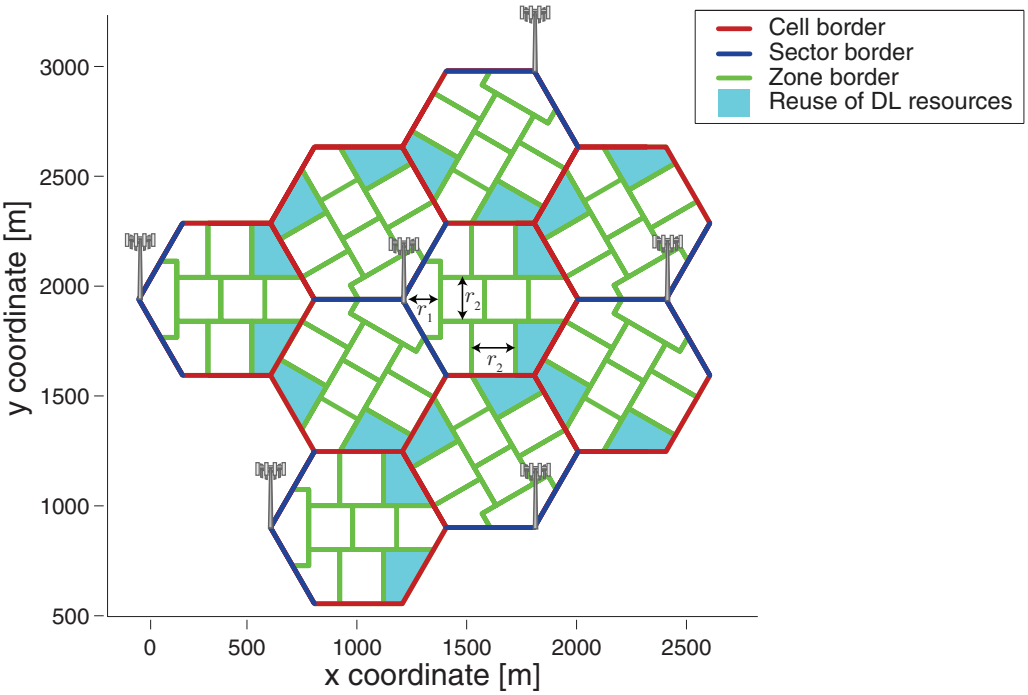

Figure 5.6: Example zone topology for an urban deployment considering the reuse of DL resources.

the signaling overhead even further.

5.6.2 Reuse of DL Resources

Similar considerations lead to criteria for the reuse of DL resources analogous to the ones detailed throughout this chapter. In order to avoid repetitions, these will not be formulated explicitly. It should be noted, however, that the roles of the guard distances r_1 and r_2 (or equivalently, the channel gain thresholds $h(r_2)$ and $h'(r_1)$) are inverted. Hereby, r_1 protects receiving V-UEs from the cross-interference due to DL transmissions by eNBs, and r_2 protects receiving C-UEs from the cross-interference due to direct transmissions. For V-UEs in zones with high (channel) separation from eNBs (i.e., the ones near the cell edge), this scheme allows for reusing DL resources, which are used for transmissions to C-UEs in zones with low (channel) separation from the eNBs (i.e., the ones close by). Hereby, the transmit power invested by the eNBs must not exceed a certain threshold, similarly to the V-UEs in the case of UL resource reuse. Figure 5.6 illustrates such a constellation. Allowing for the reuse of DL resources for D2D communication in certain zones leads to two-fold benefits: first, this allows for the decoupling of some of the vertices in the graph $\mathcal{G}$ (i.e., removing some of the edges) and, hence, reduces the computational effort required by the graph coloring algorithm (cf. Algorithm 5.2); second, the reduced restrictions on the UL resource reuse may lead to a reservation assignment with less disjoint RB sets and, hence, overall more efficient reuse of resources.

Chapter 6

Performance Evaluation

6.1 Simulation Setup

The performance of the proposed RASRFC/CDI-bRAA and LDRAS in terms of fulfilling the QoS requirements of vehicular applications (as well as conventional cellular ones) is evaluated based on extensive system level simulations. A typical urban LTE deployment with a D2D underlay network is considered. To this end, the V-UE device class reusing cellular UL radio resources is introduced. The available resources are organized in $S = 100\,\text{RBs}$ (equivalent to a bandwidth of 20 MHz) following the SC-FDMA scheme [3GP10] used in the LTE UL (cf. Figure 2.2). The simulation scenario consists of a cluster of 9 cells (see Figure 6.1); here, we consider the outer cells to generate realistic interference to the users in the central cell. Accordingly, the results shown here only refer to users within the central cell. The cell constellation is chosen in order to generate a realistic interference scenario for the receiving V-UEs near the serving eNB. The general system parameters reflect a typical urban LTE deployment and are summarized in Table 6.1.

6.1.1 Radio Propagation Environment

The distance/location-dependent component of the channel gains in the system is determined by path loss (i.e., power decay with distance) and shadowing (i.e., additional power decay due to obstacles in the environment) [TV05]. The path loss (in dB) of the links to an eNB is computed according to the WINNER II typical urban macro-cell model [KMH+07] (adapted to the considered system model). Hereby, Line-of-Sight (LOS) and Non-Line-of-Sight (NLOS) propagation conditions are considered:

$$\overline{PL}(x) = \begin{cases} 23.06 + 26\log_{10}(x), & \text{for LOS,} \\ 24.3 + 35.74\log_{10}(x), & \text{for NLOS,} \end{cases}$$

where x denotes the communication link distance (in m). The path loss model for the computation of the signal attenuation between two communicating V-UEs, or between a D2D receiver and the interfering C-UE, is based on the WINNER II urban micro-cell model [KMH+07]. Hereby, adapting the path loss function to the heights of the UEs in the considered scenario yields:

$$PL(x) = \begin{cases} 9.31 + 40\log_{10}(x) \equiv PL_{\text{LOS}}(x), \text{ for LOS,} \\ \min\left(PL'(x_1, x_2), PL'(x_2, x_1)\right), \text{ for NLOS,} \end{cases}$$

Parameter	Value
Inter-site distance	1.2 km
Carrier frequency	800 MHz
Number of available RBs S	100
eNB antenna height	25 m
UE height	1.5 m
V2X relevant communication distance	20 m
Cellular SINR threshold	2 dB
D2D SINR threshold	7 dB
Resource allocation reliability threshold r_{th}	0.01
Variance for links to eNBs	0.5
Variance for direct links	4
Shadow fading standard deviation	8 dB
Shadow fading correlation distance	50 m
Outdoor-to-indoor penetration loss	10 dB
Maximum eNB antenna gain G_0	14 dBi
eNB horizontal antenna beamwidth	70°
Maximum eNB antenna isolation	20 dB
Maximum UE transmit power P_k, $\forall k \in \mathcal{M}$	24 dBm
eNB noise floor	-117.45 dBm
V-UE noise floor	-104.5 dBm
C-UE movement speed	0 km/h
V-UE movement speed	50 km/h

Table 6.1: System and simulation parameters.

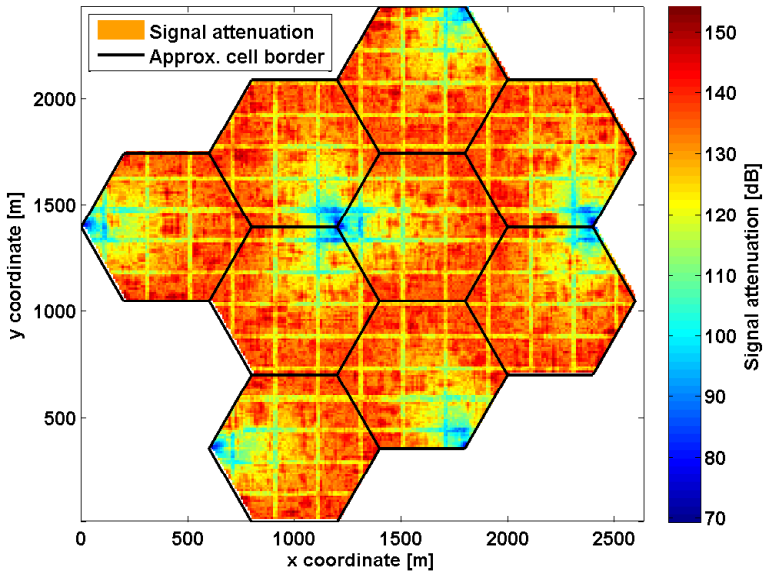

Figure 6.1: Deployment scenario considering an exemplary shadow fading realization.

where $PL'(x_a, x_b) = PL_{\text{LOS}}(x_a) + 26.01\,\text{dB} - 12.5n_j + 10n_j \log_{10}(x_b)$ and $n_j = \max(2.8 - 0.0024x_a, 1.84)$. Here, x_1 defines the distance between the considered UEs in x-direction and x_2 is the distance in y-direction in the 2D space. Note that $x_1 + x_2$ is also known as the Manhattan distance [BSH03].

In addition, log-normal distributed shadow fading taken from a 2D correlated fading map [FSA04] is considered for the links between eNBs and UEs, where each of the C eNBs is associated with a separate shadowing realization. Outdoor-to indoor propagation is subject to an additional penetration loss of 10 dB [OKI09]. Moreover, a 2D antenna pattern is adopted for the calculation of the antenna gain (in dBi) $G(\phi)$ at the eNBs as follows [GJF+08]:

$$G(\phi) = G_0 - \min\left(25, \min\left(25, 12\left(\frac{\phi}{70^\circ}\right)^2\right)\right),$$

where ϕ denotes the azimuth angle determined by the positions of the transmitter and receiver, respectively. Isotropic zero dB gain antennas are assumed for the receiving V-UEs. The effects of antenna directivity and shadowing can be seen in Figure 6.1.

The effects of multipath-induced fading are taken into account by employing the Rayleigh-fading model [Gol05] with different variances for direct and cellular links (see Table 6.1).

6.1.2 User Traffic and Mobility Models

The cellular terminals are uniformly distributed throughout the deployment area and are assumed to be static. The V-UEs, on the other hand, are distributed on fixed roads constituting a Manhattan grid [BSH03] with a distance of 200 m between adjacent roads in the x-direction and 148.4 m in the y-direction. The intermittent space is occupied by buildings, emulated by additional penetration loss. A mean vehicle speed of 50 km/h is adopted, with a probability of turning left or right at intersections of 0.125, respectively, and a probability of a U-turn of 0.05. Vehicles that leave the simulation area are replaced by a newly activated V-UE at a

random point within the road topology such that a constant number of terminals is ensured throughout the entire simulation time.

In order to reduce the simulation complexity, the full-buffer traffic model is adopted for all C-UEs in the simulated scenarios. In other words, all of the C-UEs constantly transmit data in the UL. This is done in order to always generate cross-interference to the vehicular D2D underlay and, hence, generate a worst-case scenario for RRM.

At the same time, a broadcast-based service is considered in the D2D underlay (i.e., the transmitted messages are to be received by all V-UEs around the transmitter within the desired broadcasting distance) with a packet size of 580 bytes, periodicity of 10 Hz, and a transmission delay budget of 10 ms. This traffic pattern is modeled according to the cooperative road safety use cases (like emergency electronic brake lights) defined in C-ITS [ETS09]. Hereby, the packet size and periodicity are taken in accordance to typical Cooperative Awareness Messages [ETS11], while the delay budget is chosen much smaller than the current state-of-the-art definitions [1] in an effort to anticipate future needs. The initial transmission takes place at a random time instance within the first 100 ms upon the activation of a V-UE. The broadcast distance is set to 20 m. This distance is sufficient for a braking vehicle to come to a complete stop [DE04] under the considered mobility model.

6.1.3 Reliability Requirements

The MCS 16QAM 490/1024, which is used in the LTE UL [3GP12], is selected for the timely transmission of packets in the D2D underlay. This MCS has an efficiency of 1.9141 transferred bits per used RE. Hence, the complete transmission of a 580 byte message in the D2D underlay requires 15 RBs in total. The target reliability for C-ITS applications of 99.999% is reached by said MCS at a SINR in an Additive White Gaussian Noise (AWGN) channel of $\approx 7\,\text{dB}$ [MBL+14]. Hence, $\gamma_k = \gamma_{\text{D2D}} = 7\,\text{dB}, \forall k > K$, is set throughout the simulations. In accordance, the calibration margin for the calculation of the effective SINR (cf. Section 2.3) over the entire used bandwidth is set to $\beta_{\text{MCS}} = 6.42$ [AATK13, Table 14.2].

The applications in the primary network are assumed to have lower reliability requirements with a SINR threshold of $\gamma_k = \gamma_{\text{C}} = 2\,\text{dB}, \forall k \leq K$. This threshold is sufficient for the MCS QPSK 602/1024 [3GP12] to reach reliability of 90%. This enables the support for a basic set of cellular services. Note, that the above thresholds are guaranteed with a probability of $r_{\text{p,th}}$ in the worst case scenario. A large percentage of the transmissions actually experiences much better SINR since the channel conditions are usually much better most of the time. Moreover, Hybrid Automatic Repeat reQuest (HARQ) techniques[2] [3GP16] can be used to ensure message delivery by means of repeated transmission. Hence, the supported (cellular) applications are not limited by the chosen thresholds.

6.1.4 Load Conditions and Statistical Significance

Statistical data is gathered in 100 independent simulation runs with different initial terminal locations and shadow fading realizations. Each run lasts for 60 seconds. We assess the performance of the proposed RRM schemes under different load conditions with respect to

[1] A delay budget of 100 ms is set in the current C-ITS standards.

[2] Note that HARQ techniques are not considered in the simulations, as the short delay budget and broadcast nature of V2X messages would not allow for their adoption. At the same time, C-UEs are only considered with a full buffer traffic model without explicit QoS requirements.

N	9	18	27	36	45
$r_{\mathrm{p}}(N)$	6.3×10^{-4}	9.5×10^{-6}	6.5×10^{-6}	7.7×10^{-8}	5.1×10^{-8}

Table 6.2: Example for the used values for $r_{\mathrm{p}}(N)$ in the simulations considering CDI-bRAA, as determined per Monte Carlo experiments.

the number of V-UEs. Low load is emulated by $L = 450$ V-UEs, medium load is simulated with $L = 900$ V-UEs, and a high load scenario is modeled by $L = 3600$ V-UEs, while the number of active C-UEs is fixed to $K = 270$ throughout all of the simulations. The number of V-UEs in the medium load scenario is derived from the typical vehicle density in urban environments according to [GSTW04]. The low load scenario considers half this amount in order to emulate low road traffic conditions (such as in the early morning hours). The high load scenario considers four times the typical road traffic in order to simulate rush hour conditions.

6.1.5 Application of CSI-based RRM

The values of $r_{\mathrm{p}}(N)$ used for power control in CDI-bRAA (cf. Section 4.3.4) are calibrated by means of Monte Carlo experiments, the results of which are summarized in Table 6.2. As fading channels are considered, setting $r_{p,\mathrm{th}} = 0$ is infeasible. Instead, a reasonable value of $r_{p,\mathrm{th}} = 0.01$ is selected. Note that a small threshold results in a low frequency of reusing resources in the system.

6.1.6 Application of LDRAS

A sampling distance of $d_{\mathrm{samp}} = 5\,\mathrm{m}$ (cf. Section 5.3) is selected for the application of LDRAS to the simulated environment for complexity reasons. The RSS target for cellular communication is set as $R_0 = $ -85 dBm in order to allow for a sufficient power margin to interfering signals. The resulting zone topologies further depend on the shadow fading realization and, hence, show slight differences between the different simulation runs. Nevertheless, comparable resource reservations with $Y = 14$ disjoint RB sets are found in most runs. Each of these RB sets contains 7 RBs to ensure fairness among the zones. Hence, a D2D transmission requires at least 3 TTIs in LDRAS under the selected traffic model. A representative zone topology example is shown in Figure 5.4. Again, as fading channels are considered, it is infeasible to have no outages. Reasonable values of $p_{\mathrm{out,C}} = 0.1$ and $p_{\mathrm{out,D2D}} = 0.01$ are selected. The resulting V-UE transmit power is set to $p_k^{(s)} = P_{\text{V-UE}} = 7.988\,\mathrm{dBm}$, $\forall k \in \mathcal{M}, k > K, s \in \mathcal{S}_k$.

The cellular UL traffic is scheduled according to a modified PF scheduler, as discussed in Section 5.5.2. The transmit power of the C-UEs is calculated by means of fractional power loss compensation, a mechanism used in the LTE UL [3GP12]:

$$p_k^{(s)} = \min\{P_k, R_0 + a_{\mathrm{pow}} L_{\mathrm{pow}}\}\,\mathrm{dBm},\ \forall k \in \mathcal{M}, k \leq K, s \in \mathcal{S}_k. \tag{6.1}$$

Here, $a_{\mathrm{pow}} \in [0, 1]$ denotes a power loss compensation factor and L_{pow} denotes the total power loss measured on the respective link (in dB) including path loss, shadowing and antenna gain. Hereby, the sum-power constraints in (2.1) must be satisfied. Table 6.3 summarizes the control parameters for LDRAS.

Parameter	Value
Sampling distance d_{samp}	5 m
Cellular outage probability target $p_{\text{out,C}}$	0.1
D2D outage probability target $p_{\text{out,D2D}}$	0.01
Vehicular UE transmit power $P_{\text{V-UE}}$	7.988 dBm
Target RSS at eNB R_0	-85 dBm
Power loss compensation factor a_{pow}	1

Table 6.3: LDRAS control parameters.

6.2 Reference Scheme

To compare the performance of the proposed schemes to RRM schemes that do not consider QoS requirements for direct links, the UL scheduling algorithm in [ZHS10] is used as a reference. This scheme has comparable heuristic nature and computational complexity. In this algorithm, RBs are first allocated to each C-UE according to the UL scheduling policy. Hereby, a conventional PF scheduler is selected in the simulations. In a second step, complete CSI is leveraged to determine the potential D2D transmitter expected to cause the least interference to each cellular link. Reuse of the respective RBs in the D2D underlay is only allowed, if the additional interference at the eNB, C-UE and D2D receiver, respectively, remains below a certain tolerable level. Hereby, the SINR thresholds for cellular and D2D links are used to derive said tolerable level in the simulations. This algorithm ensures that the cellular performance is not affected significantly, while the D2D underlay is only used in opportunistic fashion and lacks QoS support. Moreover, as the algorithm is to be applied in a distributed manner at each individual eNB without knowledge about the decision-making at the neighboring ones, it lacks coordination of the inter-cell (cross-) interference.

6.3 Simulation Results

6.3.1 Quality of Service

Effective SINR Distribution in the D2D Underlay

Figure 6.2 shows the cdf of the measured effective SINR (i.e., $\text{SINR}_{kr}^{\text{eff}}$) in the D2D underlay across all relevant receiving V-UEs for the different RRM schemes. Remember that each message is transmitted in broadcast manner and can be received by a multitude of receivers within the broadcast range of a transmitting V-UE. As can be seen, CDI-bRAA leads to satisfactory behavior in all three load scenarios, since the SINR threshold of 7 dB is only violated with a probability of 0.0106 in the low load scenario, 0.009 in the medium load scenario, and 0.0135 in the high load scenario, respectively. These values lay slightly above or below the reliability threshold targeted in the simulations (cf. Table 6.1). This small deviation can be expected, as the simulation results do not comply with the law of large numbers due to the limited number of runs. Hence, the performance of CDI-bRAA can be considered satisfactory.

At the same time, LDRAS leads to identical, satisfactory behavior in all three load scenarios. The SINR threshold is violated with a probability of 0.00016, which is lower than the tolerable outage probability set in the simulations (cf. Table 6.3). The cdf displays a

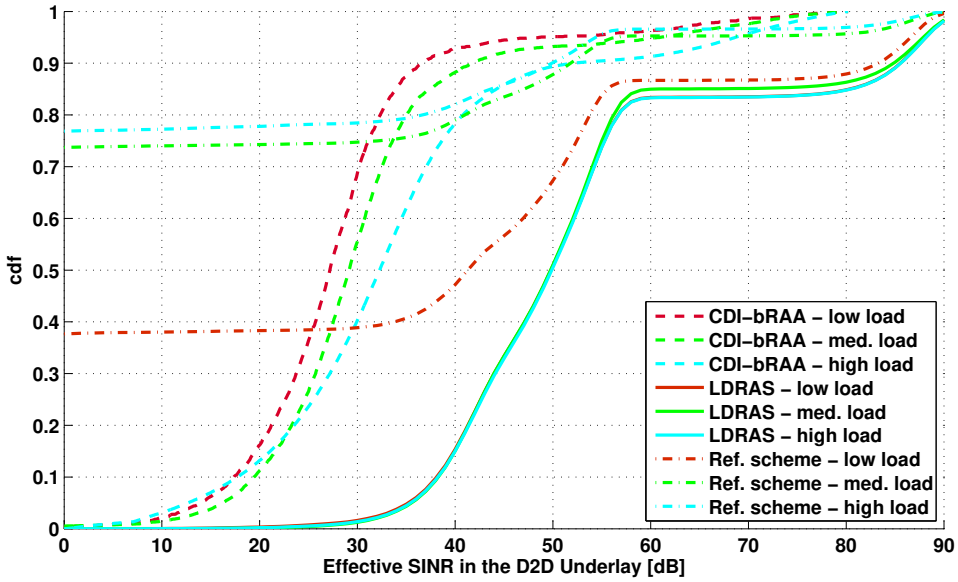

Figure 6.2: Cumulative distribution function of the measured effective SINR in the D2D underlay under different RRM algorithms and load configurations.

'step' (near the 60 dB mark) due to the heterogeneous propagation conditions. This can be attributed to the fact that transmissions tuned for reception under worst case conditions (i.e., around a corner) are also received by more favorable V-UEs (i.e., in LOS) with significantly higher SINR. The same effect can be seen in the performance of CDI-bRAA, but is slightly less evident in the cdf curves. Nevertheless, both schemes are successful in achieving their common design goal, i.e., satisfying the reliability SINR requirements of V-UEs.

In contrast, the reference scheme fails to meet the targeted requirements in all of the load scenarios. This is due to the prioritization of cellular communication in this scheme and the fact that the used scheduler is only aware of the interference between terminals served by the same eNB, and ignores the stochastic nature of wireless channels. As a result, this scheme tends to first allocate V-UEs near the cell edges, but fails to coordinate this effort and causes high interference between V-UEs served by different eNBs. Under the reference scheme, nearly 40% of the packets are received with an effective SINR that is lower than the set threshold in the low load scenario. This negative effect is even amplified with a growing number of V-UEs, and the portion of SINR violations in the D2D underlay grows to nearly 80% under high load.

Effective SINR Distribution in the Primary Network

Figure 6.3 shows the cdf of the measured effective SINR at the eNB serving the central cell in the simulation scenario. As can be seen, the SINR target of 2 dB is violated under CDI-bRAA with a probability of 0.007 in the low load scenario, 0.006 in the medium load scenario, and 0.005 in the high load scenario, respectively. These values are well within the targeted limit of $p_{\text{out,C}} = 0.1$. Furthermore, as in the case of direct communication, higher SINR values are achieved in most cases as the required transmit power is often overestimated. This fact can be exploited to facilitate adaptive modulation and coding to increase the throughput of C-UEs, as it is being done in current generation LTE networks [STB11]. Hereby, a counter-

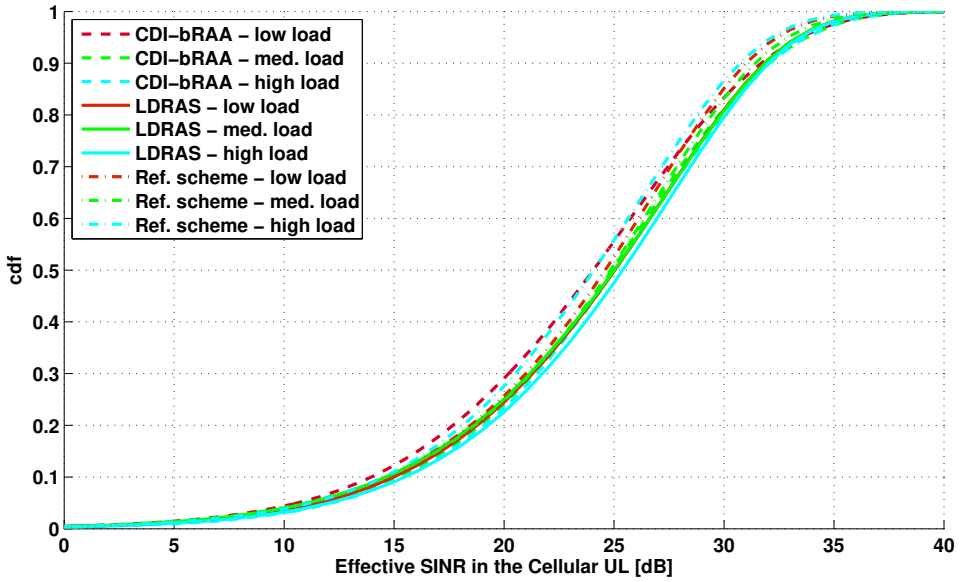

Figure 6.3: Cumulative distribution function of the measured SINR in the primary network under different RRM algorithms and load configurations.

intuitive trend can be observed in the performance of CDI-bRAA, where the scheme shows slightly better performance with increasing load. This can be explained with the higher user diversity, allowing the algorithm to build more favorable tuples of users that reuse the same RBs. Although a higher number of users is served, the resulting interference can be distributed better, and thus leads to better performance.

Similarly, LDRAS shows satisfactory behavior and meets the targeted QoS requirements. The SINR threshold is violated with probability of 0.006 throughout the different load scenarios. Its more conservative approach to the reuse of resources and the often overestimated transmit power also lead to much better effective SINR in many occasions. Again, this fact can be exploited to facilitate adaptive modulation and coding. Due to its fixed spatial resource reuse scheme, LDRAS shows slightly declining performance with increasing load.

Since cellular transmissions are prioritized by the reference scheme, it also meets the QoS requirements. All three of the investigated RRM schemes show close performance in the cellular UL under all load conditions.

Transmission Delay Distribution in the D2D Underlay

Figure 6.4 shows the cdf of the measured transmission delays (i.e., δ_k^{Tx}) for the packets in the D2D underlay. Under LDRAS over 99% of the packets in the low and medium load scenarios are transmitted within the minimum possible delay of 3 ms considering the resource availability in each zone and the chosen MCS. In the high load scenario, this portion shrinks to just over 60%.

The RB allocation to V-UEs under the reference scheme is linked to the RB allocation to C-UEs. As a result, often a larger number of RBs can be used by individual V-UEs as compared to LDRAS. This leads to a lower best case transmission delay of 2 ms. Nevertheless, the reference scheme displays higher delay variation.

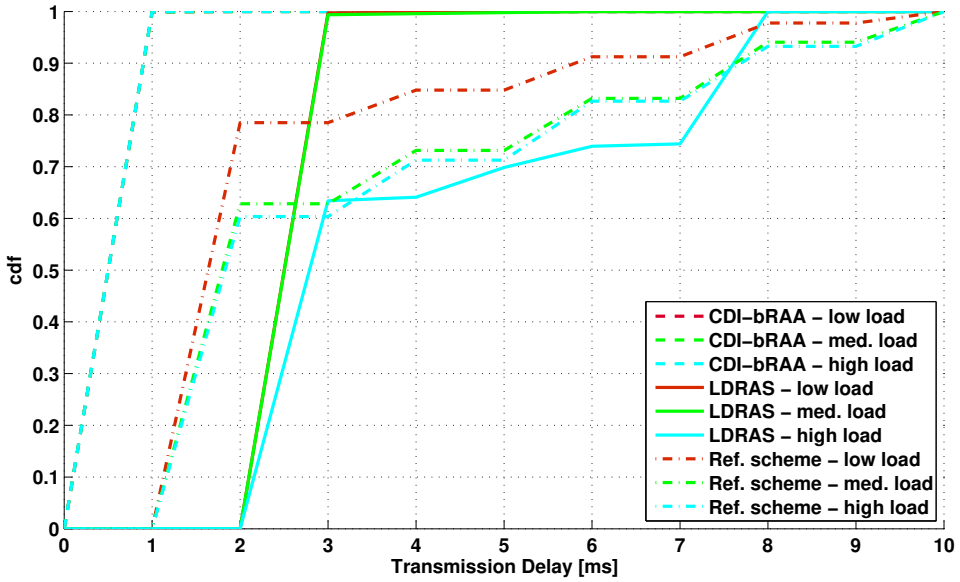

Figure 6.4: Cumulative distribution function of the measured transmission delays in the D2D underlay for different RRM algorithms and load configurations.

	CDI-bRAA	LDRAS	Ref. scheme
low load	0	$\approx 0\%$	5.7%
medium load	0	$\approx 0\%$	36.99%
high load	0	5.4%	88.9%

Table 6.4: Portion of dropped packets due to resource unavailability for different RRM algorithms and load configurations.

In contrast, CDI-bRAA is capable of allocating the required number of RBs per packet (i.e., 15 for the chosen MCS and packet size in these simulations) in a single TTI for all load conditions in more than $99,9\%$ of the cases. The remaining less than 0.1% of the packets are transmitted within 2 TTIs, i.e., 2 ms.

Dropped Packets in the D2D Underlay

All of the generated packets in the D2D underlay are transmitted within the given delay budget under CDI-bRAA. Table 6.4 summarizes the portions of packets which cannot be transmitted on time due to resource unavailability, for the different simulation scenarios. As it is shown, LDRAS is capable of satisfying the availability requirements of C-ITS applications in the low and medium load scenarios. Under high load, the uncoordinated nature of the packet generation by the V-UEs leads to occasional congestions, if the reserved RBs within a certain zone are insufficient to serve all terminals within the given transmission delay budget. Although the scheme may serve up to 4200 V-UEs in the considered deployment (assuming perfectly uniform distribution and aligned packet generation), the conservative behavior of LDRAS results in dropping 5.4% of the generated data packets under high load conditions. Higher system bandwidth would help to improve the link availability. In comparison, the reference scheme deprives a high portion of V-UEs of resources due to its mechanics. It shows

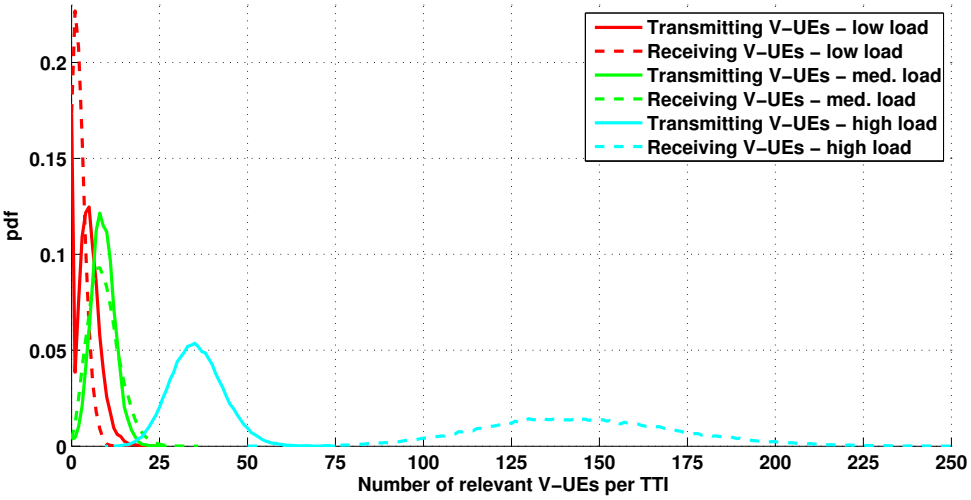

Figure 6.5: Probability density function of the number of relevant transmitting and receiving V-UEs per TTI.

unsatisfactory behavior even in the lower load scenario, and nearly 90% of the packets being discarded under high load.

6.3.2 Protocol Overhead

Figure 6.5 shows the pdf of the number of relevant V-UEs per TTI - the number of parallel transmission attempts and the number of relevant receivers under the different load conditions. Note that the number of relevant V-UEs only takes integer values, but this plot displays a linear interpolation of the discrete pdf for the sake of better readability. In the worst case, there are up to 24 parallel transmission attempts to at most 17 relevant receivers in the low load scenario, 27 parallel transmission attempts to at most 36 relevant receivers in the medium load scenario, and up to 75 parallel transmission attempts to at most 250 relevant receivers in the high load scenario. The respective mean values are measured at 4.5 transmitting V-UEs and 2.3 relevant receiving V-UEs per TTI in the low load scenario, 9 transmitting V-UEs and 9.3 receiving V-UEs per TTI in the medium load scenario, and 35 transmitting V-UEs and 144 receiving V-UEs per TTI in the high load scenario. In order to achieve the above shown QoS under this load, CDI-bRAA and LDRAS require CDI and location information, respectively. The required added SMOH is summarized in Table 6.5. Hereby, the MR of each receiving V-UE is limited to only contain information about the mean number of user per cell and not all active users in the network. This is reasonable, as a receiving V-UE may not be able to receive all SRSs with sufficient strength in order to do a measurement, but the SRSs for the users within half the cell's range around it should be sufficiently strong. Further note that the reference scheme's added SMOH in the UL is approximately 100 times higher as compared to CDI-bRAA, as it requires complete CSI (i.e., the channel coefficients for each of the $S = 100$ RBs).

A good portion of the SMOH in the case of CDI-bRAA is transmitted in the UL. This reduces the availability of resources for cellular UL transmissions. Under high load, the transmission of management and measurement data may require a significant portion of the system bandwidth and, hence, reduce the throughput of C-UEs considerably. Under pessimistic as-

case	load	CDI-bRAA	LDRAS
worst	low	UL: 8234 – 29136 (5.45 – 19.27%) and DL: 5412 (3.58%)	UL: 504 – 816 (0.33 – 0.54%) and DL: 3168 (2.1%)
	med.	UL: 16926 – 57768 (11.19 – 38.2%) and DL: 8316 (5.5%)	UL: 693 – 1044 (0.46 – 0.69%) and DL: 3564 (2.36%)
	high	UL: 185644 – 594990 (122.78 – 393.51%) and DL: 42900 (28.37%)	UL: 1701 – 2676 (1.13 – 1.77%) and DL: 9900 (6.55%)
mean	low	UL: 1312.75 – 3983.85 (0.87 – 2.63%) and DL: 897.6 (0.59%)	UL: 199.5 – 258 (0.13 – 0.17%) and DL: 594 (0.39%)
	med.	UL: 4241.7 – 14585.7 (2.8 – 9.64%) and DL: 2415.6 (1.6%)	UL: 231 – 348 (0.15 – 0.23%) and DL: 1188 (0.79%)
	high	UL: 67538 – 223044 (44.67 – 147.52%) and DL: 23628 (15.63%)	UL: 749 – 1204 (0.5 – 0.8%) and DL: 4620 (3.06%)
worst (limited MR)	high	UL: 39394 – 156240 (26.05 – 103.33%) and DL: 42900 (28.37%)	-

Table 6.5: SMOH for different load conditions and RRM schemes, measured as the sum of occupied REs (and the corresponding percentage of the required network bandwidth).

sumptions, i.e., when a low MCS is required for the transmission of the majority of MRs and an instantaneously high number of relevant receiving and/or transmitting V-UEs, the required resources can even exceed the system capacity. In such a case, the transmission of the MRs would require extra time, adding to the overall packet delay in the D2D underlay and in the cellular UL. An attempt to reduce this overhead can be made by limiting each MR to contain, e.g., the 10 strongest contributions at each receiving V-UE. For such a constellation, the worst-case SMOH in the UL is significantly lower: in the range of $26.05 - 103.33\%$ of the available bandwidth. This comes at the cost of reduced QoS, however. As it can be seen in Figure 6.6a, limiting the MRs leads to a violation of the targeted SINR threshold with a probability of ≈ 0.085, which might be unacceptable for advanced C-ITS applications. This is due to the fact that CDI-bRAA allows for the reuse of resources between UEs where the interference channels are weakest. In the case of limited reporting, exactly these channels are left unknown and the power control OP cannot derive a proper power assignment. Limiting the MRs of V-UEs does not affect the reliability of CDI-bRAA in the cellular UL significantly, as most of the relevant data (with respect to the scheduling of the C-UEs) is measured directly at the eNBs (cf. Figure 6.6b). The different power control outcome and the resulting different interference strongly affect the distribution of the measured effective SINR, however. The limited MR leads to worse performance in approximately 70% of the cases with a significant gap of $5 - 10\,\mathrm{dB}$ compared to the measured effective SINR in the simulations with complete MRs.

It is obvious that a system where at least 44.67% (in the mean case under high load) of

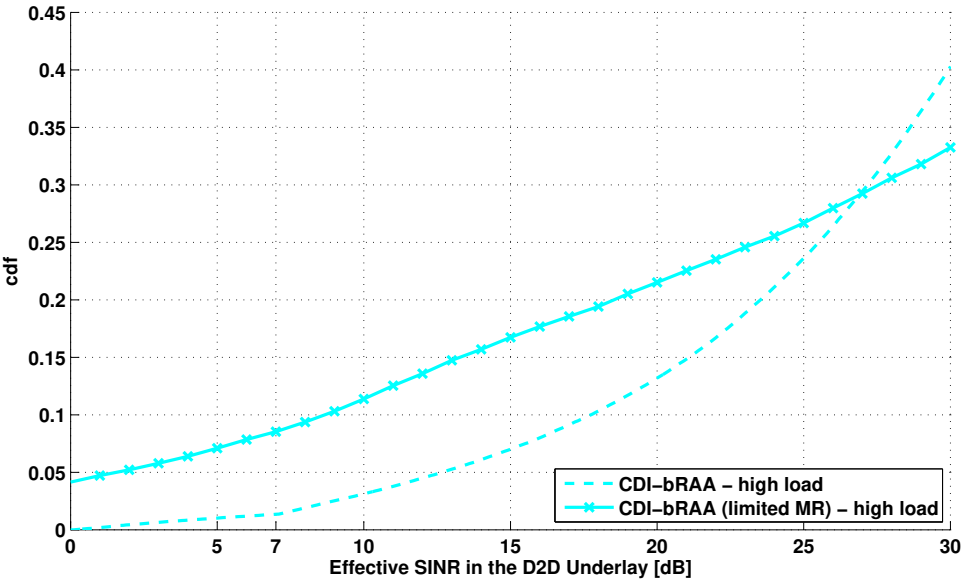

(a) D2D underlay

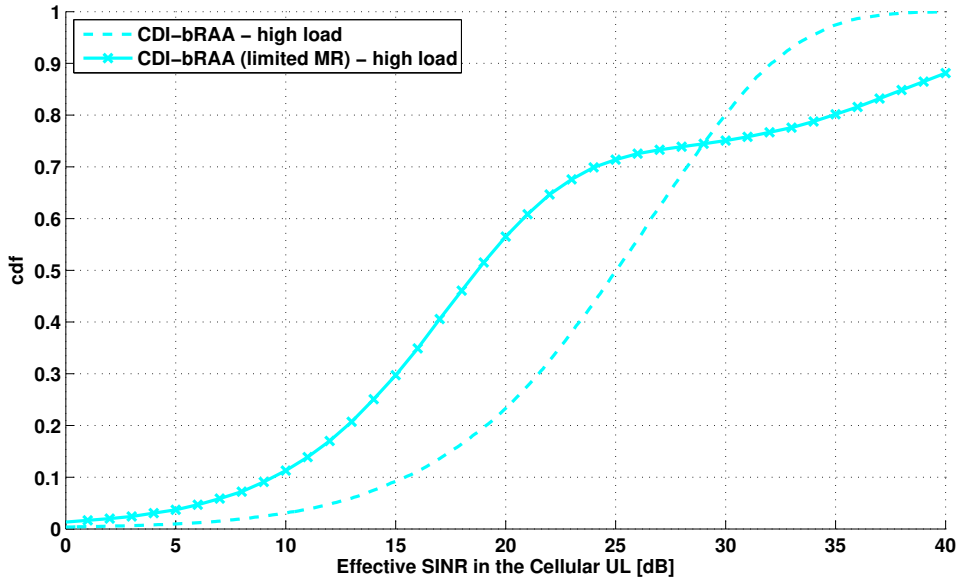

(b) Primary network

Figure 6.6: Cumulative distribution function of the measured transmission delays in the D2D underlay and the primary network under CDI-bRAA with complete and limited MR.

the available UL bandwidth needs to be invested in overhead in order for it to meet its QoS targets is not particularly efficient. In contrast, LDRAS fulfills its design goal and leads to significantly better performance. Even under the most pessimistic assumptions, the added SMOH is limited to 1.77% of the UL bandwidth and 6.55% of the DL bandwidth, and, thus, has bearable impact on the primary network's performance.

In addition to the required radio resources, the SMOH includes further delay. In the case of CDI-bRAA, the simplified protocol for periodic traffic (such as the one considered in these simulations) results in $\delta^{\mathrm{SMOH}} = 9\,\mathrm{ms}$ for the first transmitted packet of each V-UE and $\delta^{\mathrm{SMOH}} = 7\,\mathrm{ms}$ for the following packets. On the other hand, the protocol for LDRAS results in $\delta^{\mathrm{SMOH}} \leq 4\,\mathrm{ms}$ for the first packet generated after a zone change and $\delta^{\mathrm{SMOH}} = 0\,\mathrm{ms}$ for the following ones.

6.3.3 Effects of Complete CSI

It should be noted that the power control in CDI-bRAA often leads to higher than required effective SINR. This is due to its tendency to overestimate the transmit powers of users required to achieve the targeted SINR violation probability. Unfortunately, it is unlikely for the network to exploit this fact to increase the spectral efficiency of the D2D underlay (i.e., through adaptive modulation and coding) due to the limited delay budget of automotive applications, the relatively small packet sizes, and the lack of efficient feedback mechanisms in the context of broadcast communication.

Assuming the availability of complete instantaneous CSI, like in many of the state-of-the-art RRM schemes, RASRFC can be applied. Figure 6.7 shows the cdf of the measured effective SINR under this scheme and compares it against CDI-bRAA. As it can be seen, complete CSI can be leveraged to achieve perfect reliability as the set SINR threshold is exactly met at all of the worst case receiving V-UEs. The remaining receiving V-UEs do experience higher effective SINR, as it can be expected. The cdf curves for RASRFC, however, remain on the left of the corresponding curves for CDI-bRAA in all load conditions. Hence, in addition to only being able to guarantee a certain outage probability strictly greater than zero, CDI-based RRM has the drawback of lower power efficiency as compared to CSI-based RRM.

Remember, however, that the acquisition of complete instantaneous CSI is infeasible in practically relevant network deployments. At the very least, there will be some delay between the channel measurements and the actual channel use. Hence, the input to RASRFC is likely to be outdated and inaccurate which leads to worse performance. This can be seen in Figure 6.7, as RASRFC shows poor reliability in this case (denoted as 'delayed CSI'), with it failing to meet the SINR target in more than 75% of the cases. Hereby, the algorithm shows better performance with the increasing load as a result of the higher receiver diversity.

6.4 Discussion

6.4.1 Quality of Service

The simulation results clearly indicate that satisfying the stringent QoS requirements of C-ITS applications in the considered D2D underlay network is only achieved when special care is taken. The opportunistic approach taken in the reference scheme (and in many of the contributions in the literature) leads to unsatisfactory system behavior, especially with respect to the link availability. Hereby, even under the lowest simulated load conditions, more than

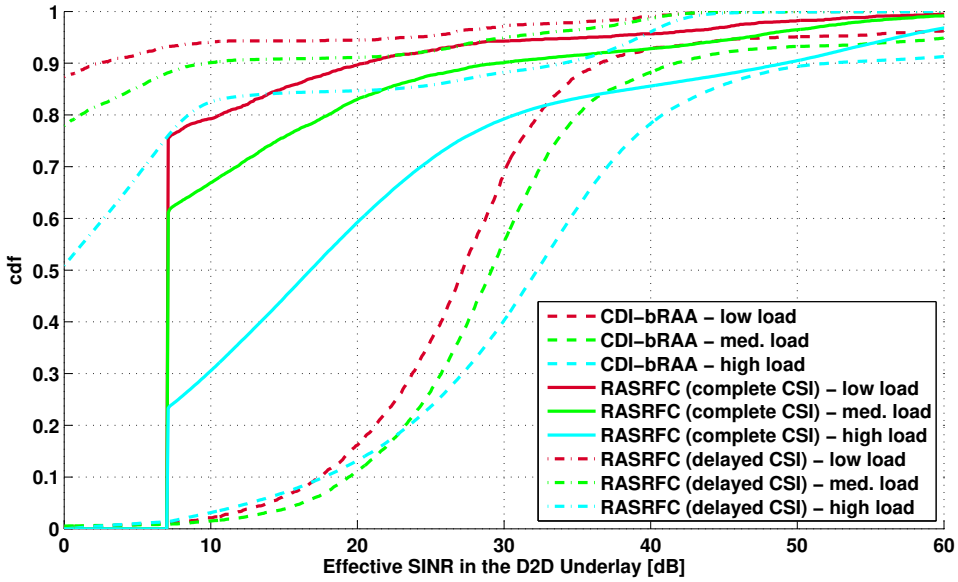

Figure 6.7: Cumulative distribution function of the measured SINR in the D2D underlay under RASRFC and CDI-bRAA.

5% of the vehicular transmissions could not be completed within the considered time budget. This is due to the prioritization of cellular traffic, the effect of which is only amplified with the increasing D2D traffic.

Moreover, the conventional CSI-based approach to RRM building upon the assumption of knowing the channel coefficients for all links in the network is incapable of satisfying the SINR requirements of C-ITS applications, as the wireless channels are, in fact, random in nature. This has been shown by the performance of the reference scheme (cf. Figure 6.2) and the herein proposed RASRFC (cf. the delayed CSI case in Figure 6.7). Hence, said channel randomness needs to be taken into account in RRM in order to enable support for (C-ITS) applications with stringent SINR requirements in a D2D underlay. The herein proposed CDI-bRAA performs well in this regard. However, to meet its set SINR threshold and outage target, this scheme requires complete CDI. The acquisition of which is associated with enormous SMOH due to the broadcast nature of V2X transmissions and the resulting need for knowledge over a huge number of channels, and may cripple the primary network. Moreover, V-UEs operating in half duplex manner may miss relevant transmissions while sending MRs, undermining the purpose of CSI-based RRM in the context of C-ITS applications. Counteracting these negative effects by limiting the acquisition of CDI leads to lower reliability, where the set outage target is exceeded. (cf. Figure 6.6a and Figure 6.3).

In an effort to address the disadvantages of CDI-based RRM, LDRAS relies on location information instead. Although it too satisfies the SINR and packet delay requirements of C-ITS applications, it cannot support as many V-UEs as CDI-bRAA. This is due to its more conservative approach to the reuse of radio resources, originating from the lack of instantaneous channel knowledge. On the other hand, LDRAS requires significantly less resources for the transmission of control information and its added SMOH is bearable.

In summary, CDI-bRAA, depending on the duplexing capabilities of V-UEs, may be preferable in situations with high V-UE density and low C-UE density. The advantages of LDRAS

are best exploited under high cellular load.

6.4.2 Algorithm Complexity

In addition to the resulting network performance, the complexity of CDI-bRAA and LDRAS needs to be taken into account in their respective application. On the one hand, LDRAS has the advantage of an allocation algorithm with minimal added computational complexity over conventional approaches. In fact, the added complexity is equivalent to keeping Z lists that track the availability of RBs for D2D communication in each zone, and matching the available RBs to the L active V-UEs at a given time instance. The allocation algorithm for V-UEs can be implemented with a computational complexity of $O(L)$, where O denotes the Big-Oh operator [BC94]. The complete allocation effort is determined by the chosen scheduler for the primary network. It should be further noted that determining the zone topology and resource reservation in LDRAS requires significant effort. However, as this effort is spent in a planning phase and does not affect the allocation algorithms' complexity during their operation, we disregard it.

On the other hand, CDI-bRAA requires the execution of convolution operations for the calculation of the feasibility metric (cf. Theorem 4.3) and solving the LP (4.54a) for power control in each of its steps (cf. Algorithm 4.2). The standard simplex method for solving the LP has a computational complexity of $O\left(M^{N_{\mathrm{Tot}}}\right)$ [RKT81], where N_{Tot} denotes the total number of allocated users, i.e., $N_{\mathrm{Tot}} = \sum_{s=1}^{S} N(s)$. The standard convolution can be implemented with computational complexity of $O\left(L_{\mathrm{conv}}^2\right)$, where L_{conv} denotes the length of the convolution [KS13]. With this, the total complexity of CDI-bRAA amounts to $O\left(S\left(SM\left(M-1\right)L_{\mathrm{conv}}^2 + M^{N_{\mathrm{Tot}}}\right)\right)$. Hence, in addition to the enormous SMOH, the higher spectral efficiency of CDI-bRAA comes at a price of higher computational complexity, as compared to LDRAS. This complexity, however, can be reduced by splitting the LP into smaller problems with respect to each RB, as mentioned previously, and adopting more efficient algorithm implementations. For example, the convolution may be calculated in the Fourier domain with a complexity of $O\left(L_{\mathrm{conv}} \log L_{\mathrm{conv}}\right)$ [KS13]. The simplex method may also be modified to reduce its complexity to $O\left(N_{\mathrm{Tot}} \log N_{\mathrm{Tot}}\right)$ [RKT81]. Moreover, due to the definition of the feasibility metric, many of the convolutions can be skipped, as the data is either available from previous calculations or the output is not changed due to convolution with the Dirac delta function.

The planning phase where the zone topology and RB reservations in LDRAS are fixed leads to the lower computational complexity in the operation of the allocation algorithm. However, this also leads to the lack of efficient support for heterogeneous QoS requirements. Naturally, different zone topologies and RB reservations may be derived for different SINR requirements and outage targets, but managing a mixture of UEs with mutually different requirements and all of the possible permutations becomes increasingly complex. Hence, it is likely to adopt only the zone topology corresponding to the most stringent requirements. This is also part of the reason behind the lower spectral efficiency of the scheme, as compared to CDI-bRAA which directly supports heterogeneous SINR requirements.

Chapter 7

Conclusions

7.1 Dissertation Summary

Motivated by the ever increasing interest in D2D communication in the context of future 5G cellular networks, and the correlation between its properties and C-ITS applications, this work investigates the D2D paradigm from an automotive perspective. Hereby, the focus of this work is set on the most challenging form of D2D communication, namely underlay D2D communication, where direct links reuse radio resources occupied by conventional cellular transmissions. The resulting cross-interference plays a key role in the network performance. Hence, effective RRM is essential in order to enable support for C-ITS services with stringent QoS requirements in a D2D underlay. In this regard, the vast majority of the state-of-the-art contributions available at the start of this work only considered opportunistic utilization of the D2D underlay and lacked QoS support or resulted in infeasible complexity. Hence, the goal of this work is to deliver feasible solutions to the problem of RRM for underlay D2D communication in future 5G networks, capable of satisfying the strict QoS requirements of C-ITS applications.

Adopting C-ITS application in a D2D underlay is associated with the additional challenge of supporting a huge amount of V-UEs. Their impact on the overall network performance is assessed in Chapter 3 based on an analysis of the system's transport capacity. The envisioned two-tier network is modeled in the context of the CSF, considering the widely adopted CSI- and location-based models. Moreover, upper bounds on the MPUTC for cellular and direct transmissions are derived. Although the transport capacity of the primary cellular network may be reduced slightly by the reuse of radio resources in the D2D underlay under the CSI-based model, the higher efficiency of direct transmissions compensates for this fact and allows for higher overall network capacity (cf. Theorem 3.1). Similar satisfactory behavior is also achieved under the location-based model (cf. Theorem 3.2). Hereby, some of the consequences of system design assumptions are more visible under this second model. The common assumption of prioritizing cellular communication may prohibit underlay D2D communication when a higher number of C-UEs is active. This is done despite the fact that direct communication is the more resource-efficient channel. Hence, the prioritization of services in the future two-tier network might need to be revised in order to enable additional applications based on the D2D paradigm (such as C-ITS services) at the cost of reduced cellular performance. Moreover, network densification through the deployment of a high number of micro and pico cells, one of the other highly interesting topics in the context of 5G networks, reduces the possibility of

reusing radio resources for direct communication whilst maintaining given QoS requirements. Hence, depending on the radio propagation environment, it is likely that only the resources available in macro cells can be reused in D2D underlay manner.

On the bright side, the demonstrated results indicate that a reasonable implementation of a macro cellular network with a D2D underlay may be possible. It should be noted, however, that the derived MPUTC bounds have no implications on their achievability or the instantaneous QoS for individual users. Nevertheless, the possible favorable system behavior motivates the remaining contributions in this work.

In this regard, we develop a feasible RRM scheme, corresponding to the CSI-based model in the context of the CSF, in Chapter 4. Hereby, building upon the common assumption in the literature of complete CSI knowledge, we propose the RASRFC first. This algorithm is based on a resource allocation feasibility check considering the spectral radius of a matrix which reflects the channel conditions in the network, and the SINR requirements of all active users. It is, however, infeasible to acquire complete instantaneous CSI in the network of interest, as wireless channels are random in nature. Hence, RASRFC is developed further to take this randomness into account. The resulting CDI-bRAA, extends the spectral radius feasibility check to the domain of random variables. Hereby, we use an upper bound of said spectral radius in order to derive an explicit function of the resource allocation as a feasibility metric. In a second step, we derive a feasible power allocation that would allow for the SINR requirements of all allocated users to be met with a predefined probability. As shown in Chapter 6, CDI-bRAA shows satisfactory performance in this regard. However, this comes at the cost of enormous added SMOH due to the acquisition of CDI for the huge amount of broadcast links in the network.

In an effort to bypass the need for CDI and the associated costly measurements, we leverage the location-based model in the context of the CSF to define LDRAS in Chapter 5. Hereby, the author's previous work under the assumption of non-fading channels is extended to the more realistic fading environment. The scheme uses previous knowledge about the propagation environment to derive guard distances between UEs that reuse the same radio resources such that the QoS requirements of all affected users can be met. In order to minimize the management overhead in this regard, LDRAS builds upon the concept of partitioning the deployment area into spatially disjoint zones. This partitioning is done by projecting the problem in the domain of clustering analysis. Hereby, the radio resources that are to be used for cellular and D2D communication in each zone are reserved such that the (cross-) interference between users in different zones is within the tolerable limits. This is done by means of a graph coloring approach, based on the derived guard distances and zone topology.

Finally, we validate the performance of the developed RRM schemes' by means of extensive system level simulations in Chapter 6. The need to explicitly consider QoS in RRM is demonstrated by a comparison to an opportunistic state-of-the-art reference scheme which fails to meet the link availability requirements of C-ITS applications. In contrast, both CDI-bRAA and LDRAS fulfill their design goal and enable reliable and timely D2D communication. Hereby, LDRAS supports a lower number of V-UEs as compared to CDI-bRAA as a result of its more conservative approach to resource reuse. This is also inline with the MPUTC bounds in Chapter 3. The more efficient resource utilization under CDI-bRAA comes at the prize of extremely high SMOH for the acquisition of the required CDI. This SMOH may even cripple the primary network under higher load scenarios. Attempting to reduce it by limiting the number of links for which CDI is acquired leads to violations of the SINR requirements.

Alternative CSI/CDI-based and location-based RRM schemes are likely to have similar (or

even higher) SMOH as CDI-bRAA and LDRAS, respectively. Hence, CSI/CDI-based schemes like CDI-bRAA, may only be preferable in situations with high V-UE density and low CUE density. The advantages of location-based schemes, such as LDRAS, are best exploited under high cellular load and moderate V-UE density.

7.2 Additional Remarks

Although reasonable, the combination of D2D broadcast distance, QoS requirements, and propagation environment models in the considered simulations may take a different shape in realistic deployments. A significant increase in the desired broadcast distance or much stricter SINR requirements, for example, would result in greater guard distances in the context of LDRAS. These may cause an inefficient zone topology where radio resources cannot be reused in the same cell. Similar behavior, but to a slightly lesser extent, is expected from CDI-bRAA. Hence, the use of orthogonal spectrum for direct transmissions (i.e., overlay or out-band D2D communication) may be necessary when considering extremely stringent QoS requirements.

The herein developed RRM schemes are defined with focus on the D2D underlay case, but are also applicable to the less challenging overlay and out-band D2D communication cases. The lack of cross-interference in such scenarios allows for significant simplifications. In the case of CDI-bRAA, the allocation problem splits into two separate ones: one for C-UEs and one for V-UEs. Hereby, the required SMOH is reduced by the fraction corresponding to the cross-interference links. The broadcast nature of the vehicular transmission, however, still results in the necessity to transmit a huge amount of channel coefficients from receiving V-UEs to their serving eNB.

In an overlay or out-band D2D communication setting, LDRAS can be reduced to only control the direct transmissions. Hereby, the expressions for the derivation of the needed guard distances are simplified due to the elimination of cross-interference terms. In fact, defining a special guard area around each eNB is not needed. Although the planning phase is simplified, the added SMOH in the operation of the allocation algorithm remains the same.

7.3 Outlook

Although the contributions in this work reach their aim of enabling reliable vehicular D2D communication, additional questions arise from their context and may serve as a basis for further investigations. For example, power economy has not been addressed in this work. In this regard, it may be possible to derive power control mechanisms with lower power consumption, especially in the case of CDI-bRAA.

Moreover, the CDI input to this algorithm is likely to suffer from estimation errors in a realistic deployment. Hence, means of mitigating the effects of such input uncertainty may be required in order to reach the herein demonstrated reliability in the error-free case. Similarly, the effect of inaccurate channel models and means for the mitigation of the resulting errors may be of interest in the context of LDRAS.

Furthermore, the set SINR targets can only be met by CDI-bRAA with the required probability when complete CDI is available. Its acquisition by means of measurements, however, may not be feasible under higher load conditions. Hence, alternative methods such as channel prediction may help reduce the SMOH whilst preserving CDI-bRAA's reliability.

Finally, the implications of using multiple antennas at each UE/eNB (i.e., considering a Multiple-Input Multiple-Output system) may be investigated in an effort to boost the spectral efficiency of the considered two-tier network even further.

Appendix A

List of Symbols

Δ	Environment-specific control parameter for successful cellular communication under the location-based model
Δ'	Environment-specific control parameter for successful D2D communication under the location-based model
$\mathbf{1}$	All-ones vector of appropriate size
$\mathbf{A}$	Interference coupling matrix for the entire system bandwidth
a	Auxiliary variable
$a_{kl}^{(s)}$	Effective interference power gain
α	Auxiliary variable
α	Environment-specific path loss exponent
α_{pow}	Power correction factor
α'	Auxiliary variable
a_{pow}	Fractional power loss compensation factor
$\mathbf{A}^{(\mathbf{s})}$	Interference coupling matrix (associated with RB s)
b_1	Auxiliary variable
β	Auxiliary variable
β_1	Auxiliary variable
β_2	Auxiliary variable
β_{MCS}	MCS-specific calibration margin
β'	Auxiliary variable
C	Number of eNBs over the area of interest
$\mathbb{C}$	The set of complex numbers
c_{kl}	Auxiliary variable
$\mathfrak{C}$	Set of available colors at a given instance in the graph coloring algorithm
$\mathfrak{C}'$	Auxiliary set of colors in the graph coloring algorithm
$\mathcal{C}_z$	Set of eNBs that may serve users in zone z
d	Desired D2D/V2X broadcast distance
δ	Auxiliary positive constant
δ_k^{E2E}	E2E transmission delay for transmission k
δ_k^{SMOH}	SMOH delay for transmission k
δ_k^{Tx}	Actual transmission delay for transmission k
d_{kl}	Distance/location-dependent channel gain component for the link between transmitter k and the worst-case receiver associated with transmitter l

$\bar{d}_{k,\tilde{r}(k)}$	Mean distance between a C-UE and its serving (i,e,, closest) eNB
$\bar{d}$	Normalized desired D2D/V2X broadcast distance
d_{samp}	Sampling distance
$\mathcal{E}$	Set of edges in a graph
$e_{kl}^{(s)}$	Element of the interference activation matrix associated with RB s
E_s	The event that a given resource allocatgion fails to meet the resouce allocation feasibility condition
$\mathbf{E}^{(s)}$	Interference activation matrix associated with RB s
$\mathfrak{e}\left(w, w'\right)$	Euclidean distance between location w and location w
$f_{\text{D},50\,\text{km/h}}$	Maximum Doppler shift at a relative speed of 50 km/h
g	Exponential random variable
$\mathbf{G}$	Effective interference coupling matrix
$\mathcal{G}$	Graph
G_0	Maximum antenna gain at the receiving eNBs
$\mathbf{\Gamma}$	Matrix collecting the SINR targets of all users for all RBs
γ_{C}	SINR requirement for cellular transmissions
γ_{D2D}	SINR requirement for D2D transmissions
γ_k	SINR requirement of user k
$\gamma_k^{(s)}$	SINR target of user k for RB s
$\boldsymbol{\gamma}^{(s)}$	Vector collecting the SINR targets of all users for RB s
$G\left(\phi\right)$	Antenna gain at the eNBs
g'	Exponential random variable
$h\left(\cdot\right)$	Distance-dependent component of the channel gain at agiven distance in the propagation model for D2D communication
$h_{kl}^{(s)}$	Channel coefficient for the link between transmitter k and the worst-case receiver associated with transmitter l, in RB s
$h'\left(\cdot\right)$	Distance-dependent component of the channel gain at agiven distance in the propagation model for cellular communication
$h^{(w)}$	Constant power gain control parameter for location w under LDRAS
$H^{(w)}$	Constant power gain for potential direct transmissions originating from a transmitting V-UE at location w to all other locations in the network
i	Numer of already allocated users in a given iteration of CDI-bRAA
$\mathbf{I}$	Identity matrix of appropriate size
$I_{kl}^{(s)}$	Auxiliary random variable, defined as $I_{kl}^{(s)} = \gamma_k^2 \pi_{ks} \frac{d_{kl}^2}{d_{kk}^2} Z_{kl}^{(s)}$
ι	Auxiliary variable in a Laplace transformation
k	Primary transmitter/transmission index
K	Total number of cellular users to be served at a given time
$\mathcal{K}_{\text{active}}$	Set of active C-UEs at a given time instance
κ_{ks}	PF metric associated with C-UE k and RB s
l	Secondary transmitter/transmission index
L	Total number of D2D users to be served at a given time
λ	MPUTC in the primary network
λ'	MPUTC in the D2D underlay
λ_x	Mean of the random variable t_x
L_{conv}	Length of the numerical convolution

L_{pow}	Power loss on a given link (in dB)
M	Total number of cellular and D2D users to be served at a given time
$\mathcal{M}$	Set of active users to be served at a given time
$\mathfrak{M}^{(w)}$	Matrix that describes the locations, where another transmitter is allowed to transmit in the same RBs as a V-UE at location w
$\mathfrak{M}'^{(c)}$	Matrix that describes the locations, where a V-UE may reuse the radio resources occupied by a cellular UL transmission
$\mathfrak{m}_{u,v}^{(w)}$	(u,v)-th element of the matrix $\mathfrak{M}^{(w)}$
$\mathfrak{m}_{u,v}^{\prime(c)}$	(u,v)-th element of the matrix $\mathfrak{M}'^{(c)}$
$\mathbb{N}_0$	The set of natural numbers and zero
$\eta_{kr}^{(s)}$	Noise power at receiver r associated with transmitter k, in RB s
n_{sim}	Number of parallel cellular transmissions
n'_{sim}	Number of parallel D2D transmissions
N_{Tot}	Total number of allocated users
$\mathcal{N}_z$	Set of relevant neighbors to zone z, which impose restrictions on the sets of RBs that can be used for D2D transmissions
$\mathcal{N}'_z$	Set of relevant neighbors to zone z, which impose restrictions on the sets of RBs that can be used for cellular transmissions
$\mathcal{O}_z$	Cluster of locations in zone z
$\mathcal{P}$	Set of feasible resource allocations
$\mathfrak{P}$	Set of feasible power assignments
$P_{\text{C-UE}}$	Maximum transmit power of C-UEs
ϕ	Azimuth angle
$\mathbf{\Pi}$	Allocation matrix
π_{ks}	(k,s)-th element of the matrix $\mathbf{\Pi}$
P_k	Maximum transmit power of user k
$p_k^{(s)}$	Transmit power of user k in RB s
$p_{\text{out,C}}$	Targeted outage probability of cellular communication
$p_{\text{out,D2D}}$	Targeted outage probability of D2D communication
$\mathbf{p}^{(s)}$	Power vector associated with RB s
$\overline{P_{\text{V-UE}}}$	Upper bound on $P_{\text{V-UE}}$
$P_{\text{V-UE}}$	Maximum transmit power of V-UEs
$\mathbf{q}$	Transmit powers of all users in all RBs
r	Receiver index
R_0	Targeted RSS at a receiving eNB
r_1	Desired minimum distance between a receiving eNB and an interfering V-UE
$\overline{r_1}$	Upper bound on r_1
r_2	Desired minimum distance between a receiving V-UE and an interfering C-UE
$\overline{r_2}$	Upper bound on r_2
$\mathcal{RB}_{\text{C},z}$	Set of RBs reserved for cellular communication in zone z
$\mathcal{RB}_{\text{D2D},z}$	Set of RBs reserved for D2D communication in zone z
$\mathcal{RB}_y$	y-th subset of RBs
$r(C)$	Radius of the coverage area of an eNB, depending on the number of deployed eNBs

$\mathbb{R}_{\geq 0}$	The set of positive real numbers and zero
$\tilde{\rho}$	Auxiliary variable defined as $\tilde{\rho} \coloneqq \max_{s} \frac{M-1}{M} \sum_{k=1}^{M} \sum_{\substack{l=1,\\ l\neq k}}^{M} \left(\gamma_k \pi_{ks} a_{kl}^{(s)}\right)^2$
$\mathbb{R}_{+}$	The set of strictly positive real numbers
$r_{\mathrm{p,th}}$	Threshold on the probability of meeting the SINR targets of all of the allocated users
$\mathfrak{R}(k)$	Set of relevant receivers associated with transmitter k
r_{th}	Fixed probability threshold
$\tilde{r}(k)$	Worst-case receiver associated with transmitter k
S	Total number of available RBs per TTI
$\mathfrak{S}$	Similarity matrix
s	RB index
σ_{C}^2	Variance of the Rayleigh fading on cellular links
σ_{D2D}^2	Variance of the Rayleigh fading on D2D links
σ_{kl}^2	Variance of the Rayleigh fading on the link between transmitter k and the (worst-case) receiver of transmitter l
$\mathrm{SINR}_{kr}^{\mathrm{eff}}$	Effective SINR measured at receiver r associated with transmitter k over the entire transmission bandwidth
$\mathrm{SINR}_{kr}^{(s)}$	SINR measured at receiver r associated with transmitter k, in RB s
S_k	Number of RBs allocated to transmitter k at a given time
$\mathcal{S}_k$	Set of RBs allocated to user k at a given time
$\mathcal{S}$	Set of available RBs
$\mathfrak{s}_{w,w'}$	(w,w')-th element of the matrix $\mathfrak{S}$
T	Transmission interval
T_{total}	Number of graph coloring trials
t_x	Auxiliary exponential random variable
U	Number of horizontal pixels
$U(k)$	Urgency metric
$\upsilon_k^{\mathrm{out}}$	Acceptable outage probability for transmission k
$\mathcal{V}$	Set of vertices in a graph
V	Number of vertical pixels
$\mathbf{V}^{(s)}$	Auxiliary variable, defined as $\mathbf{V}^{(s)} \coloneqq \mathrm{diag}\left(\boldsymbol{\gamma}^{(s)}\right)\left(\mathbf{A}^{(s)} \circ \mathbf{E}^{(s)}\right) \in \mathbb{R}_{\geq 0}^{M\times M}, s \in \mathcal{S}$
W	System bandwidth
$\mathbf{x}_k$	Coordinates of UE/eNB k
Y	Number of disjoint RB sets
Z	Number of zones
$\mathcal{Z}$	Set of all zones
z	Zone index
Z_{I}	Auxiliary variable, defined as $Z_{\mathrm{I}} \coloneqq \sum_{i=1}^{6} P_{\text{C-UE}} h(r_2) g_i + \sum_{j=1}^{3} P_{\text{V-UE}} h(r_2) g_j$
Z_{I}'	Auxiliary variable, defined as $Z_{\mathrm{I}}' \coloneqq \sum_{j=1}^{3} P_{\text{V-UE}} h'(r_1) g_j'$
$Z_{kl}^{(s)}$	Auxiliary variable, defined as $Z_{kl}^{(s)} = \frac{z_{kl}^{(s)2}}{z_{kk}^{(s)2}}$

$z_{kl}^{(s)}$	Random channel gain component for the link between transmitter k and the worst-case receiver associated with transmitter l, in RB s
Z_{S}	Auxiliary variable, defined as $Z_{\mathrm{S}} \coloneqq P_{\text{V-UE}} h\left(d\right) g$
Z'_{S}	Auxiliary variable, defined as $Z'_{\mathrm{S}} \coloneqq R_0 g'$

Appendix B

List of Figures

Appendix C

List of Tables

Appendix D

List of Abbreviations

5G	Fifth Generation of Mobile Communication
AWGN	Additive White Gaussian Noise
BSR	Buffer Status Report
C-ITS	Cooperative Intelligent Transport Systems
C-UE	Cellular User Equipment
cdf	Cumulative Distribution Function
CDI	Channel Distribution Information
CDI-bRAA	Channel-Distribution-Information-based Resource Allocation Algorithm
CE	Consumer Electronics
CSF	Capacity Scaling Framework
CSI	Channel State Information
CSMA	Carrier Sense Multiple Access
D2D	Device-to-Device
DL	Downlink
E2E	End-to-end
eNB	evolved NodeB
FDD	Frequency Division Duplex
HARQ	Hybrid Automatic Repeat reQuest
KPI	Key Performance Indicator
LBSR	Location and Buffer Status Report
LDRAS	Location Dependent Resource Allocation Scheme
LHS	Left-Hand Side
LOS	Line-of-Sight
LTE	Long Term Evolution
MAC	Medium Access Control
MCS	Modulation and Coding Scheme
MNO	Mobile Network Operator
MPUTC	Mean Per-User Transport Capacity
MR	Measurement Report
NLOS	Non-Line-of-Sight
OFDMA	Orthogonal Frequency-Division Multiple Access
OP	Optimization Problem

PF	Proportional Fair
PUCCH	Physical Uplink Control CHannel
PUSCH	Physical Uplink Shared CHannel
QoS	Quality of Service
RAN	Radio Access Network
RASRFC	Resource Allocation algorithm with a Spectral Radius Feasibility Check
RB	Resource Block
RE	Resource Element
RHS	Right-Hand Side
RRM	Radio Resource Management
RSS	Received Signal Strength
SC-FDMA	Single-Carrier Frequency Division Multiple Access
SINR	Signal-to-Interference-and-Noise-Ratio
SISO	Single-Input Single-Output
SMOH	Signaling and Measurement Overhead
SPC	Stochastic Power Control
SR	Scheduling Request
SRS	Sounding Reference Signal
TTI	Transmission Time Interval
UE	User Equipment
UL	Uplink
V-UE	Vehicular User Equipment
V2X	Vehicle-to-Anything

Publications

[BKKF14] M. Botsov, M. Klügel, W. Kellerer, and P. Fertl. Location dependent resource allocation for mobile device-to-device communications. In *IEEE Wireless Comunications and Networking Conference*, pages 1690–1695, April 2014.

[BKKF15] M. Botsov, M. Klügel, W. Kellerer, and P. Fertl. Location-based resource allocation for mobile D2D communications in multicell deployments. In *IEEE International Conference on Communications (ICC) Workshops*, pages 2456–2462, June 2015.

[Bot13] M. Botsov. Device-to-device communications for vehicular terminals as an underlay to long term evolution networks. Master's thesis, Technische Universität München, Germany, 2013.

[BSF15a] M. Botsov, S. Stańczak, and P. Fertl. Comparison of location-based and CSI-based resource allocation in D2D-enabled cellular networks. In *IEEE International Conference on Communications (ICC)*, pages 2529–2534, June 2015.

[BSF15b] M. Botsov, S. Stańczak, and P. Fertl. On the transport capacity of next-generation cellular networks with vehicular D2D underlay. In *International Symposium on Wireless Communication Systems (ISWCS)*, pages 176–180, August 2015.

[BSF16a] M. Botsov, S. Stańczak, and P. Fertl. On the overhead of radio resource management schemes for mobile underlay D2D communication. In *IEEE Vehicular Networking Conference (VNC)*, pages 84–91, December 2016.

[BSF16b] M. Botsov, S. Stańczak, and P. Fertl. Optimized zone design for location-based resource allocation in mobile D2D underlay networks. In *International Symposium on Wireless Communication Systems (ISWCS)*, September 2016.

[BSF16c] M. Botsov, S. Stańczak, and P. Fertl. Stochastic Resource Allocation and Power Optimization for Mobile D2D Communications. in preparation, 2016.

[CMB+18] D. Calabuig, D. Martín-Sacristán, M. Botsov, J. F. Monserrat et al. Comparison of LTE centralized RRM and IEEE 802.11 decentralized RRM for ITS cooperative awareness. In *IEEE Wireless Communications and Networking Conference (WCNC)*, pages 1–6, April 2018.

[CMM+18] D. Calabuig, D. Martín-Sacristán, J. F. Monserrat, M. Botsov et al. Distribution of road hazard warning messages to distant vehicles in Intelligent Transport

Systems. *IEEE Transactions on Intelligent Transportation Systems*, 19(4):1152–1165, April 2018.

[GEGSBS16] M. A. Gutierrez-Estevez, D. Gozalvez-Serrano, M. Botsov, and S. Stańczak. STFDMA: a novel technique for Ad-Hoc V2V networks exploiting radio channels frequency diversity. In *International Symposium on Wireless Communication Systems (ISWCS)*, September 2016.

[HED+16] L. Hu, J. Eichinger, M. Dillinger, M. Botsov et al. Unified device-to-device communications for low-latency and high reliable vehicle-to-x services. In *IEEE Vehicular Technology Conference (Spring)*, pages 1–7, May 2016.

[SBS+16] W. Sun, M. Botsov, E. G. Ström, F. Brännström et al. A novel framework for radio resource management in 5G enabled vehicular networks. in preparation, 2016.

Bibliography

[3GP10] 3GPP. TS 36.211 Physical channels and modulation. v. 9.1.0, March 2010.

[3GP12] 3GPP. TS 36.213 Physical layer procedures. v. 11.0.0, September 2012.

[3GP16] 3GPP. TS 36.321 Medium Access Control (MAC) protocol specification. v. 13.2.0, June 2016.

[AATK13] J. Agbinya, M. Aguayo-Torres, and R. Klempous. *4G Wireless Communication Networks: Design Planning and Applications.* River Publishers series in communications. River Publishers, 2013.

[AATSH14] N. Abu-Ali, A. E. M. Taha, M. Salah, and H. Hassanein. Uplink scheduling in LTE and LTE-Advanced: tutorial, survey and evaluation framework. *IEEE Communications Surveys & Tutorials*, 16(3):1239–1265, 2014.

[AM97] S. V. Amari and R. B. Misra. Closed-form expressions for distribution of sum of exponential random variables. *IEEE Transactions on Reliability*, 46(4):519–522, December 1997.

[AWM14] A. Asadi, Q. Wang, and V. Mancuso. A survey on device-to-device communication in cellular networks. *IEEE Communications Surveys & Tutorials*, 16(4):1801–1819, 2014.

[BC94] D. Bovet and P. Crescenzi. *Introduction to the Theory of Complexity.* Prentice Hall, 1994.

[BCGS04] S. Basagni, M. Conti, S. Giordano, and I. Stojmenovic. *Mobile Ad Hoc Networking.* John Wiley & Sons, Inc., 2004.

[Ber11] P. Bertrand. Channel gain estimation from sounding reference signal in LTE. In *IEEE Vehicular Technology Conference (Spring)*, pages 1–5, May 2011.

[BFA11] M. Belleschi, G. Fodor, and A. Abrardo. Performance analysis of a distributed resource allocation scheme for D2D communications. In *IEEE GLOBECOM Workshops*, pages 358–362, December 2011.

[BM76] J. A. Bondy and U. S. R. Murty. *Graph Theory with Applications.* Elsevier Science Publishing, 1976.

[Bon13] M. Bonamente. *Statistics and Analysis of Scientific Data.* Graduate Texts in Physics. Springer New York, 2013.

[BR07] A. Behzad and I. Rubin. Optimum integrated link scheduling and power control for multihop wireless networks. *IEEE Transactions on Vehicular Technology*, 56(1):194–205, January 2007.

[BSH03] F. Bai, N. Sadagopan, and A. Helmy. Important: a framework to systematically analyze the impact of mobility on performance of routing protocols for adhoc networks. In *INFOCOM*, volume 2, pages 825–835, March 2003.

[Cis16] Cisco. Cisco Visual Networking Index: Global mobile data traffic forecast update, 2015—2020. White paper, February 2016.

[CPG+13] F. Capozzi, G. Piro, L. A. Grieco, G. Boggia et al. Downlink packet scheduling in LTE cellular networks: Key design issues and a survey. *IEEE Communications Surveys & Tutorials*, 15(2):678–700, February 2013.

[CTV11] K. Christodoulopoulos, I. Tomkos, and E. A. Varvarigos. Elastic bandwidth allocation in flexible OFDM-based optical networks. *Journal of Lightwave Technology*, 29(9):1354–1366, May 2011.

[Cur41] J. H. Curtiss. On the distribution of the quotient of two chance variables. *The Annals of Mathematical Statistics*, 12(4):409–421, 12 1941.

[CYS15] X. Cheng, L. Yang, and X. Shen. D2D for intelligent transportation systems: A feasibility study. *IEEE Transactions on Intelligent Transportation Systems*, 16(4):1784–1793, August 2015.

[DD16] M. Deza and E. Deza. *Encyclopedia of Distances*. Springer Berlin Heidelberg, 2016.

[DE03] S. Dey and J. Evans. Optimal power control in wireless data networks with outage-based utility guarantees. In *IEEE Conference on Decision and Control*, volume 1, pages 570–575, December 2003.

[DE04] P. Delaigue and A. Eskandarian. A comprehensive vehicle braking model for predictions of stopping distances. *Proceedings of the Institution of Mechanical Engineers, Part D: Journal of Automobile Engineering*, 218(12):1409–1417, 2004.

[Dir81] P. Dirac. *The Principles of Quantum Mechanics*. International series of monographs on physics. Clarendon Press, 1981.

[DRW+09] K. Doppler, M. Rinne, C. Wijting, C. Ribeiro et al. Device-to-device communication as an underlay to LTE-Advanced networks. *IEEE Communications Magazine*, 47(12):42–49, December 2009.

[DYRJ10] K. Doppler, C. H. Yu, C. B. Ribeiro, and P. Janis. Mode selection for device-to-device communication underlaying an LTE-Advanced network. In *IEEE Wireless Communication and Networking Conference (WCNC)*, pages 1–6, April 2010.

[EE04] T. ElBatt and A. Ephremides. Joint scheduling and power control for wireless ad hoc networks. *IEEE Transactions on Wireless Communications*, 3(1):74–85, January 2004.

[ETS09] ETSI. TR 102 638 Intelligent Transport Systems (ITS); Vehicular communications; Basic set of applications; Definitions, June 2009.

[ETS11] ETSI. TS 102 637-2 Intelligent Transport Systems (ITS); Vehicular Communications; Basic Set of Applications; Part 2: Specification of Cooperative Awareness Basic Service, March 2011.

[ETS13] ETSI. TR 101 607 Intelligent Transport Systems (ITS); Cooperative ITS (C-ITS). Technical report, ETSI, May 2013.

[FDM+12] G. Fodor, E. Dahlman, G. Mildh, S. Parkvall et al. Design aspects of network assisted device-to-device communications. *IEEE Communications Magazine*, 50(3):170–177, March 2012.

[Fel71] W. Feller. Law of large numbers for identically distributed variables. *An introduction to probability theory and its applications*, 2:231–234, 1971.

[Fis13] G. Fishman. *Monte Carlo: Concepts, Algorithms, and Applications*. Springer Series in Operations Research and Financial Engineering. Springer New York, 2013.

[FLE87] N. Fisher, T. Lewis, and B. Embleton. *Statistical Analysis of Spherical Data*. Cambridge University Press, 1987.

[FLY+16] D. Feng, L. Lu, Y. W. Yi, G. Y. Li et al. QoS-aware resource allocation for device-to-device communications with channel uncertainty. *IEEE Transactions on Vehicular Technology*, 65(8):6051–6062, August 2016.

[FSA04] I. Forkel, M. Schinnenburg, and M. Ang. Generation of two-dimensional correlated shadowing for mobile radio network simulation. In *International Symposium on Wireless Personal Multimedia Communications*, September 2004.

[FTP+13] M. Fallgren, B. Timus, P. Popovski, V. Braun et al. Deliverable D1.1: Scenarios, requirements and KPIs for 5G mobile and wireless system. Deliverable, ICT-317669 METIS, April 2013.

[GJF+08] F. Gunnarsson, M. N. Johansson, A. Furuskar, M. Lundevall et al. Downtilted base station antennas - a simulation model proposal and impact on HSPA and LTE performance. In *IEE Vehicular Technology Conference (Fall)*, pages 1–5, September 2008.

[GK00] P. Gupta and P. Kumar. The capacity of wireless networks. *IEEE Transactions on Information Theory*, 46(2):388–404, March 2000.

[Gol05] A. Goldsmith. *Wireless Communications*. Cambridge University Press, August 2005.

[GSTW04] A. Gühnemann, R.-P. Schäfer, K.-U. Thiessenhusen, and P. Wagner. Monitoring traffic and emissions by floating car data, 2004. DLR, available online, `http://elib.dlr.de/6675/`.

[GT01] M. Grossglauser and D. Tse. Mobility increases the capacity of ad-hoc wireless networks. In *IEEE INFOCOM*, volume 3, pages 1360–1369, April 2001.

[Haz88] M. Hazewinkel. *Encyclopaedia of mathematics: an updated and annotated translation of the Soviet 'Mathematical Encyclopaedia'*. Number Volume 1 in Encyclopaedia of Mathematics. Kluwer Academic Publishers, 1988.

[Hoc07] D. S. Hochbaum. Complexity and algorithms for nonlinear optimization problems. *Annals of Operations Research*, 153(1):257–296, Sep 2007.

[Ibe11] O. Ibe. *Fundamentals of Stochastic Networks*. Wiley, 2011.

[IEE12] IEEE. IEEE Standard for Information technology–Telecommunications and information exchange between systems; Local and metropolitan area networks–Specific requirements Part 11: Wireless LAN Medium Access Control (MAC) and Physical Layer (PHY) Specifications. *IEEE Std 802.11-2012 (Revision of IEEE Std 802.11-2007)*, pages 1–2793, March 2012.

[JD88] A. Jain and R. Dubes. *Algorithms for clustering data*. Prentice-Hall Advanced Reference Series. Prentice Hall PTR, 1988.

[JKR+09] P. Jänis, V. Koivunen, C. Ribeiro, J. Korhonen et al. Interference-aware resource allocation for device-to-device radio underlaying cellular networks. In *IEEE Vehicular Technology Conference (VTC), Spring*, pages 1–5, April 2009.

[JLW+16] D. Jia, K. Lu, J. Wang, X. Zhang et al. A survey on platoon-based vehicular cyber-physical systems. *IEEE Communications & Surveys Tutorials*, 18(1):263–284, 2016.

[JYD+09] P. Jänis, C. Yu, K. Doppler, C. Ribeiro et al. Device-to-device communication underlaying cellular communications systems. *International Journal of Communications, Network and System Sciences*, 2(3):169–178, August 2009.

[KB02] S. Kandukuri and S. Boyd. Optimal power control in interference-limited fading wireless channels with outage-probability specifications. *IEEE Transactions on Wireless Communications*, 1(1):46–55, January 2002.

[KMH+07] P. Kyösti, J. Meinilä, L. Hentilä, X. Zhao et al. WINNER II channel models. Deliverable, IST-4-027756 WINNER II, September 2007.

[KPP04] H. Kellerer, U. Pferschy, and D. Pisinger. *Knapsack Problems*. Springer, 2004.

[KPP13] H. Kellerer, U. Pferschy, and D. Pisinger. *Knapsack Problems*. Springer Berlin Heidelberg, 2013.

[KS13] P. Karas and D. Svoboda. *Design and Architectures for Digital Signal Processing*, chapter Algorithms for Efficient Computation of Convolution. InTech, 2013. Available from: http://www.intechopen.com/books/design-and-architectures-for-digital-signal-processing/algorithms-for-efficient-computation-of-convolution.

[KTT+02] S. Kato, S. Tsugawa, K. Tokuda, T. Matsui et al. Vehicle control algorithms for cooperative driving with automated vehicles and intervehicle communications. *IEEE Transactions on Intelligent Transportation Systems*, 3(3):155–161, September 2002.

[LBFM12] C. Lottermann, M. Botsov, P. Fertl, and R. Müllner. Performance evaluation of automotive off-board applications in LTE deployments. In *IEEE Vehicular Networking Conference (VNC)*, pages 211–218, November 2012.

[Lei79] F. T. Leighton. A graph coloring algorithm for large scheduling problems. *Journal of Research of the Notional Bureau of Standards*, 84(6), June 1979.

[LPM+09] S.-B. Lee, I. Pefkianakis, A. Meyerson, S. Xu et al. Proportional fair frequency-domain packet scheduling for 3GPP LTE uplink. In *IEEE INFOCOM*, pages 2611–2615, April 2009.

[LS14] N. Lu and X. S. Shen. *Capacity Analysis of Vehicular Communication Networks.* Springer New York, 2014.

[MBL+14] A. Maltsev, I. Bolotin, A. Lomayev, A. Pudeyev et al. Deliverable D4.1: System Level Simulator Specification. Deliverable, ICT-608637 MiWEBA, December 2014.

[MDV13] M. Maso, M. Debbah, and L. Vangelista. A distributed approach to interference alignment in OFDM-based two-tiered networks. *IEEE Transactions on Vehicular Technology*, 62(5):1935–1949, June 2013.

[Mey00] C. D. Meyer. *Matrix Analysis and Applied Linear Algebra.* Society for Industrial and Applied Mathematics, 2000.

[MFP+14] G. Mange, M. Fallgren, P. Popovski, V. Braun et al. Deliverable D6.2: Initial report on horizontal topics, first results and 5G system concept, April 2014.

[MLPH11] H. Min, J. Lee, S. Park, and D. Hong. Capacity enhancement using an interference limited area for device-to-device uplink underlaying cellular networks. *IEEE Transactions on Wireless Communications*, 10(12):3995–4000, December 2011.

[NW06] J. Nocedal and S. J. Wright. *Numerical Optimization.* Springer New York, 2 edition, 2006.

[OKI09] H. Okamoto, K. Kitao, and S. Ichitsubo. Outdoor-to-indoor propagation loss prediction in 800-MHz to 8-GHz band for an urban area. *IEEE Transactions on Vehicular Technology*, 58(3):1059–1067, March 2009.

[PLW+09] T. Peng, Q. Lu, H. Wang, S. Xu et al. Interference avoidance mechanisms in the hybrid cellular and device-to-device systems. In *IEEE International Symposium on Personal, Indoor and Mobile Radio Communications (PIMRC)*, pages 617–621, September 2009.

[POC+15] G. Piro, A. Orsino, C. Campolo, G. Araniti et al. D2D in LTE vehicular networking: System model and upper bound performance. In *International*

Congress on Ultra Modern Telecommunications and Control Systems and Workshops (ICUMT), pages 281–286, October 2015.

[Rap02] T. S. Rappaport. *Wireless Communications*. Prentice Hall PTR, 2002.

[RC00] W. Rhee and J. M. Cioffi. Increase in capacity of multiuser OFDM system using dynamic subchannel allocation. In *Vehicular Technology Conference (Spring)*, volume 2, pages 1085–1089, May 2000.

[RKT81] A. Rinnooy Kan and J. Telgen. The complexity of linear programming. *Statistica Neerlandica*, 35(2):91–107, 1981.

[RW00] L. Råde and B. Westergren. *Mathematics handbook for science and engineering*. Springer, 3 edition, 2000.

[SA89] A. Sánchez-Arroyo. Determining the total colouring number is NP-hard. *Discrete Mathematics*, 78(3):315 – 319, 1989.

[SL05] G. Song and Y. Li. Cross-layer optimization for OFDM wireless networks-part II: algorithm development. *IEEE Transactions on Wireless Communications*, 4(2):625–634, March 2005.

[SMS06] G. Sharma, R. R. Mazumdar, and N. B. Shroff. On the complexity of scheduling in wireless networks. In *Proceedings of the 12th Annual International Conference on Mobile Computing and Networking*, pages 227–238. ACM, 2006.

[SSB+14] W. Sun, E. G. Ström, F. Brännström, Y. Sui et al. D2D-based V2V communications with latency and reliability constraints. In *IEEE Globecom Workshops*, pages 1414–1419, December 2014.

[SSB+16] W. Sun, E. Ström, F. Brännström, K. Sou et al. Radio resource management for D2D-based V2V communication. *IEEE Transactions on Vehicular Technology*, 65(8):6636–6650, August 2016.

[STB11] S. Sesia, I. Toufik, and M. Baker. *LTE - The UMTS Long Term Evolution: From Theory to Practice*. Wiley, 2011.

[SWB09] S. Stańczak, M. Wiczanowski, and H. Boche. *Fundamentals of Resource Allocation in Wireless Networks*, volume 3 of *Foundations in Signal Processing, Communications and Networking*. Springer, Berlin, 2009.

[SYSB16] W. Sun, D. Yuan, E. G. Ström, and F. Brännström. Cluster-based radio resource management for D2D-supported safety-critical V2X communications. *IEEE Transactions on Wireless Communications*, 15(4):2756–2769, April 2016.

[TV05] D. Tse and P. Viswanath. *Fundamentals of Wireless Communication*. Cambridge University Press, 2005.

[Ull75] J. Ullman. NP-complete scheduling problems. *Journal of Computer and System Sciences*, 10(3):384 – 393, 1975.

[Uts16] W. Utschick. *Communications in Interference Limited Networks*. Signals and Communication Technology. Springer International Publishing, 2016.

[Var09] R. Varga. *Matrix Iterative Analysis*. Springer Series in Computational Mathematics. Springer Berlin Heidelberg, 2009.

[WAJ10] S. Weber, J. Andrews, and N. Jindal. An overview of the transmission capacity of wireless networks. *IEEE Transactions on Communications*, 58(12):3593–3604, December 2010.

[WOM09] I. C. Wong, O. Oteri, and W. Mccoy. Optimal resource allocation in uplink SC-FDMA systems. *IEEE Transactions on Wireless Communications*, 8(5):2161–2165, May 2009.

[WS80] H. Wolkowicz and G. P. Styan. Bounds for eigenvalues using traces. *Linear Algebra and its Applications*, 29:471–506, 1980.

[XSH+12] C. Xu, L. Song, Z. Han, D. Li et al. Resource allocation using a reverse iterative combinatorial auction for device-to-device underlay cellular networks. In *IEEE Global Communications Conference (GLOBECOM)*, pages 4542–4547, December 2012.

[XWW+14] W. Xing, N. Wang, C. Wang, F. Liu et al. Resource allocation schemes for D2D communication used in VANETs. In *IEEE Vehicular Technology Conference (Fall)*, pages 1–6, September 2014.

[ZdV05] A. Zemlianov and G. de Veciana. Capacity of ad hoc wireless networks with infrastructure support. *IEEE Journal on Selected Areas in Communications*, 23(3):657–667, March 2005.

[ZHS10] M. Zulhasnine, C. Huang, and A. Srinivasan. Efficient resource allocation for device-to-device communication underlaying LTE network. In *IEEE International Conference on Wireless and Mobile Computing, Networking and Communications (WiMob)*, pages 368–375, October 2010.

[ZKF12] G. Z. Zhang, H. King, and M. Faulkner. The transport capacity of cellular wireless networks. In *IEEE International Symposium on Personal, Indoor and Mobile Radio Communications (PIMRC)*, pages 642–646, September 2012.